High penetration of Solar Photovoltaics into low-voltage distribution networks: developing novel feeder voltage control strategies

A thesis submitted in fulfilment

of the requirements for award of the Degree

Doctor of Philosophy

from

James Cook University

By

Nasif Mahmud

College of Science and Engineering

Supervisors: A/ Prof Ahmad Zahedi, A/ Prof Mohan Jacob

2017

CERTIFICATION

I, Nasif Mahmud, declare that this thesis, submitted in partial fulfilment of the requirements for the award of Doctor of Philosophy, in the college of science and engineering, James Cook University, is wholly my own work unless otherwise referenced and acknowledged. The document has not been submitted for qualifications at any other academic institution.

Nasif Mahmud

ACKNOWLEDGEMENT

I would like to express my sincere gratitude to my supervisor, Associate Professor Ahmad Zahedi, for his continuous support, patience, encouragement and insightful discussions throughout my PhD candidature. His supervision, as well as, encouragements helped me a lot to accomplish my research goals. I am grateful for his expert engineering intuition and endless enthusiasm.

I am thankful to my co-supervisor, Associate Professor Mohan Jacob, for his editorial advices and critical comments in preparation of my PhD thesis. Despite his busy schedule, he managed his valuable time for me and I am very grateful for this.

I would like to thank Mr. Asif Mahmud, who is a Distribution Design Engineer from Western Power, Perth, Australia for assisting me in designing realistic distribution system model with practical network data and co-authoring one of my journals.

I thank Matthew Rigano, who is an Operations Control Centre Manager from Ergon Energy, for providing me residential customer demand data that helped me in performing realistic test analysis in distribution power system.

I would also like to thank Dr Shamiur Rahman and Dr Adnan Anwar for their inspirations and their valuable discussions throughout my PhD candidature. Their encouragement to focus on different important issues is greatly acknowledged.

My sincere appreciation goes to Ms Melissa Norton, who made my PhD tenure very smooth by solving a lot of my troubles in-a-blink. Her sincere and wholehearted support is gratefully acknowledged.

I would like to send my gratitude to my colleagues and friends (Timo, Mitchell, Korah, Sathees, Elsa, Michael, Fifi, Thushara, Niroshan, Geeth and Jeanne) who made my time memorable in Townsville. Also, I want to acknowledge my gratitude to Dr Ilias Inam, Mr Farhan Masud and Dr Jakaria Ahmad for accepting me as a family member.

I want to thank my parents, elder brother, sister-in-law, my nephew and niece for the continuous inspirations, supports and indulgence.

Last, but certainly not least, I am indebted to College of Science and Engineering at James Cook University for their financial support and the opportunity to embark on this PhD journey.

STATEMENT OF CONTRIBUTION OF OTHERS

Editorial assistance: My supervisor Associate professor Ahmad Zahedi and Co-supervisor Associate professor Mohan Jacob provided editorial support and suggestions for preparing the thesis.

Contribution to co-authored publications: Associate professor Ahmad Zahedi and Associate professor Mohan Jacob assisted me with their valuable comments to edit my publications. Engr. Asif Mahmud from Western Power, Perth, Australia has assisted me in designing a realistic low-voltage distribution system model in Matlab/ Simulink environment in one of my journals.

Except for the cases stated above, I performed all the simulation, analytical and editorial works.

ABSTRACT

Integration of renewable energy sources (RES) into traditional power system is one of the most viable technologies to meet the ever-increasing energy demand efficiently. Penetrating renewable distributed generators (DGs) such as solar panels, wind turbines into low-voltage distribution network is being a popular tradition nowadays. Increased interconnection of renewable DGs such as solar PVs arise several crucial issues that actually impose limitations on the amount of solar PV penetration. The most significant issue that arises due to large-scale PV interconnection with low-voltage power distribution system is voltage regulation issue. Due to high power generation during midday by solar PVs, the excess power, after satisfying the load demand, reverses back to distribution grid, which causes voltage rise through the feeder. On the other hand, during evening, there is increased load demand and there is no PV generation. As a result, evening peak load consumes high power from distribution grid, which causes voltage sag. These phenomena cause the feeder voltage to exceed the allowable voltage zone and trip the power supply. To interconnect solar PVs into distribution grid spontaneously, intelligent and robust voltage control strategies should be designed and implemented to regulate the feeder voltage within allowable limit.

Firstly, this thesis attempts to present a detailed overview of voltage control strategies that are being utilized to mitigate voltage regulation challenges when increased amount of renewable DGs are penetrated. The impact of high PV penetration on single bus and multi-bus low-voltage distribution systems have been analysed with mathematical representations. A comprehensive qualitative analysis has been performed for different voltage control approaches with comparisons among them. In addition, recent status of ongoing research on distribution system voltage control strategies has been briefly analysed.

This thesis has proposed novel mitigation strategies for the adverse impacts of high penetration of solar PVs on feeder voltages.

A novel intelligent, adaptive and robust control strategy has been proposed for PV interfacing 3-phase inverters where the control parameters of proportional-integral-derivative control scheme is dynamically auto-tuned in real time by adaptive neuro-fuzzy inference system (ANFIS) to provide robust response during any nonlinear and fluctuating operating conditions. This ANFIS-based PID (ANFISPID) is capable of handling fluctuating operating conditions

and damping system oscillations, which ensures power system stability and reliability. ANFISPID controls the injection/ absorption of appropriate reactive power by 3-phase PV interfacing inverter and regulates the voltage at point of common coupling (PCC). A novel intelligent supervisory energy management system (EMS) based on ANFIS has been proposed to control the charge/ discharge of battery energy storage system (BESS) to provide voltage support at PCC. The performance of the cooperative operation of these two novel voltage control strategies has been analysed and evaluated in realistic low-voltage distribution system model and their performance has been compared with classic PID control scheme and classic EMS in different worst-case scenarios.

Then, the impact of high PV penetration has been evaluated on large-distribution system with multiple buses and a novel distributed cooperative voltage control strategy has been proposed to regulate the bus voltages through the feeder in a coordinated fashion. A discrete event-triggered communication-based distributed cooperative control strategy has been proposed to control BESSs and PV interfacing inverters for feeder voltage regulation that requires minimal communication. The distributed cooperative voltage control strategy has been separated into two different control layers (distributed control layer and cooperative control layer). Discrete event-triggered communication mechanism has been implemented among neighbour agents in each layer and appropriate triggering conditions have been designed that dramatically reduces the amount of communication and relax the real-time information exchange requirement among agents. A realistic radial distribution feeder has been designed in MATLAB/ Simulink environment to show that the proposed discrete event-triggered distributed cooperative voltage control strategy requires lower communication rates while preserving the desired voltage control performance.

Finally, the impact of high penetration of solar PVs on feeder bus voltages has been evaluated on a partly cloudy day. The performance of the discrete event-triggered communication based distributed cooperative control has been evaluated in the occurrences of random communication link failures. An algorithm has been designed and implemented to provide robustness against random communication link failures while implementing distributed voltage control through the feeder.

Overall, in this thesis, the impacts of large-scale solar PV penetration into low-voltage distribution network on the PCC and across the feeder have been analysed. Novel control strategies have been designed and implemented to regulate the voltage and their performances

have been evaluated in realistic low-voltage distribution system model in MATLAB/ Simulink environment.

NOMENCLATURE

DG	Distributed generation	DMSC	Distribution management system controller
PV	Photovoltaic	CBA	Cost benefit analysis
SDG	Sustainable development goal	AVC	Automatic voltage control
AEMO	Australian Electricity Market Operator	V2GQ	Vehicle-to-grid reactive power support
OLTC	On-load tap changers	VSC	Voltage source converters
SC	Switched capacitors	MAS	Multi-agent system
SVR	Step voltage regulator	FIPA	Foundation for Intelligent Physical Agents
STATCOM	Static synchronous compensator	JADE	Java Agent Development Framework
PID	Proportional-integral-derivative	LVRT	Low voltage ride-through
ANN	Artificial neural network	PVI	Photovoltaic inverter
FIS	Fuzzy inference system	NREL	National Renewable Energy Laboratory
PCC	Point of common coupling	MPPT	Maximum power point tracking
ANFISPID	ANFIS-based PID	dq	Direct-quadrature
EMS	Energy management system	SOC	State-of-charge
RES	Renewable energy sources	ITAE	Integral time absolute error
DS	Distribution substation	ITSE	Integral time square error
DNO	Distribution network operator	THD	Total harmonic distortion
PSS/E	Power System Simulator for Engineering	MPPT	Maximum power point tracking
PSO	Particle swarm optimization	BOM	Bureau of Meteorology
GA	Genetic algorithm	FEC	Forward error correction
GS	Gradient search	ACK	Acknowledgement
OPF	Optimal power flow	QoS	Quality of service
ANM	Active network management	DMRF	Dynamical jumping real-time fault-tolerant
SCADA	Supervisory control and data acquisition	DSSE	Distribution system state estimation

LIST OF FIGURES

LIST OF TABLES

CONTENTS

LIST OF PUBLICATIONS

Refereed Book Chapter

1. Mahmud, N., Zahedi, A., & Shamiur, M. (2017) “Control of Renewable Energy Systems,” in *Renewable Energy and the Environment,* Springer. (accepted, in press)

Refereed Journal Papers

2. Mahmud, N., & Zahedi, A. (2016). Review of control strategies for voltage regulation of the smart distribution network with high penetration of renewable distributed generation. *Renewable and Sustainable Energy Reviews, 64*, 582-595. (published) [chapter 2]
3. Mahmud, N., Zahedi, A., & Mahmud, A. (2017). A cooperative operation of novel PV inverter control scheme and storage energy management system based on ANFIS for voltage regulation of grid-tied PV system. *IEEE Transactions on Industrial Informatics*. (published) [chapter 3]
4. Mahmud, N., Zahedi, A., & Jacob. M. (2017) A novel event-triggered communication-based distributed cooperative voltage control strategy for large grid-tied PV system *IEEE Transactions on Industrial Informatics*. (under review) [chapter 4]
5. Mahmud, N., Zahedi, A., & Jacob. M. (2017) An event-triggered distributed cooperative voltage control with communication link failures on a partly cloudy day *IEEE Transactions on Energy Conversion*. (under review) [chapter 5]

Refereed Conference papers

6. Mahmud, N., Zahedi, A., & Mahmud, A. (2016, November). ANFISPID-based voltage regulation strategy for grid-tied renewable DG system with ESS. In *Innovative Smart Grid Technologies-Asia (ISGT-Asia), 2016 IEEE* (pp. 81-86). IEEE.
7. Mahmud, N., Zahedi, A., & Mahmud, A. (2016, September). Dynamic voltage regulation of grid-tied renewable energy system with ANFIS. In *Power Engineering Conference (AUPEC), 2016 Australasian Universities* (pp. 1-6). IEEE.
8. Mahmud, N., Zahedi, A., & Shamiur, M. (2017, November) "A novel leader-following distributed voltage control strategy in radial distribution network." *Power Engineering Conference (AUPEC), 2017 Australasian Universities*. IEEE. (accepted)

Chapter 1

INTRODUCTION

1.1 Rationale

With the major development of economies, global electricity demand is estimated to rise by 43% through 2035 [1]. Consequently, the electricity generation is gradually shifting from conventional sources (ea. fossil fuel) to renewable energy sources (ea. solar energy, wind energy etc.). The penetration of renewable energy sources into global electricity generation is increasing rapidly for reducing greenhouse gas emissions and local pollution and increasing customers' participation [2, 3]. Apart from environmental factors, social, operational and economic drivers are behind the recent evolution of renewable power generation [4, 5]. For instance, the total investment in power generation from renewable sources (wind, solar, biomass, waves) grew to $187 billion in recent times compared to $157 billion for natural gas, coal and oil [2]. Renewable distributed generation (DG) technologies include PV arrays, wind turbines, fuel cells, gas-fired turbines, mircroturbines, reciprocating engines, conventional diesel and natural gas. They can be classified into two technologies, which are 1) rotating prime mover technologies (such as wind turbines) and 2) non-rotating prime mover technologies (such as solar PV and fuel cells) [6].

The deregulation of the electricity market coupled with the recently launched sustainable development goals (SDGs) by United Nations emphasizing on the increase of renewable energy resource in the global electricity generation also serves as drivers for PV integration into the power system [3, 7, 8]. There are two broad perspectives driving the increased penetration of solar PVs into traditional electricity grids, which are the end-users perspective and public entities perspective. The end-users are driven by network reliability, deregulation of energy markets, distribution level de-monopolization and profitability [9]. As for public entities, emergence of a new industry, reliability of the national energy and environmental consideration are the major drivers. Consequently, the traditional power system is presently undergoing an evolution in terms of operations and architectural landscape. The distribution network, which used to be a passive one, is now active with the high penetration of solar PVs. The PV capacity has increased to 6 GW in 2016 from 2.44 GW in 2012 [10]. The penetration

of large-scale solar PVs into low and medium-voltage distribution network is being a popular trend nowadays. Large-scale integration of solar PVs into traditional distribution network can generate excess power comparing to consumer load during high solar irradiation period and cause reverse power flow back to the traditional grid. As the resistance to reactance ratio is more than one for distribution networks, the impact of active power flow on the voltage through the distribution feeder is significant. As a result, the voltage rise or sag created through the feeder can cause one or more bus voltages of the feeder to exceed the allowable zone.

Low voltage distribution systems have not received much attention previously, as they were passive in nature with unidirectional power flow. However, increased penetration of solar PVs is turning the network into active in nature causing bidirectional power flow. As a result, several issues are being raised in the operation and protection of the system. The evolving active distribution network with distributed solar PV interconnections now requires active management mechanisms in terms of control, protection and communication systems over the changing topology in order to improve its operational efficiency and ensure the security of supply.

Different sorts of control strategies have been proposed to mitigate the voltage regulation issues those occur when large-scale solar PVs are interconnected with low-voltage distribution systems. This voltage control operations can be performed by, 1) Utilities or 2) Customers. To mitigate voltage regulation issues, utilities require bringing radical changes to distribution network structure, which include increasing the conductor size, installing more voltage regulators, frequent tap changing of transformers etc., which are very expensive [11-13]. The conventional voltage regulators like on-load tap changers (OLTC), switched capacitors (SC) and step voltage regulators (SVR) are not efficient enough to regulate the voltage when large-scale solar PVs are integrated. This is because, solar PVs are intermittent in nature and the power generated by solar PVs is always varying. Besides, due to the dynamic behaviour of the customer loads, the voltage at PCC varies so rapidly that these conventional voltage regulators cannot operate fast enough to regulate the voltage. On the other hand, the strategies those can be followed by customers to regulate the voltage within allowable limits include power curtailment [14], reactive power injection/ absorption using static synchronous compensator (STATCOM) or interfacing inverters [15-26] and utilization of battery energy storage systems (BESS) [27-34]. In the power curtailment process, the excess power flowing back to grid causing voltage violation is curtailed. However, active power curtailment causes wastage of generated power. Reactive power compensation by power electronic converters (e.g.

STATCOM, solar PV inverters) is another strategy to control PCC voltage. However, the reactive power injection/ absorption capability of PV inverters is limited that depends upon active power generation and this strategy increases the line loss through the system. Besides, the effect of injected/ absorbed reactive power on the voltage profile of the low-voltage distribution feeder is minimal because of the R/X ratio. Utilizing battery energy storage system (BESS) is another strategy to regulate the voltage of low-voltage grid connected PV systems. This strategy is more effective in systems with higher R/X ratio as it stores/ discharges active power for voltage control. However, solo-implementation of BESS for voltage regulation needs very large battery capacity, which is very costly and not a feasible process. In that scenario, a cooperative operation of both solar PV inverter and BESS is advantageous to regulate the voltage of large-scale grid connected solar PV systems. Authors of [28] have proposed a coordinated control for PV inverter and BESS for voltage regulation, however, a detailed robust control structure was not presented for PV inverter. Moreover, this control technique operates on an hourly basis with a power flow study in each operation which is complex and not dynamic enough when large-scale solar PVs are interconnected.

To control solar PV inverters for PCC voltage regulation, classic controllers like proportional-integral-derivative (PID) controllers are long established to implement because of its simplicity in structure and linearity in nature. However, these classic controllers have some shortcomings when they are implemented in highly fluctuating system environment. When they are implemented in fluctuating operating conditions, they start to provide unstable, oscillatory or sluggish response [35-36]. To overcome these shortcomings, the control parameters of the PID controller need to be tuned in real time in accordance with system operating conditions. Conventionally, PID control parameters are manually tuned using trial-and-error approaches which are monotonous, expensive and time consuming and the tuned gain can go obsolete in short time due to fluctuating behavior of the system. This causes classic PID controllers to operate inefficiently as it is nearly impossible to set appropriate gains due to rapid change in system dynamics [37-39]. In this scenario, an intelligent adaptive control is necessary that can automatically tune the PID control parameters in real time according to system operating conditions.

Intelligent controllers, such as, artificial neural networks (ANN), fuzzy inference system (FIS), neuro-fuzzy systems etc. are invulnerable to system dynamics [40-41]. Among the neuro-fuzzy models, adaptive neuro-fuzzy inference system (ANFIS) is easier to implement, faster, stronger in generalization skills and more accurate [42] that inherits the learning and

parallel data processing ability of artificial neural networks and inference ability (like human mind) of fuzzy inference system. As PID is well established for controlling grid-interfacing PV inverters and ANFIS is well capable of handling the uncertainties, the combination of ANFIS and PID where ANFIS auto-tunes the PID control parameters in real time in accordance with system dynamics has been shown in this thesis to be advantageous to control PV inverters in fluctuating operating conditions. This is the first time that this thesis proposes a PID control scheme dynamically auto-tuned in real time by intelligent ANFIS, implemented on PV inverter for regulating the PCC voltage of three-phase grid-tied solar PV system that shows robustness at any system worst-case scenarios. One reference has been found [42] where the charge/ discharge of BESS has been controlled by ANFIS-based supervisory control. However, the objective was not voltage regulation of the system.

To control the voltage along long distribution feeder, the control action can be implemented on PV inverters and BESSs in different structures, which are: 1) centralized control, 2) decentralized control and 3) distributed control. Centralized controller requires significant investment on communication infrastructure, which is not feasible for modern large interconnected system. Besides, communication failure for the centralized controller can affect the operation of the entire system. In decentralized control strategy, control devices does not communicate with one another and works on local measurements. However, there is no coordination and cooperation among neighbour controllers in this strategy, which may cause system unbalanced conditions. The third category, distributed control, does not operate only on local measurements and does not require large communication infrastructure. In this strategy, the control devices communicate and cooperate with only neighbour control devices and initiate control action in a coordinated way. Since PV generators are located in a heterogeneous and distributed fashion through low-voltage feeders, distributed control strategies are required to improve the stability, scalability and security of the system. Distributed control strategy has become popular nowadays in controlling BESSs and PV inverters due to its robustness to individual agent errors, scalability with respect to increased number of agents and reduced computational load. However, for distributed voltage control implementation, BESSs and PV inverters from neighbour buses need to communicate with each other for information transmission. The existing research works on distributed control strategy considered that data communication among agents is performed continually at every instant of time or periodically at equidistant sampling instants. This is not practical and requires expensive communication infrastructure [43]. Besides, the communication network of a

distribution grid usually has limited bandwidth and therefore, an efficient use of the communication infrastructure is desirable [44]. In this scenario, introducing the need-based aperiodic communication scheme, such as self-triggered or event triggered communication can significantly reduce those unnecessary sample-state transmissions and make effective use of the communication network [45]-[47]. In the event-triggered communication scheme, a sample-state transmission between agents is triggered when a state-measurement error exceeds a given threshold while in the self-triggered communication scheme, the next triggering time instant is determined by the previous received data and knowledge on plant dynamics. However, self-triggered communication scheme is not an appropriate approach in a stochastic system (like grid-tied PV system) because an emergency triggering situation may appear any time before the precomputed triggering instant. In that case, implementing event-triggered communication scheme ensures better performance as the triggering instants are executed depending upon the dynamic state measurements of the stochastic system.

In the distributed voltage control strategy, proper communication between neighbour control agents is utmost important to ensure the stability and reliability of coordinated control. In almost all the existing literatures [29-34], [44], [48-50], the distributed voltage control is implemented on an explicit assumption that the control agents can transmit data to neighbour agents any time when necessary using uninterrupted communication links. This assumption is seldom practical in real scenarios. The communication links between control agents can subject to random catastrophic failures (due to externally induced events, such as, earthquakes) which interrupts data transmission [51]. This interruption in data transmission can affect the coordination among agents while implementing distributed voltage control algorithm. In this scenario, an intelligent algorithm is necessary to ensure resiliency and robustness of the distributed voltage control strategy against random communication link failures between control agents.

1.2 Motivation of current research

- As the traditional voltage regulation devices are not adequate to regulate the voltage in fast nonlinear dynamics of low-voltage grid connected PV system, new devices which are capable of fast dynamic control, should be utilized to regulate the voltage.
- As solo-implementation of PV inverter or BESS is not adequate for voltage regulation in low-voltage distribution network, cooperative performance of PV inverter and BESS can be an effective strategy to regulate the voltage appropriately.

- As the well-established classic PID controller for PV inverter control is linear in nature and is very sensitive to variation of system operating conditions, a strategy is necessary to enable it to provide robust response in any nonlinear and fluctuating operating condition.
- As the existing coordinated control for BESS to cooperate with PV inverter operates at an hourly basis and requires power flow study every hour, which makes it complex, a dynamic supervisory control strategy is required that can operate in real time and cooperate with PV inverter in feeder voltage regulation.
- The need of a strategy that reduces the necessary communication between neighbour agents while implementing distributed cooperative voltage control on a large-scale distribution system with multiple buses.
- The necessity of a need-based aperiodic communication scheme that can significantly reduce unnecessary sample-state transmissions and the occupancy of limited communication bandwidth while implementing distributed voltage control through the low-voltage distribution feeder highly penetrated with solar PVs.
- The necessity of performance evaluation of need-based aperiodic communication scheme while implementing distributed cooperative voltage control through the low-voltage distribution feeder highly penetrated with solar PVs under fluctuating operating conditions (on a partly cloudy day) and in the occurrences of random communication link failures.
- The need of an algorithm to provide robustness against random communication link failures while implementing distributed coordinated control through the feeder.

1.3 Objective of current research

- To design and implement a cooperative operation of PV inverter control scheme and storage EMS for feeder voltage regulation in real time with detailed control structures in case of introduced fast dynamics when large-scale intermittent solar PVs are penetrated.
- To design and implement an intelligent control strategy for PV inverter that will be able to provide robust response and to damp oscillation in any nonlinear and fluctuating operating condition and system worst-case scenario.
- To design and implement an adaptive intelligent supervisory energy management system for BESS that can cooperate with PV inverter in voltage regulation by reducing the PCC voltage during voltage deviations.

- To design and implement a distributed cooperative voltage control strategy for BESS and PV inverter for long residential distribution feeder that will require minimal communication instants and occupy minimal communication bandwidth.
- To evaluate the performance of the distributed cooperative voltage control strategy that require minimal communication instants and occupy minimal communication bandwidth under fluctuating operating conditions and during random communication link failures.
- To design and implement an algorithm to provide robustness in the occurrence of random communication link failures while implementing distributed coordinated control under fluctuating operating conditions.

1.4 Specific contributions of current research

Analysis:

- Analysing the impacts of large-scale penetration of solar PVs on the voltage profile of low-voltage distribution feeder.

Control design:

- The design and implementation of cooperative operation of PV inverter and BESS for voltage regulation of low-voltage distribution network interconnected with solar PVs in real time with detailed control structures.
- The design and implementation of intelligent ANFIS-based PID control scheme (ANFISPID) on PV inverters to regulate the PCC voltage in real time that provides 'plug-and-play' feature for auto-tuning the PID parameters and shows robustness at any nonlinear and fluctuating operating condition.
- The design and implementation of an intelligent ANFIS-based supervisory EMS on BESS that cooperates with PV inverter in voltage regulation by charging/ discharging when voltage deviation occurs in real time. By applying proper control, this proposed ANFIS-based supervisory EMS reduces the PCC voltage deviations and reduces reactive power injection/ absorption load on PV inverter.
- The separation of the distributed cooperative control into two different layers which reduces the necessary communications while implementing distributed cooperative voltage control along a large distribution feeder with multiple buses.

- The design and implementation of a discrete event-triggered communication scheme for data transmission between neighbour agents while implementing distributed cooperative voltage control on BESS and PV inverters.
- The performance evaluation of a discrete event-triggered communication-based distributed cooperative voltage control strategy in the occurrences of random communication link failures under fluctuating operating condition (on a partly cloudy day).
- The design and implementation of an alternate path routing algorithm for data dissemination that provides robustness against random communication link failures while implementing distributed voltage control under fluctuating operating condition (on a partly cloudy day).

1.5 Thesis organization

The organization of the thesis is outlined below:

Chapter 1 provides a brief background of the problems those have been particularly focused in this thesis and depicts the motivations, objectives and contributions of the research.

Chapter 2 provides a detailed review of the control strategies that are being utilized to mitigate voltage regulation challenges when increased amount of renewable DGs are connected within low-voltage distribution network. This chapter analyses the challenges of increased penetration of renewable DGs on the distribution network operation and evaluates ongoing research status of voltage control strategies. A comprehensive analysis is performed on the performances of conventional and advanced voltage control strategies and different communication infrastructures.

Chapter 3 develops the design and implementation of a novel cooperative control strategy of PV interfacing inverter and BESS to regulate the voltage at PCC at any nonlinear and fluctuating operating condition and analyses its performance. The proposed cooperative control scheme has been evaluated under different worst-case scenarios and its performance has been compared with classic cooperative voltage control strategies in realistic distribution system model.

Chapter 4 develops the design and implementation of a novel discrete event-triggered communication-based distributed cooperative voltage control strategy for long distribution feeder with multiple buses. In this chapter, a novel distributed cooperative voltage control algorithm has been implemented on neighbour BESSs and PV inverters that requires minimal

communication instants and minimal occupancy of bandwidth. The performance of the proposed control strategy has been evaluated in a realistic low-voltage distribution feeder highly penetrated with PVs.

Chapter 5 evaluates the performance of the proposed discrete event-triggered communication-based distributed cooperative voltage control strategy on a partly cloudy day with fluctuating solar irradiation and its performance in the occurrence of random communication link failures. It also develops the design and implementation of an alternate path routing algorithm to provide robustness against random communication link failures and its performance has been evaluated considering time delays.

Chapter 6 provides concluding remarks as well as recommendations for further development.

References

[1] International Energy Outlook 2016 by US. Energy Information Administration. Online: https://www.eia.gov/outlooks/ieo/

[2] Sustainable Energy for All. Online: http://www.se4all.org/our-vision_our-objectives_renewable-energy

[3] Sustainable Development Goals (SDGs). Online: https://sustainabledevelopment.un.org/

[4] Lasseter RH. Smart distribution: coupled microgrids. Proc IEEE 2011;99 (6):1074–82.

[5] Costanzo G, Gehrke O, Bondy D, Sossan F, Bindner H, Parvizi J, et al. A coordination scheme for distributed model predictive control: Integration of flexible DERs. In: Proceedings of the 2013 4th IEEE/PES Innovative Smart Grid Technologies Europe (ISGT EUROPE), IEEE, 2013, p. 1–5.

[6] IEEE Application Guide for IEEE Std 1547TM. IEEE Standard for Interconnecting Distributed Resources with Electric Power Systems; 2008.

[7] Tan W-S, Hassan MY, Majid MS, Rahman HA. Optimal distributed renewable generation planning: a review of different approaches. Renew Sustain Energy Rev 2013;18:626–45.

[8] Chiradeja P, Ramakumar R. An approach to quantify the technical benefits of distributed generation. IEEE Trans Energy Convers 2004;19(4):764–73.

[9] Hammons T. Integrating renewable energy sources into European grids. Int J Electr Power Energy Syst 2008;30(8):462–75.

[10] Zahedi, A. (2017) Development of large scale Solar PV in North Queensland: Sustainable Electricity for the State and Export Product for ASEAN Region. In *All-Energy Australia*, October 2017, Melbourne.

[11] Masters, C. L. (2002). Voltage rise: the big issue when connecting embedded generation to long 11 kV overhead lines. *Power engineering journal*, *16*(1), 5-12.

[12] Ranamuka, D., Agalgaonkar, A. P., & Muttaqi, K. M. (2014). Online voltage control in distribution systems with multiple voltage regulating devices. *IEEE Transactions on Sustainable Energy*, *5*(2), 617-628.

[13] Todorovski, M. (2014). Transformer voltage regulation—Compact expression dependent on tap position and primary/secondary voltage. *IEEE Transactions on Power Delivery*, *29*(3), 1516-1517.

[14] Ghosh, S., Rahman, S., & Pipattanasomporn, M. (2017). Distribution voltage regulation through active power curtailment with PV inverters and solar generation forecasts. *IEEE Transactions on Sustainable Energy*, *8*(1), 13-22.

[15] Li, H., et al. "Adaptive voltage control with distributed energy resources: Algorithm, theoretical analysis, simulation, and field test verification." *IEEE Transactions on Power Systems* 25.3 (2010): 1638-1647.

[16] Smith, J. W., et al. "Smart inverter volt/var control functions for high penetration of PV on distribution systems." *Power Systems Conference and Exposition (PSCE), 2011 IEEE/PES*. IEEE, 2011.

[17] Rizy, D. T., et al. "Volt/Var control using inverter-based distributed energy resources." *2011 IEEE Power and Energy Society General Meeting*. IEEE, 2011.

[18] Jahangiri, P., & Aliprantis, D. C. "Distributed Volt/VAr control by PV inverters." *IEEE Transactions on power systems* 28.3 (2013): 3429-3439.

[19] Camacho, A., et al. "Flexible voltage support control for three-phase distributed generation inverters under grid fault." *IEEE transactions on industrial electronics* 60.4 (2013): 1429-1441.

[20] Miret, J., et al. "Control scheme with voltage support capability for distributed generation inverters under voltage sags." *IEEE Transactions on Power Electronics* 28.11 (2013): 5252-5262.

[21] Li, H., et al. "Autonomous and adaptive voltage control using multiple distributed energy resources." *IEEE Transactions on Power Systems* 28.2 (2013): 718-730.

[22] Reid, D. "DQ rotating frame PI control algorithm for power inverter voltage regulation modelling and simulation using the OpenModelica platform." *SoutheastCon 2015*. IEEE, 2015.

[23] Khan, O., & Xiao, W. "An Efficient Modeling Technique to Simulate and Control Submodule-Integrated PV System for Single-Phase Grid Connection." *IEEE Transactions on Sustainable Energy* 7.1 (2016): 96-107.

[24] Chakraborty, C., Iu, H. H. C., & Lu, D. D. C. "Power converters, control, and energy management for distributed generation." *IEEE Transactions on Industrial Electronics* 62.7 (2015): 4466-4470.

[25] Miñambres-Marcos, V., et al. "Grid-connected photovoltaic power plants for helping node voltage regulation." *Renewable Power Generation, IET* 9.3 (2015): 236-244.

[26] Schiffer, J., Seel, T., Raisch, J., & Sezi, T. (2016). Voltage stability and reactive power sharing in inverter-based microgrids with consensus-based distributed voltage control. *IEEE Transactions on Control Systems Technology*, *24*(1), 96-109.

[27] Zeraati, M., Golshan, M. E. H., & Guerrero, J. (2016). Distributed Control of Battery Energy Storage Systems for Voltage Regulation in Distribution Networks with High PV Penetration. *IEEE Transactions on Smart Grid*.

[28] Kabir, M. N., Mishra, Y., Ledwich, G., Dong, Z. Y., & Wong, K. P. (2014). Coordinated control of grid-connected photovoltaic reactive power and battery energy storage systems to improve the voltage profile of a residential distribution feeder. *IEEE Transactions on industrial Informatics*, *10*(2), 967-977.

[29] Xin, H., Zhang, M., Seuss, J., Wang, Z., & Gan, D. (2013). A real-time power allocation algorithm and its communication optimization for geographically dispersed energy storage systems. *IEEE Transactions on Power Systems*, *28*(4), 4732-4741.

[30] Xu, Y., Zhang, W., Hug, G., Kar, S., & Li, Z. (2015). Cooperative control of distributed energy storage systems in a microgrid. *IEEE Transactions on smart grid*, *6*(1), 238-248.

[31] Oliveira, T. R., Silva, W. W. A. G., & Donoso-Garcia, P. F. (2016). Distributed secondary level control for energy storage management in dc microgrids. *IEEE Transactions on Smart Grid*.

[32] Morstyn, T., Hredzak, B., & Agelidis, V. G. (2015). Distributed cooperative control of microgrid storage. *IEEE transactions on power systems*, *30*(5), 2780-2789.

[33] Morstyn, T., Hredzak, B., & Agelidis, V. G. (2016). Cooperative multi-agent control of heterogeneous storage devices distributed in a DC microgrid. *IEEE Transactions on Power Systems*, *31*(4), 2974-2986.

[34] Wang, Y., Tan, K. T., Peng, X. Y., & So, P. L. (2016). Coordinated control of distributed energy-storage systems for voltage regulation in distribution networks. *IEEE Transactions on Power Delivery*, *31*(3), 1132-1141.

[35] Han, Yi, et al. "Robust control for microgrid frequency deviation reduction with attached storage system." *IEEE Transactions on Smart Grid* 6.2 (2015): 557-565.

[36] Li, H., et al. "Adaptive voltage control with distributed energy resources: Algorithm, theoretical analysis, simulation, and field test verification." *IEEE Transactions on Power Systems* 25.3 (2010): 1638-1647.

[37] Yacoubi, L., et al. "Linear and nonlinear control techniques for a three-phase three-level NPC boost rectifier." *IEEE Transactions on Industrial Electronics* 53.6 (2006): 1908-1918.

[38] Yang, S., et al. "A robust control scheme for grid-connected voltage-source inverters." *IEEE Transactions on Industrial Electronics* 58.1 (2011): 202-212.

[39] Espi, J. M., et al. "An adaptive robust predictive current control for three-phase grid-connected inverters." *IEEE Transactions on Industrial Electronics* 58.8 (2011): 3537-3546.

[40] Li, H., Shi, K. L., & McLaren, P. G. "Neural-network-based sensorless maximum wind energy capture with compensated power coefficient." *IEEE transactions on industry applications* 41.6 (2005): 1548-1556.

[41] Jang, J. R. "ANFIS: adaptive-network-based fuzzy inference system." *IEEE transactions on systems, man, and cybernetics* 23.3 (1993): 665-685.

[42] García, P., García, C. A., Fernández, L. M., Llorens, F., & Jurado, F. "ANFIS-based control of a grid-connected hybrid system integrating renewable energies, hydrogen and batteries." *IEEE Transactions on Industrial Informatics*, 10.2 (2014): 1107-1117.

[43] Xu, Wenying, et al. "Event-triggered schemes on leader-following consensus of general linear multiagent systems under different topologies." *IEEE transactions on cybernetics* 47.1 (2017): 212-223.

[44] Yang, Q., Barria, J. A., & Green, T. C. (2011). Communication infrastructures for distributed control of power distribution networks. *IEEE Transactions on Industrial Informatics*, *7*(2), 316-327.

[45] Li, C., Yu, X., Yu, W., Huang, T., & Liu, Z. W. (2016). Distributed event-triggered scheme for economic dispatch in smart grids. *IEEE Transactions on Industrial Informatics*, *12*(5), 1775-1785.

[46] Zhang, X. M., Han, Q. L., & Zhang, B. L. (2017). An overview and deep investigation on sampled-data-based event-triggered control and filtering for networked systems. *IEEE Transactions on Industrial Informatics*, *13*(1), 4-16.

[47] Henriksson, E., Quevedo, D. E., Peters, E. G., Sandberg, H., & Johansson, K. H. (2015). Multiple-loop self-triggered model predictive control for network scheduling and control. *IEEE Transactions on Control Systems Technology*, *23*(6), 2167-2181.

[48] Chen, X., Hou, Y., & Hui, S. R. (2017). Distributed Control of Multiple Electric Springs for Voltage Control in Microgrid. *IEEE Transactions on Smart Grid*, *8*(3), 1350-1359.

[49] Cavraro, G., & Carli, R. (2017). Local and distributed voltage control algorithms in distribution network. *IEEE Transactions on Power Systems*.

[50] Lee, S. J., Kim, J. H., Kim, C. H., Kim, S. K., Kim, E. S., Kim, D. U., ... & Khan, S. U. (2016). Coordinated control algorithm for distributed battery energy storage systems for mitigating voltage and frequency deviations. *IEEE Transactions on Smart Grid*, *7*(3), 1713-1722.

[51] Zhu, P., Han, J., Guo, Y., & Lombardi, F. (2016). Reliability and Criticality Analysis of Communication Networks by Stochastic Computation. *IEEE Network*, *30*(6), 70-76.

Chapter 2

LITERATURE REVIEW

"Mahmud, N., & Zahedi, A. (2016). Review of control strategies for voltage regulation of the smart distribution network with high penetration of renewable distributed generation. *Renewable and Sustainable Energy Reviews, 64*, 582-595. (Published)"

Abstract

Integration of renewable energy sources (RES) into traditional power system is one of the most viable technologies to meet the ever increasing energy demand efficiently. However, this technology arises a lot of challenges which are necessary to be taken care of for smooth operation of the network. Voltage regulation is the most significant technical challenge that tends to limit the amount of penetration of renewable distribution generators (DGs) into distribution network. This chapter attempts to present a detailed review of the control strategies that are being utilized to mitigate voltage regulation challenges when increased amount of renewable DGs are connected within the distribution network. This chapter analyses the direct impacts of increased accommodation of renewable DGs on the distribution network operation and evaluates current research status of voltage control strategies. Then qualitative analysis is performed for all kinds of voltage control approaches involving their pros and cons for the first time. The objective of this chapter is to present the latest research status of distribution system voltage control strategies with highly penetrated renewable DGs and a brief review of different control methodologies.

2.1 Introduction

The incorporation of RES in electric power system is being popular day by day. Previously, it was mostly off-grid connection. However, nowadays grid connected RES are coming into trend. Integration of RES into power distribution system was not any serious issue a few years ago as the amount of penetration was not that much significant. However, currently a large amount of renewable energy sources are being connected which are posing a lot of impacts on the operation and protection of the distribution network [1-3].

The characteristics of the power distribution network are different from power transmission network in several ways. They are as follows [4]:

- It works in radial topology.
- There can be significant unbalance.
- The R/X ratio of the distribution network is relatively higher than the transmission network.

For the planning and stable operation of smart distribution infrastructure, it is necessary to analyze the relation between the integration of renewable DGs and the distribution network's behavior [5]. As DGs are connected very near to customers, connecting them has significant effects on distribution network's technology, environment and economy as well as customers' [6-8]. Integration of DGs in the distribution networks is not yet problem free. The traditional grids were designed to supply the electric power from generation side to customer's loads. According to this design, the electric power flow was supposed to be unidirectional (from higher to lower voltage level) through the whole system. However, when DGs are integrated into the distribution network, the excess power generated by DGs after meeting the customer's demand, flow back to the generation side. So, the power flow remains no longer unidirectional. It is rather bi-directional which has significant adverse effect on the operation, voltage regulation and protection of the power distribution network [6], [9-10].

Several efforts have been made to review the stability issues, operations and control technologies of the power system when large-scale DGs are interconnected [11-15]. [11], [12] have discussed about different control strategies and stability issues in a systematic structure but they mainly focused on micro grids. [13], [14] have done extensive reviews on the power quality issues, reactive power management and voltage management where several control devices and methods have been discussed and relative comparisons of their performances have been presented. However, systematic classifications of voltage control structures according to

respective functionalities have not been discussed. [15] investigates some low-voltage ride-through enhancement methods during voltage dips and inter-area oscillation damping techniques for wind and photovoltaic power plants. However, control schemes for real time voltage regulation during system operation was not widely discussed.

This chapter mainly focuses on the voltage regulation challenges raised from increased renewable DG interconnection with low-voltage distribution networks and detailed review of voltage control strategies to mitigate its adverse impacts on voltage profile. Existing control methodologies have been classified into centralized, decentralized autonomous (decentralized control) and decentralized coordinated (distributed control) structures according to their respective functionalities. Then qualitative analysis is performed among these classes involving their advantages and disadvantages. This chapter is organized as follows. Section 2.2 describes the challenges that arise due to increased DG accommodation. Section 2.3 details the impacts of large-scale DG connection on the voltage profile of the network. Section 2.4 analyses several traditional and advanced voltage control methods and different control structures depending on their functionalities. Section 2.5 establishes the conclusion derived from the work.

2.2 Challenges of increased penetration of DGs in distribution network

The challenges that occur due to increased penetration of DGs in distribution networks can be classified into three categories [3].

1) Technical challenges.
2) Commercial challenges.
3) Regulatory challenges.

These challenges are going to be discussed in brief.

2.2.1 Technical challenges

2.2.1.1 Power quality

Depending on the particular circumstance, connecting DGs within the distribution network can either deteriorate or improve power quality [16-18]. DGs are connected closer to the loads and most of the loads are supplied by DGs in case of higher penetration. As a result, lesser amount of power is drawn from the distribution substation. Therefore, the amount of current flow from the distribution substation to the consumer's loads through the feeder and its laterals

is reduced. So does the power loss through the feeder [16]. However, there are other two important aspects of power quality. They are:

- Transient voltage variation.
- Harmonic distortion of the network voltage.

Single large DGs may cause power quality problems in a weak distribution network particularly during starting and stopping.

2.2.1.2 Protection

The protection of the distribution network due to integration of DGs is affected in several ways [19].

- Changes in the traditional distribution network short circuit power.
- Changes in fault current level.
- Changes in the characteristics of the fault current, such as amplitude, direction and distribution.

Most of the distribution networks were designed and built considering unidirectional power flow (without DG). So, during a fault the protection relays cannot coordinate among themselves properly in a radial distribution network when a significant amount of DGs are connected and Bi-directional power flow occurs [20], [21].

2.2.1.3 Voltage regulation

Voltage regulation issues due to high penetration of DGs are one of the key issues that limit the integration of DGs in the network. Due to bi-directional flow of power, regulating the voltage through the distribution feeder needs more advanced strategy [5], [6], [9], [10].

2.2.1.4 Stability

In case of conventional passive distribution networks, stability is not any significant considerable issue. Day by day, the penetration of DGs is increasing. As a result, the stability of the smart distribution network should be a significant consideration. Researchers tried to figure out the maximum amount of DGs that can be penetrated into a particular distribution network. But this approach was not welcome by the DG manufacturers [22].

Effects of large amount of DGs penetrated into the distribution network depend on several parameters [23],

1. The voltage level of the feeder where the DG is connected.
2. Category of the distribution network.
3. The amount of customer demand.
4. The percentage of penetration.

Depending on these parameters, integration of DGs has significant effect on voltage profile, network losses and fault level [24-27]. For most of the distribution networks, they are radial and power flows from higher voltage level to lower voltage level. The resistance to reactance ratio (R/X) is more than one for distribution network and less than one for transmission network. Due to higher resistance, the voltage drop is higher in the distribution feeder. On the other hand, due to higher values of R/X, the impact of the real power provided by DGs has more influence on voltage profile than the impact of reactive power [28].

2.2.2 Commercial challenges

If proper active management can be applied, the benefit of integrating large-scale renewable DGs in the distribution network is expected to be greater than the installation cost. However, for that, developed commercial arrangements are necessary. A well-designed incentive scheme can be stablished that can encourage the companies to apply active management on grid-connected renewable DG networks. On the other hand, implementation cost of proper active management and the incentives can put effect on the electricity price for the consumers.

2.2.3 Regulatory challenges

Low voltage distribution networks were designed to deliver power unidirectionally from generation to grid. However, it does not remain as a passive network any longer when large-scale renewable DGs are interconnected. To operate the large-scale DG connected distribution systems properly, appropriate regulatory policies need to be developed those ensure smooth and uninterrupted operation of the system.

2.3 Impact on voltage regulation of distribution network

Voltage regulation issue has been considered as the most vital issue for integration of large amount of DGs into low and medium voltage distribution networks [28-30]. Several researches have been done to mathematically describe the impact of large scale renewable DGs on the voltage profile of distribution network [5], [31], [32]. A brief discussion about the impact on voltage regulation of distribution network is as follows. Let's consider a simple conventional two bus distribution system.

In figure 2.1. (a), we can observe a two bus conventional distribution feeder. V_s stands for sending end voltage, V_R stands for receiving end voltage. R represents the resistance and X represents the reactance of the distribution feeder. DS stands for the distribution substation; OLTC stands for on-load tap changing transformer. P and Q are the active and reactive power flowing through the feeder. P_L and Q_L are the active and reactive power consumed by the load respectively. In figure 2.1. (b), a DG has been connected with the conventional simple feeder. After connecting DG in the distribution feeder, there is a voltage rise at receiving end (DG bus). Let's consider the increased voltage at the bus where DG is connected is V_g. The active and reactive powers generated by the DG are P_g and Q_g respectively.

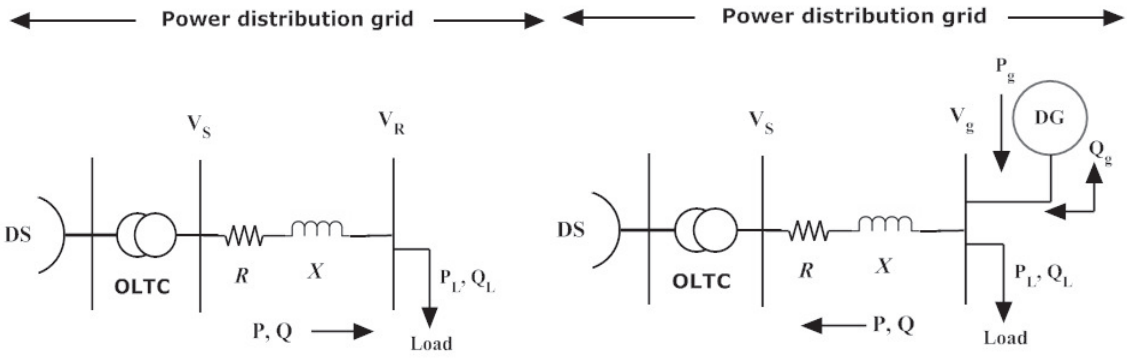

(a) (b)

Figure 2.1. (a) Conventional simple distribution feeder, and (b) Simple distribution feeder with DG

From figure (b), we can write the DG bus voltage as,

$$\widehat{V_g} = \widehat{V_S} + \hat{I}\,(R + jX) \qquad (2.1)$$

Where $\widehat{V_g}$, $\widehat{V_S}$ and $\hat{I}$ represent the corresponding phasor quantities of DG bus voltage, sending end voltage and current flowing through distribution network respectively. Power flowing through the feeder can be written as,

$$P + jQ = \widehat{V_g}\,\widehat{I^*}$$

So, the current flowing through the feeder,

$$\hat{I} = \frac{P - jQ}{\widehat{V_g^*}}$$

So, equation (2.1) can be expressed as,

$$\widehat{V_g} = \widehat{V_S} + \frac{P - jQ}{\widehat{V_g^*}}\ (R + jX) \tag{2.2}$$

$$= \widehat{V_S} + \frac{RP + XQ}{\widehat{V_g^*}} + j\,\frac{XP - RQ}{\widehat{V_g^*}} \tag{2.3}$$

The voltage drop across the feeder is approximately equal to the real part of the voltage drop as the angle between the DG bus voltage and the sending end voltage is very small. If we consider the DG bus voltage as reference bus, the angle of DG bus voltage is 0. As a result, equation (2.3) can be approximated as,

$$\Delta V \approx V_g - V_S \approx \frac{RP + XQ}{V_g} \tag{2.4}$$

Where, $\Delta V =$ voltage drop along the distribution feeder.

If we consider the DG bus voltage as the base voltage, we can assume V_g as unity. So, equation (2.4) can be written as follows,

$$\Delta V \approx V_g - V_S \approx RP + XQ \tag{2.5}$$

Where, $P = (P_g - P_L)$ and $Q = (\pm Q_g - Q_L)$.

So, equation (2.5) can be written as,

$$V_g \approx V_S + R\,(P_g - P_L) + X(\pm Q_g - Q_L) \tag{2.6}$$

From this equation, we can find the amount of maximum permissible DG in distribution feeder that can be accommodated. The worst case scenarios are (considering unity power factor):

1) Maximum generation minimum load ($P_g = P_{gmax}$, $P_L = 0$, $Q_L = 0$)
2) Maximum load minimum generation ($P_g = 0$, $Q_g = 0$, $P_L = P_{Lmax}$)

For the first scenario, considering unity power factor, (2.6) becomes,

$$V_g \approx V_S + RP_{gmax}$$

$$\text{Or,} \quad P_{gmax} \approx \frac{V_g - V_S}{R}$$

Let's consider, V_{gmax} is the maximum voltage at the generation bus within the permissible voltage limit along the feeder. Therefore, to keep the voltage within permissible limit, P_{gmax} needs to be,

$$P_{gmax} \leq \frac{V_{gmax} - V_S}{R} \tag{2.7}$$

For the second case also, considering unity power factor, (2.6) becomes,

$$V_g \approx V_S - RP_{Lmax}$$

$$\text{Or,} \quad P_{Lmax} \approx \frac{V_S - V_g}{R}$$

Let's consider, V_{gmin} is the minimum voltage at the generation bus within the permissible voltage limit along the feeder. So, to keep the voltage within permissible limit, P_{Lmax} needs to be,

$$P_{Lmax} \leq \frac{V_S - V_{gmin}}{R} \tag{2.8}$$

P_{Lmax} does not stay within this limit all the time. For larger dynamic load, the bus voltage reduces lesser than the minimum permissible limit.

Figure 2.2. compares the voltage deviation pattern along the feeder in a conventional two-bus distribution system and in a DG connected distribution system using results obtained from PSS/E and derived formula [33].

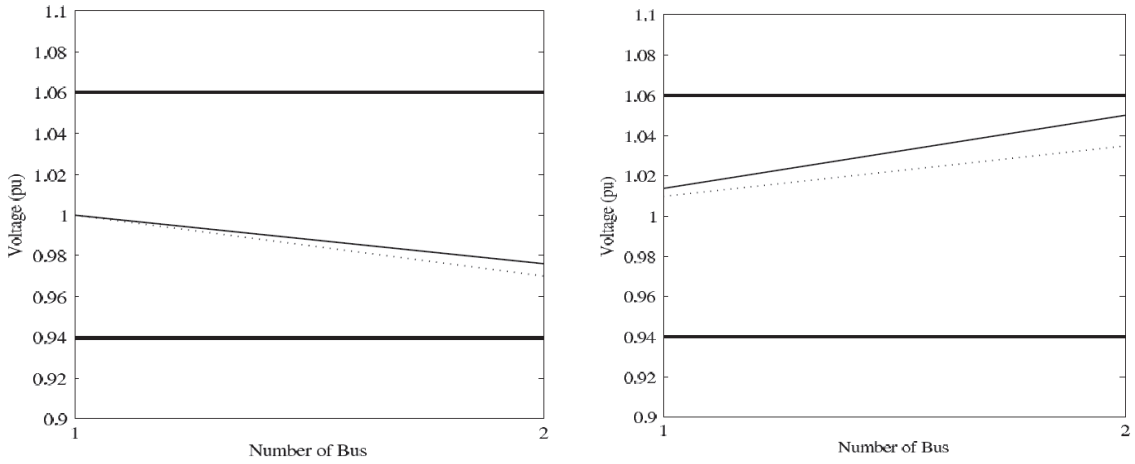

(a) (b)

Figure 2.2. (a) Voltage deviation along the feeder in a conventional two-bus distribution system, and (b) Voltage deviation along the feeder in a DG connected distribution system. The solid line represents the result obtained from PSS/E; the dotted line represents the result obtained from derived formula. Two bold solid lines indicate the permissible range of voltage variation [33].

For the steady state operation, the voltage along the feeder has to be in a permissible limit. There is no internationally applied rule for steady state voltage range along the feeder. For maximum cases, the allowable voltage variation along the feeder is $\pm 6\%$ [19]. Some cases, DNOs set the transformer secondary voltage maximum within permissible limit to ensure that voltage will remain above minimum at the far end of the long distribution feeder.

Now, let's consider a large distribution feeder with n number of buses in Fig 2.3.

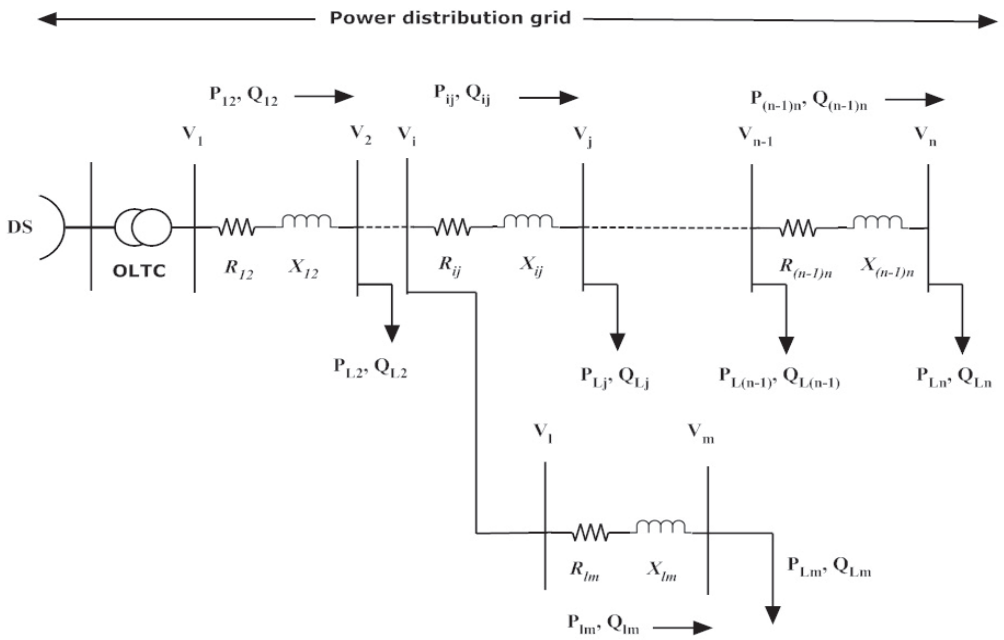

(a)

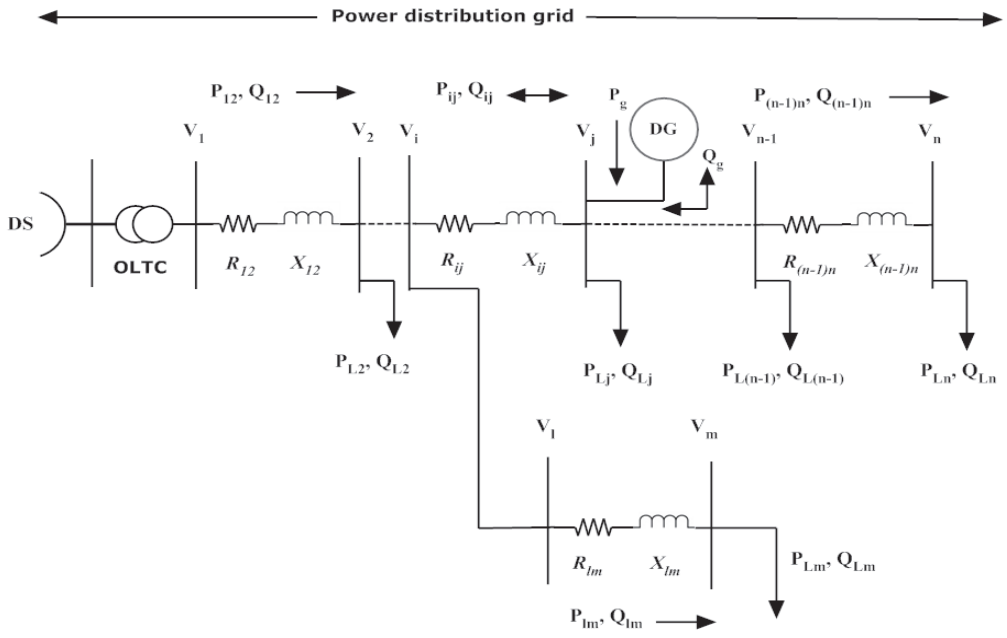

(b)

Figure 2.3. (a) Conventional n-bus distribution feeder, and (b) n-bus distribution feeder with DG

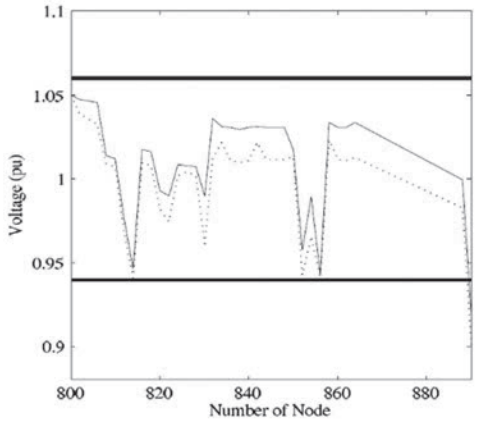

(a)

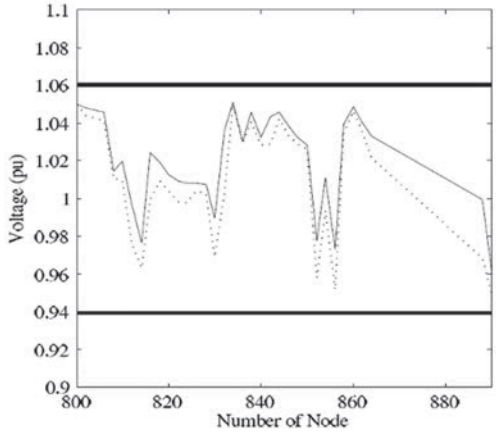

(b)

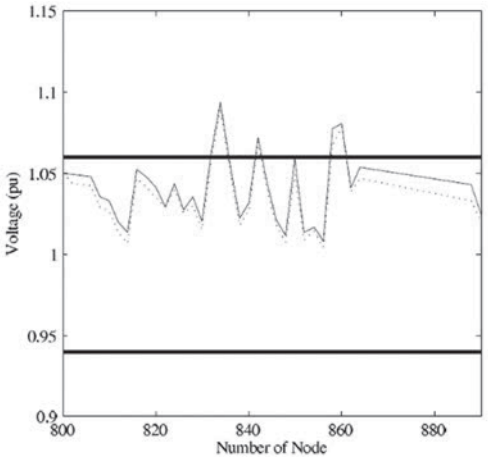

(c)

Figure 2.4. Simulation results of IEEE 34 Node Test Distribution System with 0% (a), 25% (b) and 50% (c) penetrations of DGs. The solid line represents the result obtained from PSS/E; the dotted line represents the result obtained from derived formula. Two bold solid lines indicate the permissible range of voltage variation [33].

Authors of [33] have simulated an IEEE 34 Node Test Distribution System in PSS/E (Power System Simulator for Engineering) for several percentages of DG integration and the simulation results are presented in Fig 2.4.

In order to minimize the adverse effects, distribution network operators prefer to accommodate the DGs at higher voltage level where the impact of the DGs on the voltage profile of distribution feeder is minimal. On the contrary, the developers of DGs prefer to accommodate the DGs at the lower voltage level to minimize the connection cost [67], [86]. The higher is the voltage level, the higher is the connection cost and vice versa. This conflict of interest can be settled through load flow studies.

2.4 Qualitative analysis of voltage control strategies

A significant amount of research [34-66] is going on to evaluate the optimum location where DGs should be accommodated and the amount that can be integrated into distribution network. To find the optimal size and location for DG, two kinds of approaches are followed [5]. They are,

1) To accommodate DGs with pre-specified capacities at best locations in the distribution network (DN).

2) To specify network location of interest guiding the DG capacity growth within network limits.

The first approach is done basically by using evolutionary computation. Such as particle swarm optimization (PSO) [34], genetic algorithm (GA) [35-38] and fuzzy logic based methods [39], [40]. The second approach is unable to solve continuous function of the capacity. For solving these, gradient search (GS) [41], linear programming [42] or optimal power flow (OPF) [43-48] methods are used. Both of these methods have their advantages and short comings. A hybrid method has been used in [49] and [50] (where combination of optimal power flow & genetic algorithms and combination of particle swarm optimization & optimal power flow have been used respectively). However, they have their limitations too. Some analytical approaches based on the sensitivity analysis have been done in [51-59] to optimally accommodate DGs in the distribution network. Several other different methods have been used for DG optimization and allocation in the distribution network [60-66].

In these methodologies, optimum condition is usually measured by improving the voltage profile. However, unpredictable events as wind gusts, solar radiation excursion or sudden overload may push the node voltages out of permissible limit resulting in cascaded events.

Active network management (ANM), a form of centralized strategy, is proposed as a key to integrate DG units in the distribution network as much as possible. It helps the distribution network operators (DNO) to utilize the maximum use of the existing network circuit by taking several management strategies similar to the transmission system [67], [68]. It provides real time monitoring, communication and control of the network by taking the advantages of generation dispatch, OLTC (on-load tap changing transformer), voltage regulators, shunt capacitors, reactive power compensation etc.

Another alternative approach proposed to control the voltage within acceptable limits is the intelligent distributed control of DG and other network parameters [69]. There are several different approaches for the distributed control. The effect of integration of DGs on the voltage profile mainly depends on the location of integration in distribution feeder. So, the distribution network configuration should be taken into account while designing the control strategy. Because, same amount of DGs, integrated in different parts of the network, make different impacts.

2.4.1 Traditional methods

In traditional distribution systems, the voltage regulation is being done usually by,

1) On load tap changer (OLTC).
2) Switched capacitors (SC).
3) Step voltage regulator (SVR).

On load tap changer is a tap changing autotransformer. It adjusts its taps automatically to adjust the voltage by measuring the feeder current at the substation end and estimating the voltage drop along the distribution feeder. Integration of DGs makes the power flow bi-directional and the voltage profile of the network depends on DGs location, injection of active power and power factor of DGs. So, the overall situation through the feeder is unpredictable and uncontrollable by OLTC [22]. Moreover, due to the naturally intermittent renewable DG's varying output and dynamic behavior of loads, the voltage variations occur so rapidly that traditional OLTCs or SCs cannot regulate as fast as they require. Another simple solution is to lower the set point of the OLTC at the substation so that the increased voltage at DG bus remains within upper permissible limit. However, this method is unable to ensure that the

voltages of all the network nodes will be within permissible limits throughout the feeder. In addition, other feeders might be connected to the same transformer. Then, this strategy can adversely affect other feeders. Currently, over traditional mechanical OLTCs, new solid state OLTCs are there which are performing better with lesser maintenance cost. They provide significant control capability such as coordinated control with communication [70]. Step voltage regulator (SVR) is also a tap changing automatic voltage regulator that locates along the feeder [71]. A switched capacitor (SC) is an electronic circuit element. It works by moving charges into and out of capacitors when switches are opened and closed.

2.4.2 Advanced methods

Several alternative methods with different controllable components were evaluated in several literatures to solve the voltage rise mitigation problem. A brief discussion about the controllable components is as follows:

a) **Generation curtailment during low demand:** Voltage along the distribution feeder is controlled by constraining the injection of active power from DG. However, it results in spilling of useful solar energy which is being highly discouraged by the PV panel owners.
b) **Reactive power control (VAR compensation) by reactive compensator:** To control the feeder voltage, reactive compensators absorb/ inject reactive power at the connection point of DG.
c) **Area based OLTC coordinated voltage control:** Voltage is managed within the permissible limits by continuously changing the tap changer setting at the substation.
d) **Inverters at DG sites:** Inverter interfaced DGs (PV and wind) can be utilized to control the reactive power absorption/ injection to regulate the voltage along the feeder.
e) **Consumption shifting and curtailing:** Shifting or curtailing the energy consumption by DGs can be another approach to regulate voltage.
f) **Energy storage:** By controlling the charging and discharging of the distributed battery energy storage system (BESS), the voltage fluctuation along the distribution network can be reduced.

Numerous alternative control solutions have been proposed in a number of literatures. Some common control structures were discussed in [72], [73], which are,

i) Centralized control.
ii) Decentralized autonomous control (Decentralized control).
iii) Decentralized coordinated control (Distributed control).

Now, these control structures are going to be discussed below:

2.4.2.1 Centralized control

In this approach, the control decisions on different issues are solely taken by the central coordinator body. Status information from different network components is provided to the central coordinator via communication channels. Then the network management system analyzes the data and coordinator takes the control decisions and sends control effort signals to remote equipment.

To regulate the voltage along the distribution feeder and keep it within permissible limit, the centralized controller requires having an accurate knowledge about the voltage at each network node. However, complete supervisory control and data acquisition (SCADA) system is hardly available in distribution networks. As for example: 11 kV distribution networks provide real time measurements only at primary substation. As a result, enough real time measurements throughout the feeders are seldom available. This shortages of real time measurements need to be compensated with estimated measurements. State estimation algorithms have been useful for long time designated for power transmission systems with lots of real time measurements [74]. However, transmission system state estimation algorithms cannot be directly used for the distribution network system for above reasons.

- **Distribution system state estimation**

A significant amount of researches has been done on the transmission system state estimation (TSSE) and distribution system state estimation (DSSE) [74-84]. According to the researches, lack of real time measurements in the distribution network needs to be compensated with estimated pseudo-measurements. DSSE provides methodology to estimate the voltage at each node of the distribution network from available real time measurements and information. For the estimation, the estimator needs the following information,

1) Distribution network topology.
2) Impedance data.
3) Customer's load information.
4) Few real time measurements.

A functional block diagram for the estimator and controller is given below in Fig 2.5.

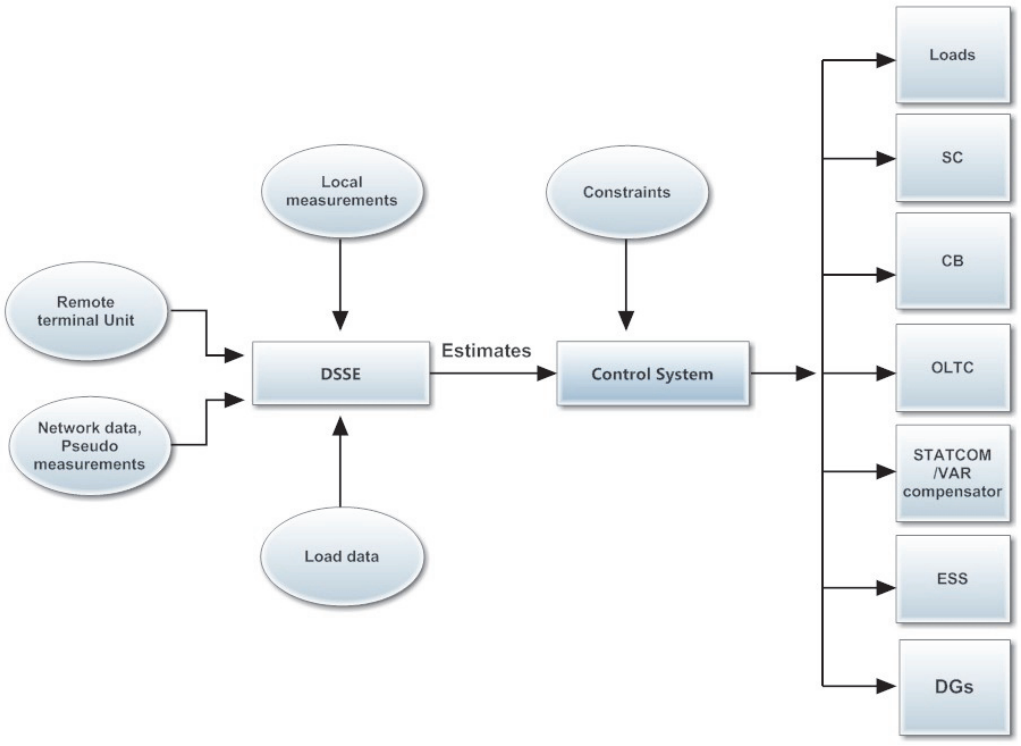

Figure 2.5. A functional block diagram of distribution management system controller (DMSC)

Significant difference between the real time measured value and the estimated pseudo value can cause significant instability within the system. So, the critical points to measure the voltage should be carefully and strategically chosen. Strategically located measurements at key network nodes (such as at point of common coupling of DG or at a crucial network node where significant variation of voltage is expected) can supple the pseudo measurements. A series of load flow analysis might help to choose the critical points which will result in minimizing the variance on the unmeasured nodes.

We can minimize the error between the measurements and calculated values from the following equations [73].

$$\min J(x_1, x_2, \dots\dots\dots x_N) = \sum_{m=1}^{M} \frac{[z_m - f_m(x_1, x_2, \dots\dots\dots x_N)]^2}{{\sigma_m}^2} \quad (2.9)$$

$$x_{n+1} = x_n + G(x_n)\, H^T(x_n) W\, [z - f(x_n)] \quad (2.10)$$

$$G(x_n) = [\, H^T(x_n) W H(x_n)]^{-1} \quad (2.11)$$

Where,

$x =$ State variables.

$Z_m =$ Measurements.

$f_m(x_1, x_2, \ldots\ldots\ldots x_N) =$ Measurement values calculated from state variables.

σ_m = Standard deviation.

$H =$ Jacobean of the measurement set.

$W =$ Diagonal matrix whose elements are the inverse of the measurement variance.

$G =$ Variance of the estimated quantities.

The solution of (2.9) is the set of state variables that minimizes the difference between measurements and calculated values. The minimization leads to iterative process where (2.10) is evaluated with the most recent values of state variables until convergence condition is met. With more integration of DGs, the network becomes more complex and interconnected. A distribution system state estimation (DSSE) algorithm that can be applicable for both radial and meshed networks is required.

▪ Review of control methodologies

A centralized operation based active network management (ANM) has been discussed in [67]. In this article, three alternative approaches are evaluated to solve the voltage rise mitigation problem:

1) Generation curtailment during low demand.
2) Reactive power control by reactive compensator.
3) Area based OLTC coordinated voltage control.

The performance of different control strategies has been relatively examined and evaluated. Revenue obtained from the coordinated OLTC control was found highest. However, the coordinated control scheme was not explained. For a higher penetration of DG, the annual generation curtailment was far lesser. Proposed control strategies likely increased the amount of integrated DGs. Similar to transmission networks, centralized distribution system controllers have been discussed in [68] and [73]. State estimation method has been used to assess the voltage at each network locations and a wide area voltage control has been done by reactive power compensation and DG curtailment. OPF and cost benefit analysis (CBA) have been performed after that to evaluate the performance of voltage control. Capital costs, operation, maintenance and repair costs, AM schemes costs, savings from economies of scale, revenues

from energy sales and environmental incentives were considered for cost benefit analysis (CBA). Distribution System State Estimation and active control of OLTC were performed in [85] and [86] to regulate the voltage. Variation of voltages has been done at substation for controlling the voltage through the feeder. A control algorithm has been proposed to control (lower or rise) the automatic voltage control (AVC) target in such a way that the maximum and minimum node voltages along the feeder stay inside the permissible range. Similar to the control strategy of transmission system, coordinated voltage and reactive power control scheme have been followed in [87-89]. Alike [89], an objective function to minimize active power losses through distribution network has been considered in [90-94]. A multi-objective optimal voltage regulation algorithm is presented in [90]. In this chapter, control devices (like load ratio transformer, static VAR compensator (SVC), Shunt capacitors and reactors) have been operated in a coordinated manner to minimize system losses and voltage deviation at each bus. With an active control over OLTC and reactive power support, voltage has been controlled in [91], [92]. In [93], voltage regulation has been performed by controlling network parameters and power factor at which DG operates over several different periods in the day with different load levels. [95] focuses purely on reactive power control with an objective to minimize voltage deviation at each bus from specified reference voltage like [96] and does not utilize control equipment like OLTC tap settings, shunt capacitors similar to [69]. Voltage regulation was done in [96] by varying the settings of OLTC & load ratio control transformer and by utilizing shunt capacitors & SVC. A combined constant power factor control and variable reactive power control has been applied with an objective function to maximize the DG real power capacity in [69]. Comparison between centralized and decentralized control by some case studies has been done in [97]. In [98], control action has been done by utilizing OLTC and SVR. An objective function to maximize the magnitude of the lowest bus voltage has been considered in [99]. The aim was to keep the voltage at each bus within specified limits and the power supplied by each DG within its limits. [100] and [101] analyzed the effect of line drop compensation in distribution network. Line drop compensation is imperfect when DGs are accommodated in the distribution network. This is because current measured at the OLTC terminals does not include the current supplied by the DGs. The proposed methodology in these articles mitigates voltage rise due to integration of DGs. However, the method does not utilize any voltage regulation equipment other than OLTCs. With minimum DG reactive support, an optimal volt/ VAR control technique has been proposed for voltage regulation in [102]. However, minimizations of DG, active power injection curtailment and coordination of voltage regulation devices have not been considered. In [103], to reduce the optimization complexity,

the distribution network has been divided into sub-networks but again coordination among OLTCs is not considered. An algorithm has been proposed in [104] to minimize system losses and tap operations in radial distribution network by coordinating OLTCs and static VAR compensators (SVC). In [105], decoupled active/ reactive power control methodology through feedback linearization has been proposed for voltage regulation. However, this methodology has not coordinated voltage regulation devices. A one-day-ahead forecasting of load and renewable resources has been used to utilize the PV reactive power in [106]. The tap operations are minimized in this approach but active power injection curtailment is not considered during limited reactive power support. There can also be forecasting errors due to uncertain intermittent nature of renewable sources. The author of [107] proposed a methodology for voltage regulation by utilizing reactive power produced by PV-inverters. An algorithm operating in continuous time domain has been adopted to solve a constrained dynamic optimization problem to minimize voltage deviation from reference value along the feeder. However, supplementary injection of reactive power increases inverter losses which reduces PV income. An optimal coordinated voltage regulation method in distribution network with vehicle-to-grid reactive power support (V2GQ) strategy has been proposed in [108]. A reactive market based on uniform price auction has been proposed by [109]. A control strategy of distributed battery energy storage system (BESS) utilizing OLTC, SVR and other traditional regulators has been proposed in [110] to reduce tap changer operation, to shave DN's peak load and to reduce power losses.

Centralized control methodology can provide the best performance possible, especially for small scale systems and for those networks where power flow is unidirectional. However, this methodology may become unpopular in future distribution networks for several reasons which are as follows:

- These centralized control approaches require significant investments in communication assets and sensors. For high penetration of DGs into large interconnected and complex distribution networks, the implementation of centralized approach is not feasible.
- A large number of small scale DGs need to be controlled.
- Increased amount of uncertainties (due to intermittent renewable sources, faults, electric vehicles, storage units, dynamic loads, restoration, reconfiguration etc.).
- It causes large computational burden and numerical stability issues as it requires power flow solution at each time step.

- This methodology does not satisfy the effort to achieve '*plug and play*' property in which DGs can be connected to the distribution system with minimum revisions on feeder control and protection.

2.4.2.2 Decentralized autonomous control

In decentralised autonomous voltage control methodology, distribution network voltage regulation devices operate in response to the localised issues surrounding them. The controllers receive and analyse information from sensors surrounding them and perform necessary control effort on their respective locality [111].

▪ Review of control methodologies

In [112], an intelligent decentralized hybrid voltage-power factor control (switching between the voltage control mode and power factor control mode) and a fuzzy logic based control strategy have been proposed and discussed to solve the voltage rise problem along the distribution feeder. As the distribution network is rapidly expanding and being complicated day-by-day, distribution network operators would require incorporating more voltage control devices. However, the discussed hybrid voltage/ power factor control can only be applied when no other voltage control device is near in the vicinity. On the other hand, to keep the power factor constant at the injection point, the generator settings need to vary with the load, which needs constant monitoring of generation and load. In [113], a methodology has been suggested to utilize voltage source converters (VSC) with DGs to control the voltage by controlling the reactive power independent of the active power. Uniformly distributed generators and loads have been considered which is seldom practical. Most distributed energy resources (DGs) are preferred to operate at unity or constant power factor. Such as, PVs are required to operate at unity power factor to provide maximum power [114]. Sizes of DGs are considered small to put effect on the voltage regulation of the distribution feeder. On the other hand, in large interconnected systems, the inverter based distributed generators with voltage control capability compete with one another to control the voltage and result in hunting among the generating units. Sometimes, they interfere with distribution network system operators' control (On load tap changing transformer operation) too and pose the possibility of undesired islanding [115]. For this reason, several countries do not allow voltage regulation by inverter interfaced distributed generators to prevent the risk of unwanted islanding.

A reactive power control approach has been made in [116] to turn large amount of DG connection into a non-perturbing power supply system along the distribution feeder. In this chapter, instead of controlling the bus voltage, an approach has been made to ensure that generators' active power injection alone does not occur significant voltage rise. Effectiveness and adequacy were analyzed and effect on DNO control was examined. Q* control, Constant leading power factor and constant lagging power factor approaches were examined for voltage rise mitigation for two different cases (high load and no load). It was found that, Q* control approach regulates the voltage rise problem for both the load situations and in between but with significantly increased tap changing efforts. It may allow to accommodate more DGs but in traditional fit and forget manner. Also, for a weak distribution network, if the DGs are operated in power factor control mode, it has an adverse effect on the generator terminal bus voltage. [117] suggested a decentralized line drop compensation method using OLTCs to mitigate voltage deviation. It also suggests that voltage control with DGs is possible when DG technology allows dispatching. [118] proposed an improved strategy from [112] to control the voltage. It suggested utilizing generation curtailment strategy when hybrid voltage-power factor control is not effective. It prevented excessive voltage rise in a cost effective manner. [119] proposed a method that optimized the existing network infrastructure. Tap settings of the OLTC were reduced in such a way that it can accommodate the raised voltage within the permissible limit. However, traditional OLTCs are not fast enough during the situations of sudden dynamics as they require some physical adjustments to make. Also, the amount of tap changes should be kept within limited value. The DG operating power factor was varied to reduce the distribution network dependency on transmission network for reactive power supply at any given period in [120]. [121] examined different operation modes (constant voltage, constant current and constant power factor) of DG and found that the losses are higher when DGs are operated at constant power factor mode. [122] suggested a decentralized control method where the network was divided into groups of adjacent buses. DGs monitor voltage within their respective groups and vary the reactive power utilizing inverters to adjust their terminal voltages.

Currently, inverter interfaced DGs are not permitted to control voltage locally according to 1547 IEEE Standard [123]. However, IEEE P1547.8 has developed practice for establishing methods for expanded use of 1547 [124]. Researchers are working on the situations when local voltage control by inverter interfaced DGs should be allowed. Moreover, inverter interfaced DGs can deliver fast reactive power support. As a continuation, [125-134] have showed that the reactive power capability of inverter interfaced distributed generators can improve

distribution network systems operation. They mainly focused on the volt/ VAR control strategy of inverter interfaced DGs. The voltage control objective is accomplished with a piecewise linear droop characteristic in [127-131], which determines the reactive power injection as a function of the voltage magnitude at the PV inverter terminals. [135-139] showed how distributed control of reactive power (part of volt/ VAR control strategy) could serve to regulate voltage and minimize resistive losses in a distribution circuit. [140] and [141] suggested that the integration of MPPT (maximum power point tracker) with real and reactive power control capability can improve the overall efficiency of the system. [142-147] suggested local linear controllers to improve voltage quality but they need high bandwidth communication with distribution network system controllers. [148] suggested a local linear controller that substitutes reactive power for real power for mitigating voltage deviations. This controller does not require high bandwidth communication like [142-147] but its performance was not assessed in larger interconnected distribution systems with multiple DGs. [149] showed that DGs have the ability to provide flexibilities on curtailing or shifting their energy consumption for mitigating voltage fluctuations.

Being autonomous is one of the main advantages of decentralized local control. Controllers receive information of their local network status, analyze it, select an appropriate control effort and then implement that effort. As a result, decentralized autonomous controllers have the capability and flexibility to respond to load fluctuations. There are some drawbacks too. They are as follows:

- Voltage control devices undergo high stress.
- Local voltage controllers compete with one another and interfere one another's operations.
- Power losses through distribution feeder are increased.
- DGs energy capture is not maximized.

2.4.2.3 Decentralized coordinated control

In this control methodology, DGs communicate with one another to recognize the local states of whole distribution system. They exchange information of their individual states, control actions, plans and requests to coordinate with one another for achieving a global approach to mitigate the voltage rise issue in an efficient way.

Voltage control devices should coordinate with one another for proper voltage regulation. With proper coordination, voltage deviation issue can be tackled efficiently. As a result, peer-

to-peer, multiagent, coordinated control methodology has been motivated by operators. Multi-agent system (MAS) has been introduced recently as a potential technology for voltage regulation applications. Some basic definitions of MAS concept and its applications in power system have been discussed in [150]. They are briefly described below:

- **Agent**

An agent is a software (or hardware) entity that is located in some environment and capable of reacting autonomously to changes in that environment. It monitors its environment either physically through sensors or collecting data from other resources.

- **Intelligent agent**

Intelligent agents show some intelligent features and flexible autonomy while taking decisions for reactions to the changes in the environment. They are:

- Intelligent agents can react to changes in a timely fashion based on the changes in the environment.
- Intelligent agents can set their own goals and can alter over time.
- Intelligent agents can interact with other intelligent agents. They not only exchange data but also negotiate and solve complex interactive problems.

- **Multi-agent system**

Combination of more than one *intelligent agent* and *agent* within a cooperative system is called multi-agent system (MAS). MAS is capable of dynamic re-organization of its overall function. This decision is taken by intelligent agents based on the signals, information and data from the environment on an ongoing basis. A functional diagram of the active network with MAS control in radial distribution network is given below in Figure 2.6.

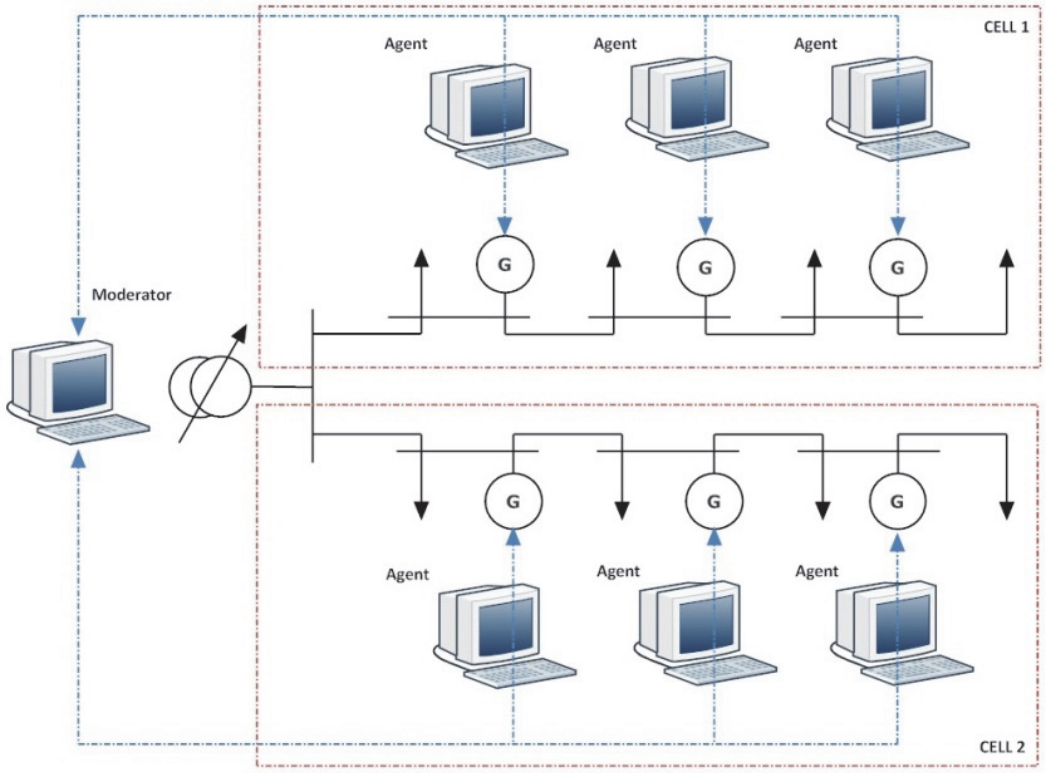

Figure 2.6. An active network with MAS control in radial distribution network divided into subnetworks (cells).

▪ Review of Control methodologies

An active network needs to be constructed with the support of MAS. The radial distribution network is divided into several sub networks (feeders). For each feeder a local control area (cell) needs to be established. Within the local control area (Cell), each controllable component (such as, controllable generators, loads etc.) will have an agent that can operate autonomously with local goals or cooperate with other agents to achieve global goals. Intelligent agents can communicate with one another in two approaches [151].

1) Phone-based communication.
2) Internet-based communication.

A multi-agent optimal reactive power dispatching strategy was suggested in [151] for voltage rise mitigation in a single feeder. This study can be advanced by considering voltage regulators and shunt capacitors in operation and providing a proper simulation model. [152-157] suggested multi-agent frame works for proper voltage control in distribution network.

However, a well-defined control structure and operation mechanism could be presented. This study can be upgraded by developing proper communication and coordination protocols among voltage controllers. [158] considered these issues that were not well discussed in [152-157]. A methodology has been proposed to achieve decentralized coordination among distributed systems in [159], [160] via multi-agent consensus theory. A secondary voltage control strategy has been discussed in [161] using multi-agent system theory but it focused on transmission systems. [162-164] suggested a strategy where each network node can request for reactive power support in the situations of voltage deviation throughout the feeder. [165] suggested a methodology where each node of the distribution network observes the deviation of its local voltage from the nominal value and voltage deviation state is initialized. Then, all the nodes share information and inverters coordinate to control the voltage jointly.

To implement multi-agent system, several things need to be considered. They are: data standardization, intelligent agents design, platforms and communication languages. Foundation for Intelligent Physical Agents (FIPA) is the body that develops agent's standards and sets agent communication languages. Java Agent Development Framework (JADE) is a popular platform for multi-agent system in power engineering applications. As JADE acts as a middleware for developing distributed applications, its scalability needs to be evaluated. Three important variables need to be considered while evaluating scalability of JADE. They are, 1) the number of agents in a platform, 2) the number of messages for a single agent and 3) the number of simultaneous conversations a single agent gets involved in [166]. JADE tries to support as large system as possible, but in case of large-scale implementation, the processing load tends to increase [167] as agents are usually programmed with interpreted language and need to keep rigorous interoperability standards in check which may cause data processing overheads.

2.5 Conclusion

Voltage regulation challenge along the distribution feeder has attracted the rapidly growing attention of industries and researchers and this issue will be more significant in near future due to increased integration of renewable DGs in the lower/ medium voltage network. In this chapter, we presented how the operation, protection and stability of the distribution network gets impact due to increased accommodation of renewable DGs. Traditional control devices are not fast enough to regulate the voltage when large amount of intermittent renewable DGs

are connected. Development of advanced control strategy is the fundamental key to penetrate large amount of intermittent renewable DGs without putting significant adverse impact on distribution network operation and stability. Many researches are going on to establish better control over the feeder voltage when large amount of renewable DGs are accommodated. Utilization of energy storage devices is also a promising strategy to mitigate these issues and to ensure a sustainable power supply. Energy storage devices can support the grid during high peak demand and they can be utilized to shift consumer loads from peak time to off-peak time [168].

Qualitative analysis was performed in this chapter for all kinds of voltage control approaches. Researchers have used several control devices like OLTCS, SVRs, SCs, STATCOM/ FACTs devices, PWM inverters, energy storage devices etc. and have utilized several control methodologies. This chapter also summarized recent developments in control approaches like centralized control approach, decentralized autonomous control approach and decentralized coordinated control approach. These control approaches have their own advantages and disadvantages, which have been discussed in previous sections. Centralized control approach is very popular for small networks where power flow is unidirectional. As power system is expanding day-by-day and power flow is being bi-directional nowadays due to increased accommodation of DGs, this approach is losing its popularity. On the other hand, decentralized autonomous control approach shows the flexibility to respond to load fluctuations due to its autonomous characteristics. However, it has got some disadvantages too like high stress, operational interference, increased power loss etc. Decentralized coordinated control approach is gaining interest of researchers nowadays because of its coordination capability among control devices which helps to achieve a global goal. In addition, as I have reviewed, voltage regulation of the modern distribution network is a challenging research area and still under development. Researches are going on and significant efforts are still necessary to mitigate this issue.

References:

[1] Masters, C. L. (2002). Voltage rise: the big issue when connecting embedded generation to long 11 kV overhead lines. *Power engineering journal*, *16*(1), 5-12.

[2] Quezada, V. M., Abbad, J. R., & Roman, T. G. S. (2006). Assessment of energy distribution losses for increasing penetration of distributed generation. *IEEE Transactions on power systems*, *21*(2), 533-540.

[3] Lopes, J. P., Hatziargyriou, N., Mutale, J., Djapic, P., & Jenkins, N. (2007). Integrating distributed generation into electric power systems: A review of drivers, challenges and opportunities. *Electric power systems research*, *77*(9), 1189-1203.

[4] Zhu, Y., & Tomsovic, K. (2002). Adaptive power flow method for distribution systems with dispersed generation. *IEEE Transactions on Power Delivery*, *17*(3), 822-827.

[5] Mahmud, M. A., Hossain, M. J., & Pota, H. R. (2014). Voltage variation on distribution networks with distributed generation: Worst case scenario. *IEEE Systems Journal*, *8*(4), 1096-1103.

[6] Chiradeja, P., & Ramakumar, R. (2004). An approach to quantify the technical benefits of distributed generation. *IEEE Transactions on energy conversion*, *19*(4), 764-773.

[7] Tsikalakis, A. G., & Hatziargyriou, N. D. (2007). Environmental benefits of distributed generation with and without emissions trading. *Energy Policy*, *35*(6), 3395-3409.

[8] Gil, H. A., & Joos, G. (2008). Models for quantifying the economic benefits of distributed generation. *IEEE Transactions on Power Systems*, *23*(2), 327-335.

[9] Zahedi, A. (2011). Maximizing solar PV energy penetration using energy storage technology. *Renewable and Sustainable Energy Reviews*, *15*(1), 866-870.

[10] Zahedi, A. (2010). A review on feed-in tariff in Australia, what it is now and what it should be. *Renewable and Sustainable Energy Reviews*, *14*(9), 3252-3255.

[11] Jiayi, H., Chuanwen, J., & Rong, X. (2008). A review on distributed energy resources and MicroGrid. *Renewable and Sustainable Energy Reviews*, *12*(9), 2472-2483.

[12] Dragičević, T., Lu, X., Vasquez, J. C., & Guerrero, J. M. (2016). DC microgrids—Part I: A review of control strategies and stabilization techniques. *IEEE Transactions on power electronics*, *31*(7), 4876-4891.

[13] Pathak, A. K., Sharma, M. P., & Bundele, M. (2015). A critical review of voltage and reactive power management of wind farms. *Renewable and Sustainable Energy Reviews*, *51*, 460-471.

[14] Kow, K. W., Wong, Y. W., Rajkumar, R. K., & Rajkumar, R. K. (2016). A review on performance of artificial intelligence and conventional method in mitigating PV grid-tied related power quality events. *Renewable and Sustainable Energy Reviews*, *56*, 334-346.

[15] Eltigani, D., & Masri, S. (2015). Challenges of integrating renewable energy sources to smart grids: a review. *Renewable and Sustainable Energy Reviews*, *52*, 770-780.

[16] El-Khattam, W., & Salama, M. M. A. (2002, March). Impact of distributed generation on voltage profile in deregulated distribution system. In *Proceedings of the Power Systems 2002 Conference, Impact of Distributed Generation, Clemson, SC, USA* (pp. 13-15).

[17] McDermott, T. E., & Dugan, R. C. (2002). Distributed generation impact on reliability and power quality indices. In *Rural Electric Power Conference, 2002. 2002 IEEE* (pp. D3-1). IEEE.

[18] Khadem, S. K., Basu, M., & Conlon, M. (2010). Power quality in grid connected renewable energy systems: Role of custom power devices.

[19] Chen, Z., & Kong, W. (2007, January). Protection Coordination Based on a Multi-agent for Distribution Power System with Distribution Generation Units. In *International Workshop on Next Generation Regional Energy System Development*.

[20] El-Khattam, W., & Sidhu, T. S. (2009). Resolving the impact of distributed renewable generation on directional overcurrent relay coordination: a case study. *IET Renewable power generation*, *3*(4), 415-425.

[21] de Britto, T. M., Morais, D. R., Marin, M. A., Rolim, J. G., Zurn, H. H., & Buendgens, R. F. (2004, November). Distributed generation impacts on the coordination of protection systems in distribution networks. In *Transmission and Distribution Conference and Exposition: Latin America, 2004 IEEE/PES* (pp. 623-628). IEEE.

[22] El-Markabi, I. M. S. (2004). Control and Protection for Distribution Networks with Distributed Generators.

[23] Ruiz-Romero, S., Colmenar-Santos, A., Mur-Pérez, F., & López-Rey, Á. (2014). Integration of distributed generation in the power distribution network: The need for smart grid control systems, communication and equipment for a smart city—Use cases. *Renewable and sustainable energy reviews*, *38*, 223-234.

[24] Gross, A., Bogensperger, J., & Thyr, D. (1997). Impacts of large scale photovoltaic systems on the low voltage network. *Solar Energy*, *59*(4), 143-149.

[25] Begovic, M., Pregelj, A., Rohatgi, A., & Novosel, D. (2001, January). Impact of renewable distributed generation on power systems. In *System Sciences, 2001. Proceedings of the 34th Annual Hawaii International Conference on* (pp. 654-663). IEEE.

[26] Hernández, J. C., Medina, A., & Jurado, F. (2008). Impact comparison of PV system integration into rural and urban feeders. *Energy conversion and management*, *49*(6), 1747-1765.

[27] González, C., Ramirez, R., Villafafila, R., Sumper, A., Boix, O., & Chindris, M. (2007, October). Assess the impact of photovoltaic generation systems on low-voltage network: software analysis tool development. In *Electrical Power Quality and Utilisation, 2007. EPQU 2007. 9th International Conference on* (pp. 1-6). IEEE.

[28] Voltage control in distribution grids with Distributed Generation(I). Annals of Mechanics and Electricity. ICAI Engineers Association (Catholic Institute of Arts and Industries) 13th ICAI April

2012. (Revista Anales de la asociación de ingenieros del ICAI). ⟨http://www.revista-anales.es/web/n_13/seccion_3.html⟩; 13 April 2012 [accessed16.02.13].

[29] Zahedi, A. (2011). A review of drivers, benefits, and challenges in integrating renewable energy sources into electricity grid. *Renewable and Sustainable Energy Reviews*, *15*(9), 4775-4779.

[30] Dugan, R. C., McGranaghan, M. F., & Beaty, H. W. (1996). Electrical power systems quality. *New York, NY: McGraw-Hill,| c1996.*

[31] Doumbia, M. L., & Agbossou, K. (2007, October). Voltage variation analysis in interconnected electrical network-distributed generation. In *Electrical Power Conference, 2007. EPC 2007. IEEE Canada* (pp. 525-530). IEEE.

[32] Scott, N. C., Atkinson, D. J., & Morrell, J. E. (2002). Use of load control to regulate voltage on distribution networks with embedded generation. *IEEE Transactions on Power Systems*, *17*(2), 510-515.

[33] Mahmud, M. A., Hossain, M. J., & Pota, H. R. (2011, July). Worst case scenario for large distribution networks with distributed generation. In *Power and Energy Society General Meeting, 2011 IEEE* (pp. 1-7). IEEE.

[34] El-Zonkoly, A. M. (2011). Optimal placement of multi-distributed generation units including different load models using particle swarm optimisation. *IET generation, transmission & distribution*, *5*(7), 760-771.

[35] Celli, G., Ghiani, E., Mocci, S., & Pilo, F. (2005). A multiobjective evolutionary algorithm for the sizing and siting of distributed generation. *IEEE Transactions on power systems*, *20*(2), 750-757.

[36] Ochoa, L. F., Padilha-Feltrin, A., & Harrison, G. P. (2008). Time-series-based maximization of distributed wind power generation integration. *IEEE Transactions on Energy Conversion*, *23*(3), 968-974.

[37] Celli, G., & Pilo, F. (2001). Optimal distributed generation allocation in MV distribution networks. In *Power Industry Computer Applications, 2001. PICA 2001. Innovative Computing for Power-Electric Energy Meets the Market. 22nd IEEE Power Engineering Society International Conference on* (pp. 81-86). IEEE.

[38] de Queiroz, L. M., & Lyra, C. (2006, July). A genetic approach for loss reduction in power distribution systems under variable demands. In *Evolutionary Computation, 2006. CEC 2006. IEEE Congress on* (pp. 2691-2698). IEEE.

[39] Ameli, M. T., Shokri, V., & Shokri, S. (2010, October). Using Fuzzy Logic & Full Search for Distributed generation allocation to reduce losses and improve voltage profile. In *Computer Information Systems and Industrial Management Applications (CISIM), 2010 International Conference on* (pp. 626-630). IEEE.

[40] Savier, J. S., & Das, D. (2007). Impact of network reconfiguration on loss allocation of radial distribution systems. *IEEE Transactions on Power Delivery*, *22*(4), 2473-2480.

[41] Rau, N. S., & Wan, Y. H. (1994). Optimum location of resources in distributed planning. *IEEE Transactions on Power Systems*, *9*(4), 2014-2020.

[42] Keane, A., & O'Malley, M. (2005). Optimal allocation of embedded generation on distribution networks. *IEEE Transactions on Power Systems*, *20*(3), 1640-1646.

[43] Dent, C. J., Ochoa, L. F., Harrison, G. P., & Bialek, J. W. (2010). Efficient secure AC OPF for network generation capacity assessment. *IEEE Transactions on Power Systems*, *25*(1), 575-583.

[44] Vovos, P. N., Harrison, G. P., Wallace, A. R., & Bialek, J. W. (2005). Optimal power flow as a tool for fault level-constrained network capacity analysis. *IEEE Transactions on Power Systems*, *20*(2), 734-741.

[45] Vovos, P. N., & Bialek, J. W. (2005). Direct incorporation of fault level constraints in optimal power flow as a tool for network capacity analysis. *IEEE Transactions on Power Systems*, *20*(4), 2125-2134.

[46] Ochoa, L. F., Dent, C. J., & Harrison, G. P. (2010). Distribution network capacity assessment: Variable DG and active networks. *IEEE Transactions on Power Systems*, *25*(1), 87-95.

[47] Harrison, G. P., & Wallace, A. R. (2005). Optimal power flow evaluation of distribution network capacity for the connection of distributed generation. *IEE Proceedings-Generation, Transmission and Distribution*, *152*(1), 115-122.

[48] Dent, C. J., Ochoa, L. F., & Harrison, G. P. (2010). Network distributed generation capacity analysis using OPF with voltage step constraints. *IEEE Transactions on Power systems*, *25*(1), 296-304.

[49] Harrison, G. P., Piccolo, A., Siano, P., & Wallace, A. R. (2008). Hybrid GA and OPF evaluation of network capacity for distributed generation connections. *Electric Power Systems Research*, *78*(3), 392-398.

[50] Gomez-Gonzalez, M., López, A., & Jurado, F. (2012). Optimization of distributed generation systems using a new discrete PSO and OPF. *Electric Power Systems Research*, *84*(1), 174-180.

[51] Wang, C., & Nehrir, M. H. (2004). Analytical approaches for optimal placement of distributed generation sources in power systems. *IEEE Transactions on Power systems*, *19*(4), 2068-2076.

[52] Acharya, N., Mahat, P., & Mithulananthan, N. (2006). An analytical approach for DG allocation in primary distribution network. *International Journal of Electrical Power & Energy Systems*, *28*(10), 669-678.

[53] Gözel, T., & Hocaoglu, M. H. (2009). An analytical method for the sizing and siting of distributed generators in radial systems. *Electric Power Systems Research*, *79*(6), 912-918.

[54] Hung, D. Q., Mithulananthan, N., & Bansal, R. C. (2010). Analytical expressions for DG allocation in primary distribution networks. *IEEE Transactions on energy conversion*, *25*(3), 814-820.

[55] Hung, D. Q., & Mithulananthan, N. (2013). Multiple distributed generator placement in primary distribution networks for loss reduction. *IEEE Transactions on industrial electronics*, *60*(4), 1700-1708.

[56] Willis, H. L. (2000). Analytical methods and rules of thumb for modeling DG-distribution interaction. In *Power Engineering Society Summer Meeting, 2000. IEEE* (Vol. 3, pp. 1643-1644). IEEE.

[57] Le, A. D., Kashem, M. A., Negnevitsky, M., & Ledwich, G. (2005, November). Maximising voltage support in distribution systems by distributed generation. In *TENCON 2005 2005 IEEE Region 10* (pp. 1-6). IEEE.

[58] Shivarudraswamy, R., & Gaonkar, D. N. (2011). Coordinated voltage control using multiple regulators in distribution system with distributed generators. *International journal of World Academy of Science, Engineering and Technology*, *74*, 574-578.

[59] Gopiya-Naik, S., Khatod, D. K., & Sharma, M. P. (2012). Optimal allocation of distributed generation in distribution system for loss reduction. In *Proc. IACSIT Coimbatore Conferences* (Vol. 28, pp. 42-46).

[60] Lantharthong, T., & Rugthaicharoenchep, N. (2013). Network reconfiguration for load balancing in distribution system with distributed generation and capacitor placement. *Journal of Energy and Power Engineering*, *7*(8).

[61] Musa, H., & Adamu, S. S. (2012). PSO based DG sizing for improvement of voltage stability index in radial distribution systems. In *Proceedings of the IASTED International Conference Power and Energy Systems and Applications* (pp. 175-180).

[62] Sharma, M., & Vittal, K. P. (2010). A heuristic approach to distributed generation source allocation for electrical power distribution systems. *Iranian Journal of Electrical and Electronic Engineering*, *6*(4), 224-231.

[63] Rao, P. R., & Raju, S. S. (2010). Voltage regulator placement in radial distribution system using plant growth simulation algorithm. *International Journal of Engineering, Science and Technology*, *2*(6).

[64] Wu, C. N., & Lv, X. Q. (2012). Analysis on power flow of distribution network with DGs. In *Network Computing and Information Security* (pp. 323-331). Springer, Berlin, Heidelberg.

[65] Kumar, I. S., & Navuri, P. K. (2012). An efficient method for optimal placement and sizing of multiple distributed generators in a radial distribution systems. *Distributed Generation & Alternative Energy Journal*, *27*(3), 52-71.

[66] Abu-Mouti, F. S., & El-Hawary, M. E. (2011). Optimal distributed generation allocation and sizing in distribution systems via artificial bee colony algorithm. *IEEE transactions on power delivery*, *26*(4), 2090-2101.

[67] Liew, S. N., & Strbac, G. (2002). Maximising penetration of wind generation in existing distribution networks. *IEE Proceedings-Generation, Transmission and Distribution*, *149*(3), 256-262.

[68] Bopp, T., Shafiu, A., Cobelo, I., Chilvers, I., Jenkins, N., Strbac, G., Li, H. & Crossley, P. (2003, May). Commercial and technical integration of distributed generation into distribution networks. In *Proc. CIRED, 17th Int. Conf. Electricity Distribution*.

[69] Vovos, P. N., Kiprakis, A. E., Wallace, A. R., & Harrison, G. P. (2007). Centralized and distributed voltage control: Impact on distributed generation penetration. *IEEE Transactions on Power Systems*, *22*(1), 476-483.

[70] Echavarría, R., Claudio, A., & Cotorogea, M. (2007). Analysis, design, and implementation of a fast on-load tap changing regulator. *IEEE transactions on power electronics*, *22*(2), 527-534.

[71] Liu, Y., Bebic, J., Kroposki, B., De Bedout, J., & Ren, W. (2008, November). Distribution system voltage performance analysis for high-penetration PV. In *Energy 2030 Conference, 2008. ENERGY 2008. IEEE* (pp. 1-8). IEEE.

[72] Han, X., Kosek, A. M., Bondy, D. E. M., Bindner, H. W., You, S., Tackie, D. V., ... & Thordarson, F. (2014, October). Assessment of distribution grid voltage control strategies in view of deployment. In *Intelligent Energy Systems (IWIES), 2014 IEEE International Workshop on* (pp. 46-51). IEEE.

[73] Shafiu, A., Bopp, T., Chilvers, I., & Strbac, G. (2004, June). Active management and protection of distribution networks with distributed generation. In *Power Engineering Society General Meeting, 2004. IEEE* (pp. 1098-1103). IEEE.

[74] Wood, A. J., & Wollenberg, B. F. (2012). *Power generation, operation, and control*. John Wiley & Sons.

[75] Wu, F. F. (1990). Power system state estimation: a survey. *International Journal of Electrical Power & Energy Systems*, *12*(2), 80-87.

[76] Lu, C. N., Teng, J. H., & Liu, W. H. (1995). Distribution system state estimation. *IEEE Transactions on Power Systems*, *10*(1), 229-240.

[77] Baran, M. E., & Kelley, A. W. (1994). State estimation for real-time monitoring of distribution systems. *IEEE Transactions on Power Systems*, *9*(3), 1601-1609.

[78] Li, K. (1996). State estimation for power distribution system and measurement impacts. *IEEE Transactions on Power Systems*, *11*(2), 911-916.

[79] Monticelli, A. (1999). *State estimation in electric power systems: a generalized approach* (Vol. 507). Springer Science & Business Media.

[80] Handschin, E., Schweppe, F. C., Kohlas, J., & Fiechter, A. A. F. A. (1975). Bad data analysis for power system state estimation. *IEEE Transactions on Power Apparatus and Systems*, *94*(2), 329-337.

[81] Ghosh, A. K., Lubkeman, D. L., & Jones, R. H. (1997). Load modeling for distribution circuit state estimation. *IEEE Transactions on Power Delivery*, *12*(2), 999-1005.

[82] Ghosh, A. K., Lubkeman, D. L., Downey, M. J., & Jones, R. H. (1997). Distribution circuit state estimation using a probabilistic approach. *IEEE Transactions on Power Systems*, *12*(1), 45-51.

[83] Baran, M. E., & Kelley, A. W. (1995). A branch-current-based state estimation method for distribution systems. *IEEE transactions on power systems*, *10*(1), 483-491.

[84] Beddoes, A. J., & Collinson, A. (2001). *Likely changes to network design as a result of significant embedded generation*. Harwell Laboratory, Energy Technology Support Unit.

[85] Fila, M., Reid, D., Taylor, G. A., Lang, P., & Irving, M. R. (2009, July). Coordinated voltage control for active network management of distributed generation. In *Power & Energy Society General Meeting, 2009. PES'09. IEEE* (pp. 1-8). IEEE.

[86] Hird, C. M., Leite, H., Jenkins, N., & Li, H. (2004). Network voltage controller for distributed generation. *IEE Proceedings-Generation, Transmission and Distribution*, *151*(2), 150-156.

[87] Viawan, F. A., & Karlsson, D. (2008, July). Coordinated voltage and reactive power control in the presence of distributed generation. In *Power and Energy Society General Meeting-Conversion and Delivery of Electrical Energy in the 21st Century, 2008 IEEE* (pp. 1-6). IEEE.

[88] Richardot, O., Viciu, A., Besanger, Y., Hadjsaid, N., & Kiény, C. (2006, May). Coordinated voltage control in distribution networks using distributed generation. In *Transmission and Distribution Conference and Exhibition, 2005/2006 IEEE PES* (pp. 1196-1201).

[89] Sarmin, M. K. N. M., Nakawiro, W., Wanik, M., Siam, M. F., Hussien, Z., Ibrahim, A. A., & Hussin, A. K. M. (2013). Coordinated Voltage Control in Distribution Network with Renewable Energy Based Distributed Generation. *Engineering*, *5*(01), 208.

[90] Senjyu, T., Miyazato, Y., Yona, A., Urasaki, N., & Funabashi, T. (2008). Optimal distribution voltage control and coordination with distributed generation. *IEEE Transactions on power delivery*, *23*(2), 1236-1242.

[91] Wanik, M. Z. C., Erlich, I., Mohamed, A., & Shareef, H. (2010, October). Predictive var management of distributed generators. In *IPEC, 2010 Conference Proceedings* (pp. 619-624). IEEE.

[92] Madureira, A. G., & Lopes, J. P. (2009). Coordinated voltage support in distribution networks with distributed generation and microgrids. *IET Renewable Power Generation*, *3*(4), 439-454.

[93] Ochoa, L. F., & Harrison, G. P. (2011). Minimizing energy losses: Optimal accommodation and smart operation of renewable distributed generation. *IEEE Transactions on Power Systems*, *26*(1), 198-205.

[94] Lam, A., Dominguez-Garcia, A., Zhang, B., & Tse, D. (2012). *Optimal distributed voltage regulation in power distribution networks* (No. arXiv: 1204.5226).

[95] Van Cutsem, T., & Valverde, G. (2013). Coordinated voltage control of distribution networks hosting dispersed generation.

[96] Shivarudraswamy, R., & Gaonkar, D. N. (2012). Coordinated voltage regulation of distribution network with distributed generators and multiple voltage-control devices. *Electric Power Components and Systems*, *40*(9), 1072-1088.

[97] El Ela, A. A., Abido, M. A., & Spea, S. R. (2011). Differential evolution algorithm for optimal reactive power dispatch. *Electric Power Systems Research, 81*(2), 458-464.

[98] Su, C. L. (2009, July). Comparative analysis of voltage control strategies in distribution networks with distributed generation. In *Power & Energy Society General Meeting, 2009. PES'09. IEEE* (pp. 1-7). IEEE.

[99] Wang, M., & Zhong, J. (2011, July). A novel method for distributed generation and capacitor optimal placement considering voltage profiles. In *Power and Energy Society General Meeting, 2011 IEEE* (pp. 1-6). IEEE.

[100] O'gorman, R., & Redfern, M. (2005, June). The impact of distributed generation on voltage control in distribution systems. In *Electricity Distribution, 2005. CIRED 2005. 18th International Conference and Exhibition on* (pp. 1-6). IET.

[101] Hiscock, J., Hiscock, N., & Kennedy, A. (2007, May). Advanced voltage control for networks with distributed generation. In *19th International Conference on Electricity Distribution* (p. 0148).

[102] Deshmukh, S., Natarajan, B., & Pahwa, A. (2012). Voltage/VAR control in distribution networks via reactive power injection through distributed generators. *IEEE Transactions on smart grid*, *3*(3), 1226-1234.

[103] Yu, L., Czarkowski, D., & De León, F. (2012). Optimal distributed voltage regulation for secondary networks with DGs. *IEEE Transactions on Smart Grid*, *3*(2), 959-967.

[104] Daratha, N., Das, B., & Sharma, J. (2014). Coordination between OLTC and SVC for voltage regulation in unbalanced distribution system distributed generation. *IEEE Transactions on Power Systems*, *29*(1), 289-299.

[105] Bonfiglio, A., Brignone, M., Delfino, F., & Procopio, R. (2014). Optimal control and operation of grid-connected photovoltaic production units for voltage support in medium-voltage networks. *IEEE Transactions on Sustainable Energy*, *5*(1), 254-263.

[106] Agalgaonkar, Y. P., Pal, B. C., & Jabr, R. A. (2014). Distribution voltage control considering the impact of PV generation on tap changers and autonomous regulators. *IEEE Transactions on Power Systems*, *29*(1), 182-192.

[107] Cagnano, A., & De Tuglie, E. (2015). Centralized voltage control for distribution networks with embedded PV systems. *Renewable Energy*, *76*, 173-185.

[108] Azzouz, M. A., Shaaban, M. F., & El-Saadany, E. F. (2015). Real-time optimal voltage regulation for distribution networks incorporating high penetration of PEVs. *IEEE Transactions on Power Systems*, *30*(6), 3234-3245.

[109] Zhong, J., Nobile, E., Bose, A., & Bhattacharya, K. (2004). Localized reactive power markets using the concept of voltage control areas. *IEEE Transactions on Power Systems*, *19*(3), 1555-1561.

[110] Liu, X., Aichhorn, A., Liu, L., & Li, H. (2012). Coordinated control of distributed energy storage system with tap changer transformers for voltage rise mitigation under high photovoltaic penetration. *IEEE Transactions on Smart Grid*, *3*(2), 897-906.

[111] Kigen, C., & Odero, N. A. (2012). Optimising voltage profile of distribution networks with distributed generation. *International Journal of Emerging Technology and Advanced Engineering*, *2*(12), 89-95.

[112] Kiprakis, A. E., & Wallace, A. R. (2004). Maximising energy capture from distributed generators in weak networks. *IEE Proceedings-Generation, Transmission and Distribution*, *151*(5), 611-618.

[113] Bollen, M. H. J., & Sannino, A. (2005). Voltage control with inverter-based distributed generation. *IEEE transactions on Power Delivery*, *20*(1), 519-520.

[114] Kim, I. S. (2006). Sliding mode controller for the single-phase grid-connected photovoltaic system. *Applied Energy*, *83*(10), 1101-1115.

[115] Dugan, R. C., McGranaghan, M. F., & Beaty, H. W. (1996). Electrical power systems quality. *New York, NY: McGraw-Hill,| c1996*.

[116] Carvalho, P. M., Correia, P. F., & Ferreira, L. A. (2008). Distributed reactive power generation control for voltage rise mitigation in distribution networks. *IEEE transactions on Power Systems*, *23*(2), 766-772.

[117] O'gorman, R., & Redfern, M. (2005, June). The impact of distributed generation on voltage control in distribution systems. In *Electricity Distribution, 2005. CIRED 2005. 18th International Conference and Exhibition on* (pp. 1-6). IET.

[118] Sansawatt, T., Ochoa, L. F., & Harrison, G. P. (2010, July). Integrating distributed generation using decentralised voltage regulation. In *Power and Energy Society General Meeting, 2010 IEEE* (pp. 1-6). IEEE.

[119] Keane, A., Ochoa, L. F., Vittal, E., Dent, C. J., & Harrison, G. P. (2011). Enhanced utilization of voltage control resources with distributed generation. *IEEE Transactions on Power Systems*, *26*(1), 252-260.

[120] Ochoa, L. F., Keane, A., & Harrison, G. P. (2011). Minimizing the reactive support for distributed generation: Enhanced passive operation and smart distribution networks. *IEEE Transactions on Power Systems*, *26*(4), 2134-2142.

[121] Guo, Y., Lin, Y., & Sun, M. (2011, July). The impact of integrating distributed generations on the losses in the smart grid. In *Power and Energy Society General Meeting, 2011 IEEE* (pp. 1-6). IEEE.

[122] Tsuji, T., Hashiguchi, T., Goda, T., Horiuchi, K., & Kojima, Y. (2009, October). Autonomous decentralized voltage profile control using multi-agent technology considering time-delay. In *Transmission & Distribution Conference & Exposition: Asia and Pacific, 2009* (pp. 1-8). IEEE.

[123] See http://standards.ieee.org/findstds/standard/1547-2003.html.

[124] See http://grouper.ieee.org/groups/scc21/1547.8/1547.8_index.html.

[125] Smith, J. W., Sunderman, W., Dugan, R., & Seal, B. (2011, March). Smart inverter volt/var control functions for high penetration of PV on distribution systems. In *Power Systems Conference and Exposition (PSCE), 2011 IEEE/PES* (pp. 1-6). IEEE.

[126] Rizy, D. T., Xu, Y., Li, H., Li, F., & Irminger, P. (2011, July). Volt/Var control using inverter-based distributed energy resources. In *Power and Energy Society General Meeting, 2011 IEEE* (pp. 1-8). IEEE.

[127] Jahangiri, P., & Aliprantis, D. C. (2013). Distributed Volt/VAr control by PV inverters. *IEEE Transactions on power systems*, *28*(3), 3429-3439.

[128] Braun, M., Stetz, T., Reimann, T., Valov, B., & Arnold, G. (2009, September). Optimal reactive power supply in distribution networks-technological and economic assessment for PV-systems. In *European Photovoltaic Solar Energy Conference (EU PVSEC 2009), Hamburg (Germany)*.

[129] Neal, R., & Bravo, R. (2011, March). Advanced Volt/VAr control element of Southern California Edison's Irvine smart grid demonstration. In *Power Systems Conference and Exposition (PSCE), 2011 IEEE/PES* (pp. 1-3). IEEE.

[130] Demirok, E., Sera, D., Teodorescu, R., Rodriguez, P., & Borup, U. (2010, September). Evaluation of the voltage support strategies for the low voltage grid connected PV generators. In *Energy Conversion Congress and Exposition (ECCE), 2010 IEEE* (pp. 710-717). IEEE.

[131] Bletterie, B., Goršek, A., Fawzy, T., Premm, D., Deprez, W., Truyens, F., ... & Uljanič, B. (2012). Development of innovative voltage control for distribution networks with high photovoltaic penetration. *Progress in Photovoltaics: Research and Applications*, *20*(6), 747-759.

[132] Varma, R. K., Khadkikar, V., & Seethapathy, R. (2009). Nighttime application of PV solar farm as STATCOM to regulate grid voltage. *IEEE transactions on energy conversion*, *24*(4), 983-985.

[133] Dall'Anese, E., Dhople, S. V., & Giannakis, G. B. (2014). Optimal dispatch of photovoltaic inverters in residential distribution systems. *IEEE Transactions on Sustainable Energy*, *5*(2), 487-497.

[134] Juamperez, M., Guangya, Y. A. N. G., & Kjær, S. B. (2014). Voltage regulation in LV grids by coordinated volt-var control strategies. *Journal of Modern Power Systems and Clean Energy*, *2*(4), 319-328.

[135] Niknam, T., Ranjbar, A. M., & Shirani, A. R. (2003, June). Impact of distributed generation on Volt/Var control in distribution networks. In *Power Tech Conference Proceedings, 2003 IEEE Bologna* (Vol. 3, pp. 7-pp). IEEE.

[136] Niknam, T., Ranjbar, A. M., Shirani, A. R., & Ostadi, A. (2005). A new approach based on ant algorithm for Volt/Var control in distribution network considering distributed generation. *Iranian Journal of Science & Technology, Transaction B*, *29*(B4), 1-15.

[137] Niknam, T. (2008). A new approach based on ant colony optimization for daily Volt/Var control in distribution networks considering distributed generators. *Energy Conversion and Management*, *49*(12), 3417-3424.

[138] Niknam, T., Firouzi, B. B., & Ostadi, A. (2010). A new fuzzy adaptive particle swarm optimization for daily Volt/Var control in distribution networks considering distributed generators. *Applied Energy*, *87*(6), 1919-1928.

[139] Turitsyn, K., Šulc, P., Backhaus, S., & Chertkov, M. (2010, July). Distributed control of reactive power flow in a radial distribution circuit with high photovoltaic penetration. In *Power and Energy Society General Meeting, 2010 IEEE* (pp. 1-6). IEEE.

[140] Li, H., Xu, Y., Adhikari, S., Rizy, D. T., Li, F., & Irminger, P. (2012, July). Real and reactive power control of a three-phase single-stage PV system and PV voltage stability. In *Power and Energy Society General Meeting, 2012 IEEE* (pp. 1-8). IEEE.

[141] Chudamani, N. S. R., & Chudamani, R. (2012, July). Single-stage grid interactive PV system using novel fuzzy logic based MPPT with active and reactive power control. In *Industrial Electronics and Applications (ICIEA), 2012 7th IEEE Conference on* (pp. 1667-1672). IEEE.

[142] Liao, Y., Fan, W., Cramer, A., Dolloff, P., Fei, Z., Qui, M., ... & Gregory, B. (2012, September). Voltage and var control to enable high penetration of distributed photovoltaic systems. In *North American Power Symposium (NAPS), 2012* (pp. 1-6). IEEE.

[143] Farivar, M., Clarke, C. R., Low, S. H., & Chandy, K. M. (2011, October). Inverter var control for distribution systems with renewables. In *Smart Grid Communications (SmartGridComm), 2011 IEEE International Conference on* (pp. 457-462). IEEE.

[144] Farivar, M., Neal, R., Clarke, C., & Low, S. (2012, July). Optimal inverter VAR control in distribution systems with high PV penetration. In *Power and Energy Society General Meeting, 2012 IEEE* (pp. 1-7). IEEE.

[145] Pyo, G. C., Kang, H. W., & Moon, S. I. (2008, July). A new operation method for grid-connected PV system considering voltage regulation in distribution system. In *Power and Energy Society General Meeting-Conversion and Delivery of Electrical Energy in the 21st Century, 2008 IEEE* (pp. 1-7). IEEE.

[146] Turitsyn, K., Sulc, P., Backhaus, S., & Chertkov, M. (2010, October). Local control of reactive power by distributed photovoltaic generators. In *Smart Grid Communications (SmartGridComm), 2010 First IEEE International Conference on* (pp. 79-84). IEEE.

[147] Turitsyn, K., Sulc, P., Backhaus, S., & Chertkov, M. (2011). Options for control of reactive power by distributed photovoltaic generators. *Proceedings of the IEEE*, *99*(6), 1063-1073.

[148] Liu, X., Cramer, A. M., & Liao, Y. (2014, April). Reactive-power control of photovoltaic inverters for mitigation of short-term distribution-system voltage variability. In *T&D Conference and Exposition, 2014 IEEE PES* (pp. 1-5). IEEE.

[149] Douglass, P. J., Garcia-Valle, R., Østergaard, J., & Tudora, O. C. (2014). Voltage-sensitive load controllers for voltage regulation and increased load factor in distribution systems. *IEEE Transactions on Smart Grid*, *5*(5), 2394-2401.

[150] McArthur, S. D., & Davidson, E. M. (2005, November). Concepts and approaches in multi-agent systems for power applications. In *Intelligent Systems Application to Power Systems, 2005. Proceedings of the 13th International Conference on* (pp. 5-pp). IEEE.

[151] Baran, M. E., & El-Markabi, I. M. (2007). A multiagent-based dispatching scheme for distributed generators for voltage support on distribution feeders. *IEEE Transactions on power systems*, *22*(1), 52-59.

[152] Nguyen, P. H., Kling, W. L., & Myrzik, J. M. (2007, September). Promising concepts and technologies for future power delivery systems. In *Universities Power Engineering Conference, 2007. UPEC 2007. 42nd International* (pp. 47-52). IEEE.

[153] Jiang, Z. (2006, December). Agent-based control framework for distributed energy resources microgrids. In *Proceedings of the IEEE/WIC/ACM international conference on Intelligent Agent Technology* (pp. 646-652). IEEE Computer Society.

[154] Lund, P. (2007, June). The danish cell project-part 1: Background and general approach. In *Power Engineering Society General Meeting, 2007. IEEE* (pp. 1-6). IEEE.

[155] Oyarzabal, J. R. A. E. J., Jimeno, J., Ruela, J., Engler, A., & Hardt, C. (2005, November). Agent based micro grid management system. In *Future Power Systems, 2005 International Conference on* (pp. 6-pp). IEEE.

[156] Pipattanasomporn, M., Feroze, H., & Rahman, S. (2009, March). Multi-agent systems in a distributed smart grid: Design and implementation. In *Power Systems Conference and Exposition, 2009. PSCE'09. IEEE/PES* (pp. 1-8). IEEE.

[157] Nguyen, P. H., Myrzik, J. M. A., & Kling, W. L. (2008, April). Coordination of voltage regulation in active networks. In *Transmission and Distribution Conference and Exposition, 2008. T&D. IEEE/PES* (pp. 1-6). IEEE.

[158] Farag, H. E., El-Saadany, E. F., & Seethapathy, R. (2012). A two ways communication-based distributed control for voltage regulation in smart distribution feeders. *IEEE Transactions on Smart Grid*, *3*(1), 271-281.

[159] Olfati-Saber, R., Fax, J. A., & Murray, R. M. (2007). Consensus and cooperation in networked multi-agent systems. *Proceedings of the IEEE*, *95*(1), 215-233.

[160] Olfati-Saber, R., & Murray, R. M. (2004). Consensus problems in networks of agents with switching topology and time-delays. *IEEE Transactions on automatic control*, *49*(9), 1520-1533.

[161] Wang, H. F. (2001). Multi-agent co-ordination for the secondary voltage control in power-system contingencies. *IEE Proceedings-Generation, Transmission and Distribution*, *148*(1), 61-66.

[162] Dominguez-Garcia, A. D., & Hadjicostis, C. N. (2010, October). Coordination and control of distributed energy resources for provision of ancillary services. In *Smart Grid Communications (SmartGridComm), 2010 First IEEE International Conference on* (pp. 537-542). IEEE.

[163] Robbins, B. A., Dominguez-Garcia, A. D., & Hadjicostis, C. N. (2011, August). Control of distributed energy resources for reactive power support. In *North American Power Symposium (NAPS), 2011* (pp. 1-5). IEEE.

[164] Robbins, B. A., Hadjicostis, C. N., & Domínguez-García, A. D. (2013). A two-stage distributed architecture for voltage control in power distribution systems. *IEEE Transactions on Power Systems*, *28*(2), 1470-1482.

[165] Polymeneas, E., & Benosman, M. (2014, July). Multi-agent coordination of DG inverters for improving the voltage profile of the distribution grid. In *PES General Meeting| Conference & Exposition, 2014 IEEE* (pp. 1-5). IEEE.

[166] Castelfranchi, C., & Lespérance, Y. (2001). Developing Multi-agent Systems with JADE Intelligent Agents. *Intelligent Agents VII Agent Theories Architectures and Languages, 1986*, 42-47.

[167] Bellifemine, F. L., Caire, G., & Greenwood, D. (2007). *Developing multi-agent systems with JADE* (Vol. 7). John Wiley & Sons.

[168] Zahedi, A. (2015) Intermittent Energy sources and their impact on feeder voltage, IRCET International Research Conference on Engineering and Technology, ISBN 978-986-89844-6-2.

Chapter 3

A Cooperative Operation Of Novel PV Inverter Control Scheme And Storage Energy Management System Based On ANFIS For Voltage Regulation Of Grid-Tied PV System

"Mahmud, N., Zahedi, A., & Mahmud, A. (2017). A cooperative operation of novel PV inverter control scheme and storage energy management system based on ANFIS for voltage regulation of grid-tied PV system. *IEEE Transactions on Industrial Informatics*. (Published)"

Abstract

In this chapter, the voltage regulation problem in low-voltage power distribution networks integrated with increased amount of solar photovoltaics (PV) has been addressed. This chapter proposes and evaluates the cooperative performance of a novel proportional-integral-derivative (PID) control scheme for PV interfacing inverter based on intelligent adaptive neuro-fuzzy inference system (ANFIS) and an ANFIS-based supervisory storage energy management system (EMS) for regulating the voltage of three-phase grid connected solar PV system under any nonlinear and fluctuating operating conditions. The proposed ANFIS-based PID control scheme (ANFISPID) dynamically controls the PV inverter to inject/ absorb appropriate reactive power to regulate the voltage at point of common coupling (PCC) and provides robust response at any system worst case scenarios and grid faults. In addition, the proposed ANFIS-based supervisory EMS controls the charge/ discharge of the battery energy storage system (BESS) when there is voltage deviation to cooperate with ANFISPID in PCC voltage regulation. The proposed ANFISPID-based PV inverter control scheme and ANFIS-based supervisory EMS are developed and simulated in MATLAB/ Simulink environment and their dynamic cooperative performances are compared with cooperative performances of conventional PID-based PV inverter control scheme and state-based EMS.

3.1 Introduction

Power distribution systems are undergoing substantial changes because of the new advents and technologies such as integration of large-scale renewable distributed generators (DGs), advanced control & communication schemes and storage capable loads [1]. Integration of large-scale renewable DGs in traditional power system is being popular day-by-day because of its capability to satisfy ever-increasing energy demands, increased power quality, zero carbon emission and expandability.

Currently, large amounts of renewable DGs are being connected with low-voltage weak distribution networks that are posing significant impacts on the operation and protection of the system [2-4]. Moreover, increased accommodation of renewable DGs introduces new dynamics that have significant adverse impacts on the voltage profile at PCC [5-7]. The three-phase grid connected renewable DG systems are generally composed of renewable energy sources such as solar PVs, wind turbines, fuel cells etc. integrated with grid. These renewable sources are naturally intermittent and the generation of power at any given time depends on uncontrollable and nonlinear natural elements (such as solar irradiation, wind speed etc.). As the resistance to reactance ratio (R/X) is more than one for low-voltage distribution networks, the impact of power injected by renewable DGs has significant influence on voltage profile of the feeders [8]. For the steady state operation of the system, the voltage along the distribution feeder needs to be within a permissible limit. Though, there is no internationally applied rule for steady state voltage range along the feeder, for maximum cases, the allowable voltage variation along the feeder is $\pm 6\%$ of the nominal voltage [9]. Conventional voltage regulators like on-load tap changers (OLTC), switched capacitors (SC), step voltage regulators (SVR) etc. are inefficient in the newly introduced dynamics of grid-tied solar PV systems. In that case, utilization of grid interfacing power electronic converters (e.g. PV inverters) can be an efficient alternative as they can deliver fast, dynamic and continuous reactive power support, which can be utilized for voltage control. However, the allowable PV inverter reactive power generation is limited and the impact of reactive power on PCC voltage of low-voltage system is lesser due to higher R/X ratio. Utilization of BESS is another efficient strategy for voltage regulation of low-voltage systems with PVs. However, frequent charge/ discharge reduce the life span of BESS and the solo-implementation of BESS for voltage profile enhancement needs excessively large capacity of batteries that is not economically feasible. In this scenario, the cooperative operation of both the PV inverter and BESS for voltage regulation can ensure enhanced performance [10]. Moreover, as power injected by solar PVs is uncertain, utilization of BESS

can improve the state of power availability, operability and degree of controllability of the system [11].

Classic controllers like PID controllers are long established in controlling the three-phase grid interfacing PV inverters. This control algorithm is widely used method in industrial automation because of its simplicity in structure and linear nature. However, this type of classical controllers require exact mathematical model of the system and are very sensitive to variation of operating conditions [12]. If the PID gain parameters are not selected properly, the response of the PID controller gets unstable, oscillatory or sluggish [13-14]. Therefore, it is necessary to tune the appropriate PID gains in real time in accordance with varying operating conditions to have stable and acceptable responses. Manual trial-and-error based tuning approaches would be very monotonous, expensive and time consuming and the tuned gains could become obsolete in a short time. As a result, conventional PID controllers may appear deficient as it is nearly impossible to set optimal gains due to rapid changes in dynamics of highly nonlinear grid-tied PV system environment [15-17] which may result in large overshoot and system oscillation. In this situation, an adaptive intelligent system is necessary that can atomically tune the PID control parameters in accordance with system operating conditions in real time.

Several intelligent control schemes are being used for industrial automation in recent days like artificial neural networks (ANN), fuzzy inference system (FIS) or neuro-fuzzy systems. These intelligent control schemes do not require exact system model to operate and they are invulnerable to system dynamics. As a result, these intelligent controllers are advantageous in operating in highly nonlinear systems [18-19]. Among the neuro-fuzzy models, ANFIS is easier to implement, faster, stronger in generalization skills and more accurate [11] that inherits the learning and parallel data processing ability of artificial neural networks and inference ability (like human mind) of fuzzy inference system. As PID is already a well stablished and widely used control scheme in power industry, the combination of the simplicity of PID and the capability of ANFIS in handling the uncertainties has been proved advantageous while controlling the PV inverters under fluctuating operating conditions. The proposed ANFIS-based intelligent PID control scheme adapts the dynamic states of distribution system voltage profile and tunes the PID gain parameters automatically to improve the potential of PID control scheme in providing transient responses.

The reactive power capability of inverter interfaced DGs has been utilized for voltage regulation and enhancement of low voltage ride-through (LVRT) capability during grid faults in many literatures [14], [20-29]. Authors of [14], [21] and [25] have theoretically analysed and tested the significance and performance of tuned PID with adaptive gains but the strategy to obtain an acceptable voltage profile along the feeder has not been presented. Previously, some efforts have been made to incorporate fuzzy logic system to auto-tune PID control parameters [30-33]. However, this approach involves laborious design steps such as manual tuning of membership functions, selection of fuzzy rules, selection of scaling factors etc., which are usually obtained by trial-and-error method. This turns it into a time consuming and error-prone process [34].

To our knowledge, this is the first time that a PID control scheme dynamically auto-tuned in real time by intelligent ANFIS has been implemented on PV inverter for regulating the PCC voltage of three-phase grid-tied solar PV system that shows robustness at any system worst-case scenarios. On the other hand, one reference has been found where ANFIS has been applied as a 'supervisory controller' [11] for BESS where the objective of charge/ discharge of BESS was not the voltage regulation of the system. In our study, an intelligent ANFIS-based supervisory EMS has been proposed that cooperates with the ANFISPID-based PV inverter control scheme in voltage regulation by reducing reverse power flow to the grid or supplying power when there are voltage deviations. It reduces the voltage deviation at PCC and the volume of reactive power injection/ absorption by the PV inverter for voltage control that eventually results in reduction of line losses through the system. The authors of [35] have proposed a coordinated control of PV inverter and energy storage for voltage profile improvement but a detailed robust control structure for PV inverter was not presented. Besides, the coordinated control operates at an hourly basis that requires a power flow study every hour which is complex and not prompt enough in cases of introduced fast nonlinear dynamics when large-scale intermittent PVs are interconnected.

The main contributions of this chapter are:

1) The design and application of intelligent ANFIS-based PID control scheme (ANFISPID) on PV inverters to regulate the PCC voltage in real time that provides 'plug-and-play' feature for auto-tuning the PID parameters and shows robustness at any nonlinear and fluctuating operating condition.

2) The design and application of an intelligent ANFIS-based supervisory EMS on BESS that cooperates with PV inverter in voltage regulation by charging/ discharging when voltage deviation occurs in real time. By applying proper control, this proposed ANFIS-based supervisory EMS minimizes the PCC voltage deviations and reduces reactive power injection/ absorption load on PV inverter.

This chapter is organized as follows. Section 3.2 describes the PV system interconnected with traditional grid. Section 3.3 details the mathematical representation of the system. Section 3.4 illustrates the proposed PV inverter control methodology. Section 3.5 depicts the design method of the proposed PV inverter control scheme and EMS. Section 3.6 summarizes the algorithm for cooperative operation of PV inverter control scheme and storage EMS. Section 3.7 details the case studies and simulation results and Section 3.8 establishes the conclusion derived from the work.

3.2 Grid-tied solar PV system

The low voltage weak distribution system interconnected with large-scale PVs under study is shown in figure 3.1.

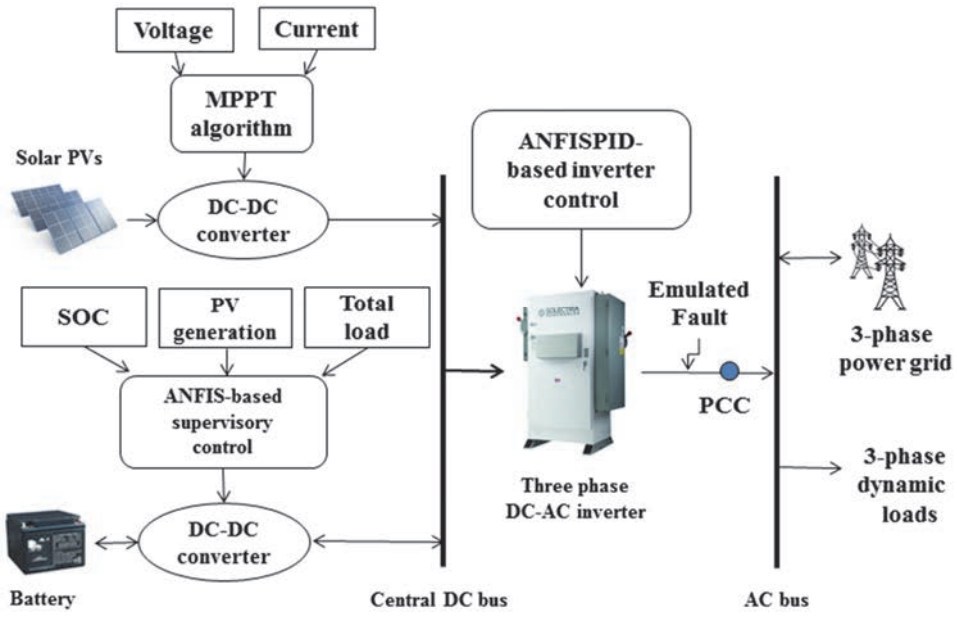

Figure 3.1. Grid-tied solar PVs with BESS

It consists of following equipment:

1) PV array consists of 66 strings of 305 W Sunpower SPR-305-WHT modules connected in parallel, each string consisting of 5 modules connected in series.
2) 240 kWh lead acid battery bank consists of 10 parallel strings of 25 Fullriver deep-cycle AGM (Absorbent Glass Mat) 12 Volt 80 Ah batteries connected in series.
3) A three-phase Solectria PVI (photovoltaic inverter) 100 kW 240 VAC Inverter PVI-100-240V.

Dynamic modelling has been done for this grid-tied PV system with BESS in MATLAB/ Simulink environment. The 100-kW PV array consists of 66 strings of 5 series-connected 305 W (standard test condition power rating) modules connected in parallel. Specifications (V_{oc}, I_{sc}, V_{mp}, and I_{mp}) of the modules are selected according to manufacturer data sheets [36] and characteristics of the modules are extracted from National Renewable Energy Laboratory (NREL) System Advisor Model [37]. Solar irradiance (W/m^2) and ambient temperature (^oC) data have been provided to the PV models as inputs and these data have been collected from [38]. A DC-DC boost converter boosts the output dc voltage of PV to direct current (DC) bus voltage V_{dc}. A maximum power point tracking (MPPT) controller controls the DC-DC boost converter to maximize the PV power output by generating duty cycles. This MPPT controller is implemented by 'perturb and observe' algorithm [39]. A 240 kWh lead acid battery bank has been connected with the central DC bus through a bidirectional buck-boost DC-DC converter. A generic dynamic model of the battery bank is implemented in MATLAB/ Simulink environment [40] parameterized to represent a bank of 240 kWh 300 volt 800 Ah consisting of 10 parallel strings of 25 units connected in series [41]. An ANFIS-based supervisory EMS is implemented on the bidirectional buck-boost converter to apply proper energy management on the system by generating power reference (P^*_{BESS}) for BESS. The DC power from the central DC bus then is transformed into AC by an interfacing 100 kW 240 VAC three phase inverter. ANFISPID-based intelligent control scheme has been applied on the three-phase PV inverter to control appropriate regulation of reactive power and active power for voltage control at PCC and DC bus. The three-phase, three-wire dynamic loads have been modelled by three-phase dynamic load block included in SimPowerSystems [42] whose active power demand and reactive power demand can be set externally. The varying active and reactive power demand data of a group of residential consumers have been collected from local distribution network operator (DNO) [43]. Some key parameters of the system are listed in Table 3.I:

TABLE 3.I. SYSTEM PARAMETERS

Parameter	Value
DC bus voltage, V_{dc}	600 V
Inverter output voltage	240 Vrms
AC system frequency, F	50 Hz
DC-link capacitor, C_{dc}	24, 000 μF
Grid connection inductor, L	625 μH

The diagram of the system is depicted in figure 3.2.

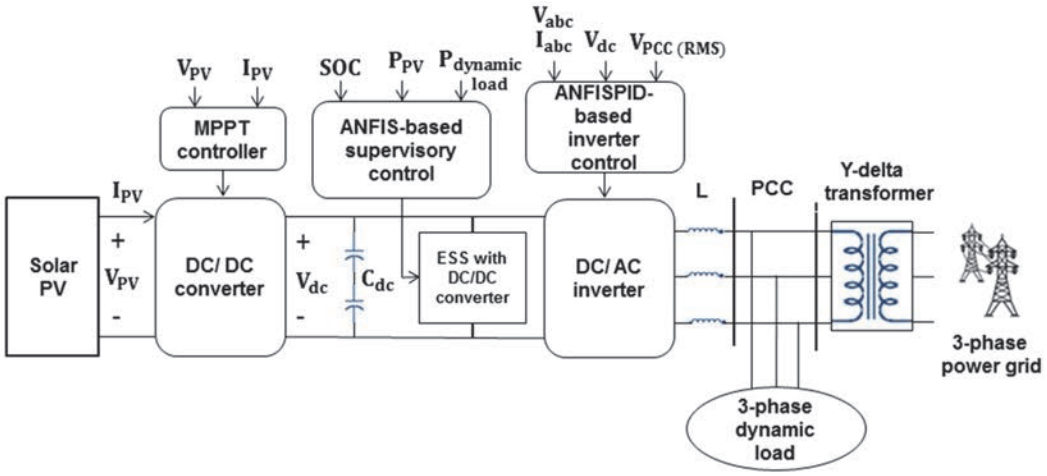

Figure 3.2. Diagram of grid-tied solar PVs with ESS

3.3 Mathematical representation of the system

In this study, the PV inverter control of grid-tied PV system with BESS is implemented based on rotating (synchronous) direct-quadrature (dq) reference frame as it can eliminate steady state error and has fast transient response by decoupling control [44]. The three-phase voltages and currents are represented by V_a, V_b, V_c and I_a, I_b, I_c. Applying the transformation method on three-phase voltages and currents we can transform the three-phase system (abc) into dq rotating frame (dq):

$$\begin{bmatrix} V_d \\ V_q \end{bmatrix} = \sqrt{\frac{2}{3}} \begin{bmatrix} \cos wt & \cos(wt - 120°) & \cos(wt + 120°) \\ -\sin wt & -\sin(wt - 120°) & -\sin(wt + 120°) \end{bmatrix} \begin{bmatrix} V_a \\ V_b \\ V_c \end{bmatrix} \quad (3.1)$$

And for three phase inverter current, we get:

$$\begin{bmatrix} I_d \\ I_q \end{bmatrix} = \sqrt{\frac{2}{3}} \begin{bmatrix} \cos wt & \cos(wt - 120°) & \cos(wt + 120°) \\ -\sin wt & -\sin(wt - 120°) & -\sin(wt + 120°) \end{bmatrix} \begin{bmatrix} I_a \\ I_b \\ I_c \end{bmatrix} \quad (3.2)$$

Here, V_d and I_d represent the direct components of three-phase voltages and currents respectively while V_q and I_q represent the quadrature components respectively. A phase lock loop (PLL) has been implemented on the three phase signals to track the frequency and phase by using an internal frequency oscillator and to obtain angular position wt for dq reference frame. The three phase active (P) and reactive power (Q) produced by the inverter is [45],

$$P = \frac{3}{2}(V_d I_d + V_q I_q) \quad (3.3)$$

$$Q = \frac{3}{2}(V_q I_d - V_d I_q) \quad (3.4)$$

Assuming that the d-axis is perfectly aligned with the grid voltage V_q = 0, the active power and the reactive power will therefore be proportional to I_d and I_q respectively:

$$P = \frac{3}{2} V_d I_d \quad (3.5)$$

$$Q = -\frac{3}{2} V_d I_q \quad (3.6)$$

So, the current d component I_d is controlled by generating reference I_d^* to manage inverters active power exchange and DC bus voltage regulation while current q component I_q is controlled by generating reference I_q^* to manage reactive power injection/ absorption to regulate the PCC voltage.

3.4 PV inverter Control methodology

The structure of ANFIS-based PID control scheme that controls the grid interfacing PV inverter is illustrated in figure 3.3. It consists of two control loops, (1) Outer control loop, and (2) Inner control loop. The outer control loop is to generate the reference values of the d-axis and q-axis component currents (I_d^*, I_q^*) to manage inverters active and reactive power exchange and to regulate the voltages at DC-bus and PCC as discussed in the previous section. This consists of two intelligent ANFIS-based PID control schemes. They are, (1) ANFISPID-I (consists of ANFIS- I and PID- I), and (2) ANFISPID- II (consists of ANFIS- II and PID- II)

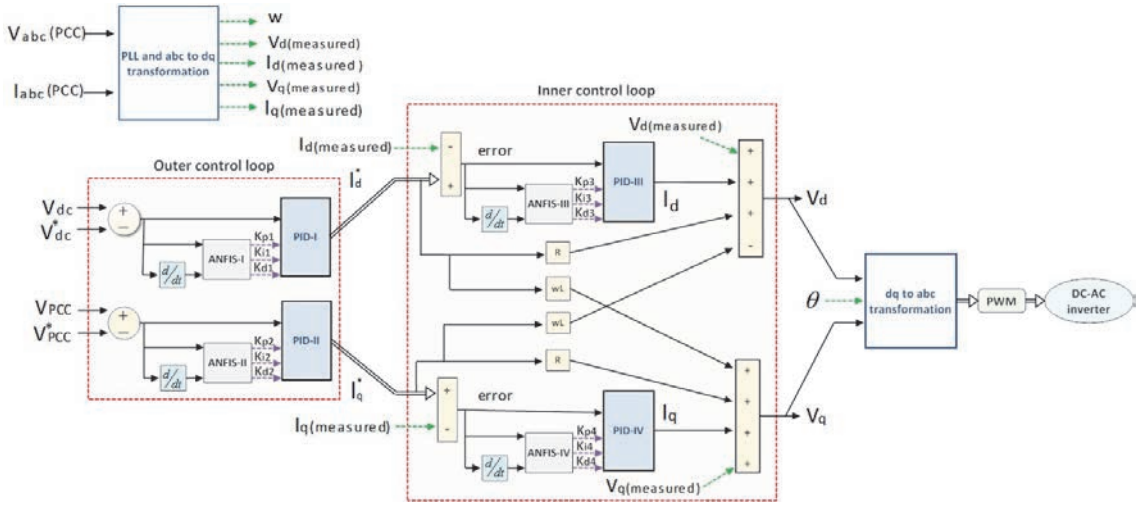

Figure 3.3. ANFISPID-based PV inverter control scheme

The voltage deviations from references at the DC bus and PCC and the derivative of this deviations (as a prediction of future deviations) are given as inputs into ANFISPID- I and ANFISPID- II respectively. V_{dc}^{*} is referred as DC bus voltage reference (600 volts) and V_{PCC}^{*} is referred as PCC voltage reference (240 volts phase-to-neutral). In ANFISPID- I, intelligent ANFIS-I tunes the gains (K_{p1}, K_{i1} and K_{d1}) of the PID-I controller to generate the appropriate d-axis component current reference I_{d}^{*} for regulating the DC bus voltage to its reference value. On the other hand, in ANFISPID- II, ANFIS- II tunes PID- II control gains (K_{p2}, K_{i2} and K_{d2}) to provide the appropriate q-axis component current reference I_{q}^{*} to control the PCC voltage.

$$I_{d}^{*} = K_{p1}(V_{dc}^{*} - V_{dc}) + K_{i1} \int (V_{dc}^{*} - V_{dc})\, dt + K_{d1} \frac{d(V_{dc}^{*} - V_{dc})}{dt} \tag{3.7}$$

$$I_{q}^{*} = K_{p2}(V_{PCC}^{*} - V_{PCC}) + K_{i2} \int (V_{PCC}^{*} - V_{PCC})\, dt + K_{d2} \frac{d(V_{PCC}^{*} - V_{PCC})}{dt} \tag{3.8}$$

The reference values of the d-axis and q-axis component currents ($I_{d}^{*},\ I_{q}^{*}$) are then provided to the inner control loop where the measured d-axis and q-axis component currents ($I_{d\ (measured)},\ I_{q\ (measured)}$) are regulated (independent to each other) by ANFIS-based PID controllers to follow the corresponding reference values ($I_{d}^{*},\ I_{q}^{*}$). Feedforward decoupling method has been implemented to allow independent control of I_{d} and I_{q}. Decoupling of the coupling terms is necessary as cross coupling can affect the dynamic performance of the inner control loop [44].

The inner control loop of the PV inverter control structure also consists of two intelligent ANFIS-based PID control schemes, (1) ANFISPID- III (consists of ANFIS- III and PID- III), and (2) ANFISPID- IV (consists of ANFIS- IV and PID- IV)

$$I_d = K_{p3}\left(I_d^* - I_{d\,(measured)}\right) + K_{i3}\int\left(I_d^* - I_{d\,(measured)}\right)dt + K_{d3}\frac{d\left(I_d^* - I_{d\,(measured)}\right)}{dt} \tag{3.9}$$

$$I_q = K_{p4}\left(I_q^* - I_{q\,(measured)}\right) + K_{i4}\int\left(I_q^* - I_{q\,(measured)}\right)dt + K_{d4}\frac{d\left(I_q^* - I_{q\,(measured)}\right)}{dt} \tag{3.10}$$

In ANFISPID- III, ANFIS- III auto-tunes the PID- III control gains (K_{p3}, K_{i3} and K_{d3}) to control the measured d-axis component current $I_{d(measured)}$ to follow corresponding reference I_d^*. On the other hand, in ANFISPID- IV, ANFIS- IV auto-tunes the control gains (K_{p4}, K_{i4} and K_{d4}) of PID- IV to regulate the measured q-axis component current $I_{q(measured)}$ to follow corresponding reference I_q^*.

The outputs of the controllers are the voltage direct-axis and quadrature-axis components ($V_d$and V_s) that the pulse width modulation (PWM) inverter has to generate. Then, V_d and V_s voltages are converted into phase voltages V_a, V_b and V_c which are used to synthesize the PWM voltages.

3.5 Adaptive neuro-fuzzy inference system design

Adaptive neuro-fuzzy inference system is an intelligent system based on learning and parallel data processing ability of artificial neural network and inference ability of Takagi–Sugeno fuzzy inference system. Figure 3.4 shows a general architecture of a 5-layer ANFIS where both square nodes and circle nodes are used to reflect different adaptive capabilities. For figure 3.4, the 5 layered ANFIS has 2 inputs (α and β) and one output (γ). Node functions in the different layers inside of a five-layered ANFIS are described below:

First layer: The first layer or fuzzification layer consists of square nodes (A_1, A_2, B_1 and B_2 in figure 4) those contain membership functions assigned to corresponding inputs (α and β in figure 3.4). If α and β are inputs to node m (where, m= 1, 2, 3…) of layer 1 then,

$$O_{A_m}^1 = \mu_{A_m}(\alpha) \quad \text{and} \quad O_{B_m}^1 = \mu_{B_m}(\beta) \tag{3.11}$$

Where, A_m and B_m are the linguistic labels and $O^1_{A_m}$ and $O^1_{B_m}$ are the membership functions of A_m and B_m respectively. In our work, triangular membership functions have been used. They can be expressed as,

$$\mu_{A_m}(\alpha),\ \mu_{B_m}(\beta) = \begin{cases} 0 & \alpha, \beta > x_m \\ \frac{x_m - \alpha,\beta}{x_m - y_m} & x_m > \alpha, \beta > y_m \\ 1 & \alpha, \beta < y_m \end{cases} \quad (3.12)$$

Here, x_m and y_m are the parameters of the membership functions that are adaptively tuned by the learning process in accordance with the variable inputs.

Second layer: In this layer, fixed nodes identify the corresponding rules. The incoming signals are multiplied and forwarded to the next layer as W_n (W_1, W_2 in figure 4).

$$W_n = \mu_{A_m}(\alpha)\, \mu_{B_m}(\beta) \quad \text{where, } m, n = 1, 2, 3\ldots \quad (3.13)$$

Third layer: Third layer of ANFIS calculates the normalized firing strength of each rule ($\bar{W}_n$) and forwards to next layer ($\bar{W}_1, \bar{W}_2$ in figure 4).

$$\bar{W}_n = \frac{W_n}{W_1 + W_2 + W_3 + W_4 + \cdots} \quad \text{where, } n = 1, 2, 3\ldots \quad (3.14)$$

Forth layer: The forth layer consists of square nodes where the node function can be written as,

$$O^4_n = \bar{W}_n \gamma_n \quad \text{where, } \gamma_n = p_n \alpha + q_n \beta + r_n \quad (3.15)$$

Here, $\bar{W}_n$ is the output from previous layer and p_n, q_n and r_n are the parameters where, n = 1, 2, 3…..

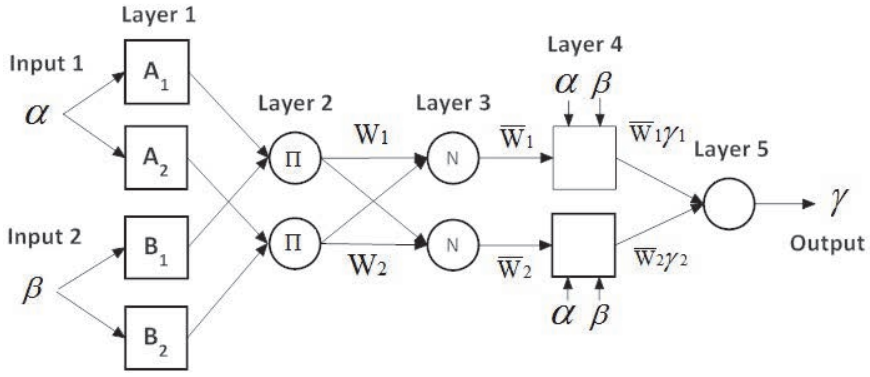

Figure 3.4. A general 5-layered ANFIS structure [19]

Fifth layer: The fifth and last layer computes the output by summing all incoming signals. For figure 4, the computed output is, $\gamma = (W_1\gamma_1 + W_2\gamma_2)/ (W_1 + W_2)$ or $\bar{W}_1\gamma_1 + \bar{W}_2\gamma_2$.

3.5.1 ANFISPID-based PV inverter control scheme design

Four ANFISPID-based control schemes (ANFISPID- I, ANFISPID- II, ANFISPID- III and ANFISPID- IV) have been applied on the grid-interfacing PV inverter to regulate active and reactive power appropriately to regulate the voltage during normal conditions and to provide LVRT during three-phase symmetric grid fault condition. Each of the ANFISPID-based control scheme has one intelligent ANFIS control scheme (ANFIS- I, ANFIS- II, ANFIS- III or ANFIS- IV repectively) to auto-tune the control parameters (K_p, K_i and K_d) of each PID (PID- I, PID- II, PID- III or PID- IV repectively). Each of the ANFIS control scheme consists of three intelligent ANFIS controllers (ANFIS- K_p, ANFIS- K_i and ANFIS- K_d) appointed to control each of the control parameters. In total, twelve intelligent ANFIS controllers have been appointed in four ANFISPID-based control schemes (where three have been appointed to each).

Figure 3.5 illustrates the general structure of the ANFISPID-based intelligent control scheme that has been developed and analysed in this chapter to control the grid interfacing three-phase PV inverter. Each of the twelve intelligent ANFIS controllers has been trained by corresponding training data set that has been gathered from simulations in MATLAB/ Simulink environment.

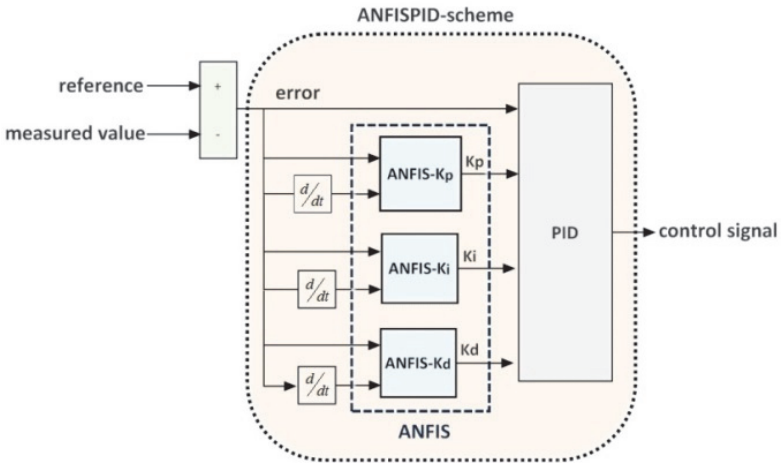

Figure 3.5. General structure of ANFISPID-based control scheme

To tune the fuzzy systems parameters of ANFIS controllers properly, a set of data for each has been collected from simulations that fully represents the dynamic features of highly

nonlinear nature of the weak distribution system integrated with large-scale PVs. The collected data set has been divided into three subsets, which are, training data set (70% of the data), testing data set (15% of the data) and checking data set (15% of the data) to validate the performance of each trained intelligent ANFIS controller [46]. Grid partitioning technique on the training data has been followed to generate the initial fuzzy inference system structure. For reducing the computational burden, triangular membership functions have been used for both the inputs [47]. A hybrid method that combines the least squares estimation method and backpropagation method has been used to tune the membership function parameters to emulate the training data.

3.5.2 ANFIS-based supervisory energy management system design for BESS

Connecting BESS with grid-tied solar PV system enhances the controllability, power quality and reliability and it provides ancillary services such as voltage regulation support if proper EMS is applied [48], [49].

The structure of proposed ANFIS-based supervisory EMS has been illustrated in figure 3.6. It has three inputs. They are, the total power generated by solar PVs (P_{PV}), the total demand of the dynamic load connected with the grid-tied PV system ($P_{dynamic\ load}$) and the state of charge (SOC%) of the battery bank (BESS). SOC is the available capacity of BESS expressed as the percentage of the rated capacity. As output, the ANFIS-based supervisory EMS provides power references (P^*_{BESS}) to the DC-DC buck-boost converter through which the battery bank is connected with the central DC bus.

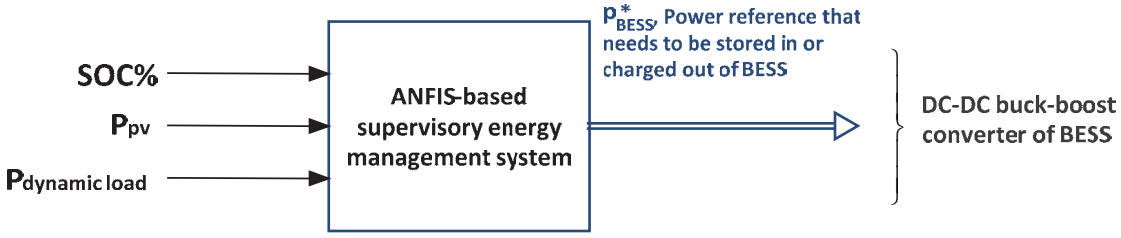

Figure 3.6. Structure of ANFIS-based supervisory EMS for BESS

Generally, the generated power from PV gradually increases and reaches to peak at midday and starts to decrease after that. The amount of surplus energy after satisfying the consumers

depends upon the nonlinear behaviour of the dynamic loads varying through the parts of the day and seasons of the year [50]. In this study, the ANFIS-based supervisory EMS intelligently controls the charge/ discharge of BESS to balance the PV power generation and dynamic load demand that enhances the voltage support for the system (during short-term fluctuations too) by cooperating with PV inverter control scheme. This control scheme is advantageous over constant charging/ discharging rate strategy that may leave the storage capacity unused [51].

Several researchers have implemented classic state-based EMS to control the charge/ discharge states of BESS [52], [53]. The performance of the proposed ANFIS-based supervisory EMS for BESS has been compared with a classic state-based EMS in section VII (E). Figure 3.7 illustrates the control algorithm of a classic state-based EMS for the grid-tied solar PV system under study.

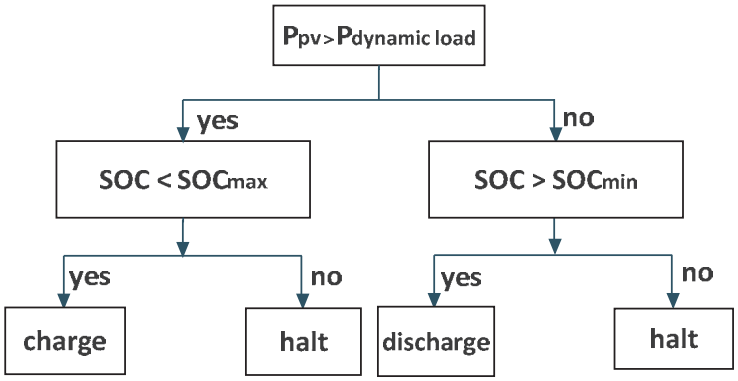

Figure 3.7. Control algorithm of a classic state-based EMS for the system under study

To prevent the battery bank from over-charging/ over-discharging, the SOC should be retained within appropriate allowable range [54], [55]. The ANFIS-based supervisory EMS prevents the BESS to be charged more than SOC_{max} (100% of rated storage capacity in this study) and to be discharged less than SOC_{min} (20% of rated storage capacity in this study). Supervisory ANFIS has been trained with a set of data to emulate the proposed supervisory management system. Initial fuzzy inference system structure was generated by grid partitioning technique on the training data. A hybrid method that combines the least squares estimation method and backpropagation method tunes the membership function parameters.

3.6 Algorithm for cooperative operation of PV inverter control scheme and storage EMS

A two-stage cooperative voltage regulation operation has been implemented on the PCC of low-voltage distribution system interconnected with large-scale PVs. Voltage at PCC (V_{PCC}) is monitored continuously at each time step (5e-5 second in this study). If V_{PCC} is same as reference voltage V_{PCC}^{*}, no action is taken. If V_{PCC} starts to deviate from V_{PCC}^{*}, the two-stage cooperative voltage regulation starts to operate. The algorithm for the two-stage cooperative voltage regulation is illustrated as follows:

Stage 1. At the first stage, PCC voltage deviation is reduced by ANFIS-based supervisory EMS. If V_{PCC} is above V_{PCC}^{*}, ANFIS-based supervisory EMS charges the BESS with the excess PV power after satisfying load demand. It suppresses the reverse power flow and reduces the voltage rise at injection point. If V_{PCC} is below V_{PCC}^{*}, BESS is discharged out to elevate PCC voltage and reduce the deviation.

Stage 2. At the second stage, the reduced voltage deviation (at stage 1) is completely mitigated with a robust response by ANFISPID-based PV inverter control scheme. It controls the PV inverter to inject (when $V_{PCC} < V_{PCC}^{*}$) or absorb (when $V_{PCC} > V_{PCC}^{*}$) reactive power to eliminate the voltage deviation.

This process repeats at each time step and keeps the voltage profile within acceptable limit in real time.

3.7 Case studies and discussions

Simulations have been performed to evaluate the cooperative performance of the proposed ANFISPID-based PV inverter control scheme and ANFIS-based supervisory EMS for voltage regulation at any worst-case scenarios (which are [56]: low or no PV generation during evening with peak dynamic loads (maximum load minimum generation), high PV generation during midday with low dynamic loads (minimum load maximum generation), sudden voltage fluctuations due to cloud passing, large load start etc.) and for enhancing LVRT capability during three-phase balanced grid fault condition. Solar irradiance data, temperature data [38] and dynamic load demand (active and reactive power demand) data of a group of residential customers [43] have been used to simulate and analyse the performance in real scenario. The cooperative performance of the proposed ANFISPID-based PV inverter control scheme and ANFIS-based supervisory EMS has been compared with the cooperative performance of

classic PID-based PV inverter control scheme and classic state-based EMS for regulating the voltage. The indexes that have been used to compare the dynamic performances of the proposed cooperative PV inverter control scheme and storage EMS are stated below [34], [57]:

Integral time absolute error, ITAE= $\int_0^T t\,|e(t)|dt$ (3.16)

Integral time square error, ITSE= $\int_0^T t\,e^2(t)dt$ (3.17)

Battery efficiency, η_{bat}= $\frac{\eta_{conv}^2 \int_0^T P_{bat}^{dis}\,dt}{\int_0^T P_{bat}^{char}\,dt}$ (3.18)

The variables in these indexes are t (time), e (t) (error at time t), η_{conv} (DC/ DC power converter efficiency), P_{bat}^{dis} (power discharged out of battery) and P_{bat}^{char} (power charged into battery).

3.7.1 Case 1: High PV generation during midday with low dynamic loads

In this case, the impact of high PV generation on the voltage profile at PCC during midday has been assessed. The impact of high PV generation has been illustrated in Figure 3.8 where per unit voltage at PCC exceeds the upper permissible limit (considering allowable voltage variation is ±6% of the nominal voltage) from time= 330.59 seconds to 415.31 seconds, from time= 633.69 seconds to 754.42 seconds and again from time= 788.08 seconds resulted from the increase of excess power flowing back to grid.

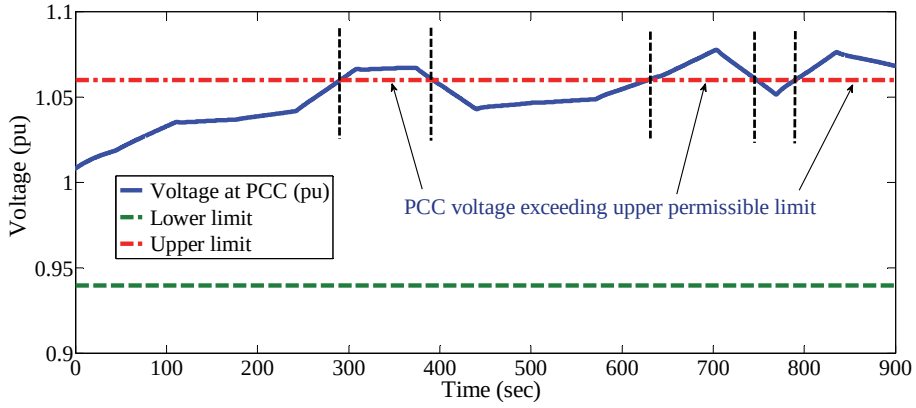

Figure 3.8. Impact of high PV integration on PCC voltage during midday

The voltage profile at PCC after applying cooperative ANFISPID-based PV inverter control scheme and ANFIS-based supervisory control on BESS is illustrated in Figure 3.9 (a).

ANFIS-based supervisory EMS controls the charging and discharging of the BESS to store the excess energy and prevent it from flowing back to grid. In figure 3.9 (b), the power delivered by PVs, dynamic load demand, power exchange with grid and the charged/ discharged power by BESS have been illustrated. When the BESS is being charged, the signing convention is negative and positive when it is discharging.

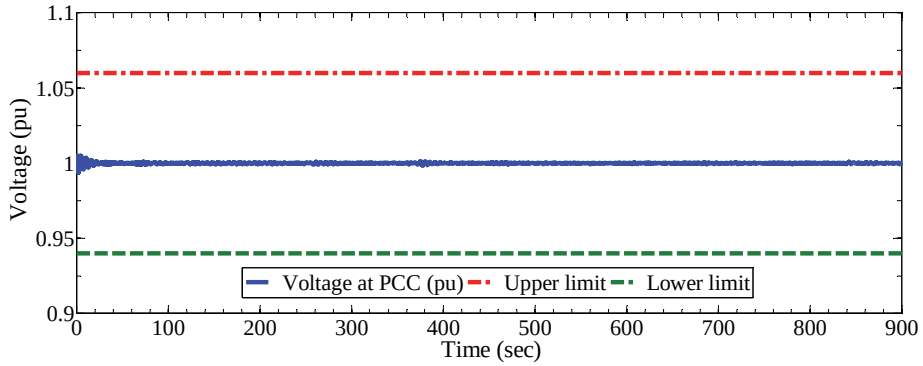

(a)

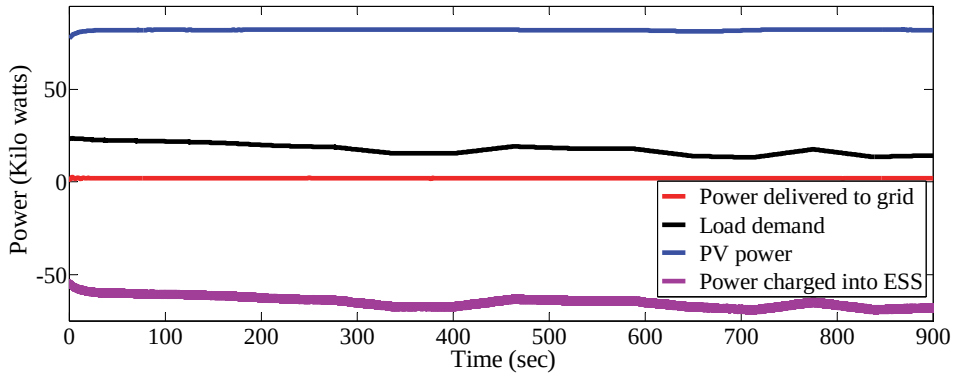

(b)

Figure 3.9. (a) Per unit voltage at PCC when applying cooperative ANFISPID-based PV inverter control scheme and ANFIS-based supervisory EMS during midday (b) the power provided by PV (considering DC to AC derate factor 0.77), active power demand by dynamic loads, charged/ discharged power by BESS and power exchange with the traditional grid.

Figure 3.10 depicts the injected/ absorbed reactive power by PV inverter both in the presence and absence of cooperative BESS. It shows that necessary reactive power injection/ absorption gets lessened when BESS is implemented to cooperate simultaneously for voltage regulation.

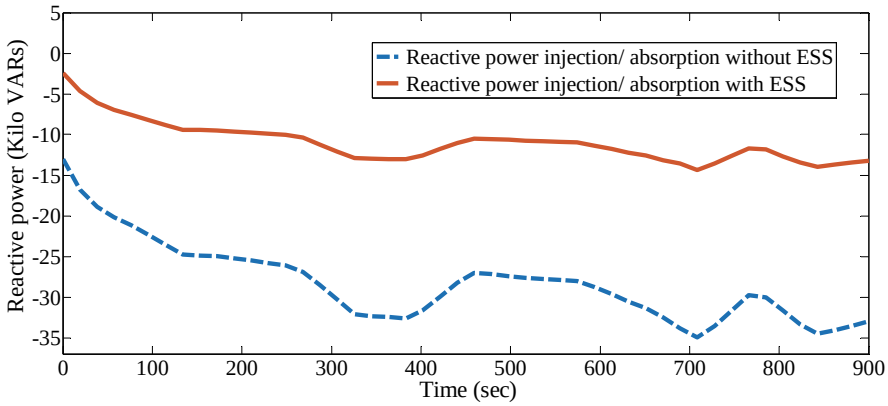

Figure 3.10. Reactive power absorbed by PV inverter during midday with and without cooperative ESS.

Now, the comparison of the proposed ANFISPID-based control scheme with classic PID-based control scheme is illustrated in figure 3.11. If a classic PID with constant control parameters is applied on PV inverter for voltage regulation, it starts to provide oscillatory response due to dynamic changes in operating conditions. In figure 3.11, we can see that, classical PID starts to provide oscillatory response from time= 295 seconds while ANFISPID-based control scheme is showing robustness and keeping the PCC and DC bus voltage around its nominal value without oscillation.

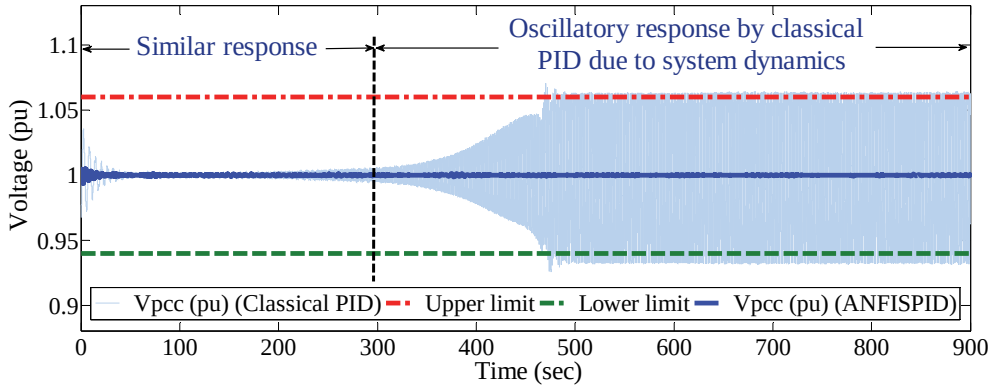

(a)

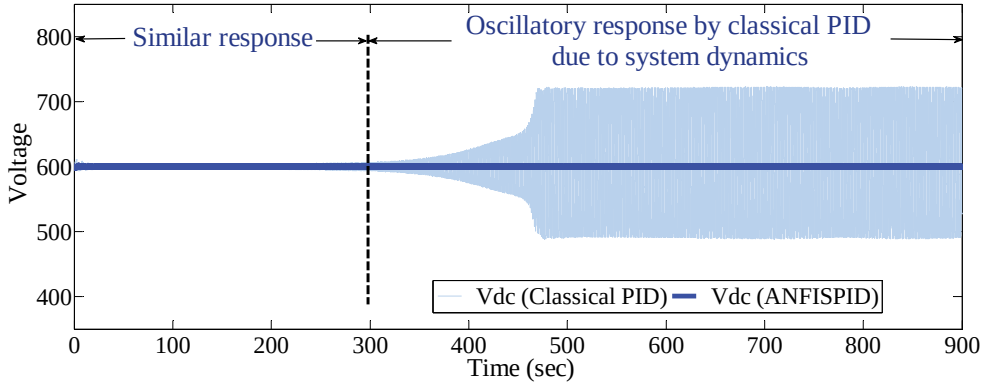

(b)

Figure 3.11. Comparison of the proposed ANFISPID-based PV inverter control scheme with classic PID-based PV inverter control scheme for PCC (a) and dc-bus (b) voltage regulation during midday

3.7.2 Case 2: Low or no PV generation with evening peak loads

Figure 3.12 illustrates the voltage profile during evening when the PV generation is minimal and the consumer load is at peak. Voltage at PCC exceeds lower permissible limit and remains in non-permissible zone from time= 651 seconds to time= 800 seconds.

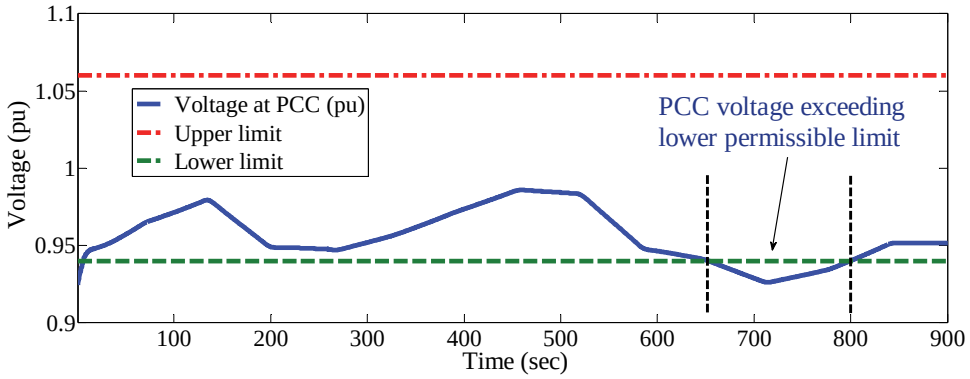

Figure 3.12. Impact of low or no PV generation with evening peak load on PCC voltage

Figure 3.13 (a) shows that per unit voltage at PCC is being regulated nearly around nominal voltage (1 per unit (pu) or 240 Volts) and within the permissible zone when proposed cooperative voltage regulation is implemented. Figure 3.13 (b) illustrates the power sharing of the system.

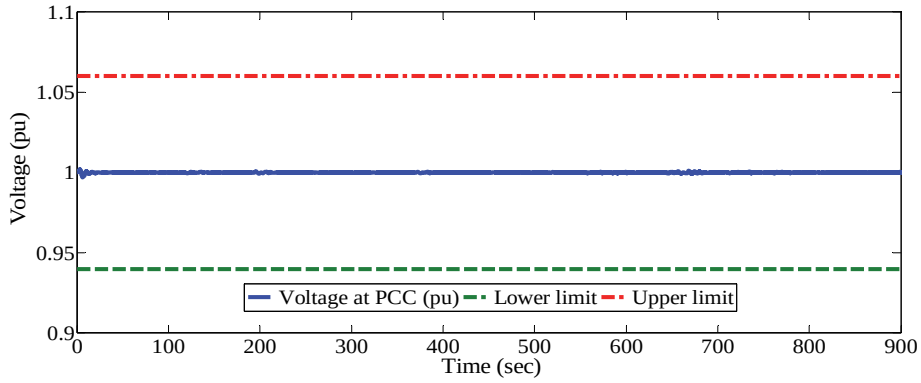

(a)

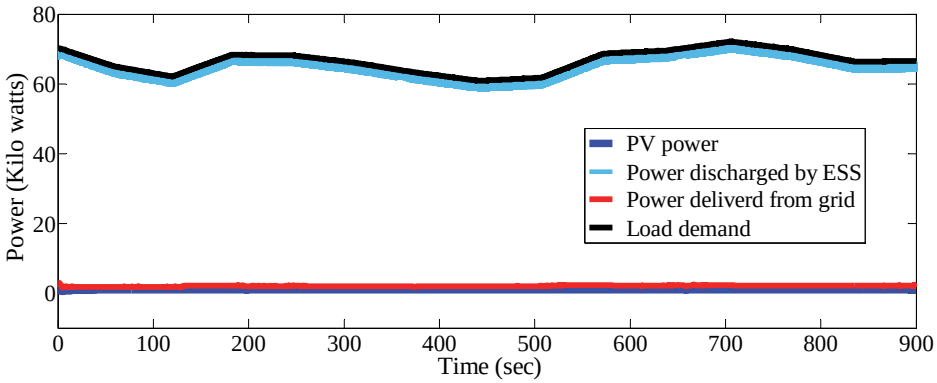

(b)

Figure 3.13. (a) Per unit voltage at PCC when applying cooperative ANFISPID-based PV inverter control scheme and ANFIS-based supervisory control on BESS during evening peak load (b) The Power provided by PV (considering DC to AC derate factor 0.77), active power demand by dynamic loads, charged/ discharged power by BESS and power delivered from grid during evening peak load.

Figure 3.14 illustrates the reactive power being injected by the PV inverter to raise the voltage sags during evening peak load demand both in the presence and absence of cooperative BESS.

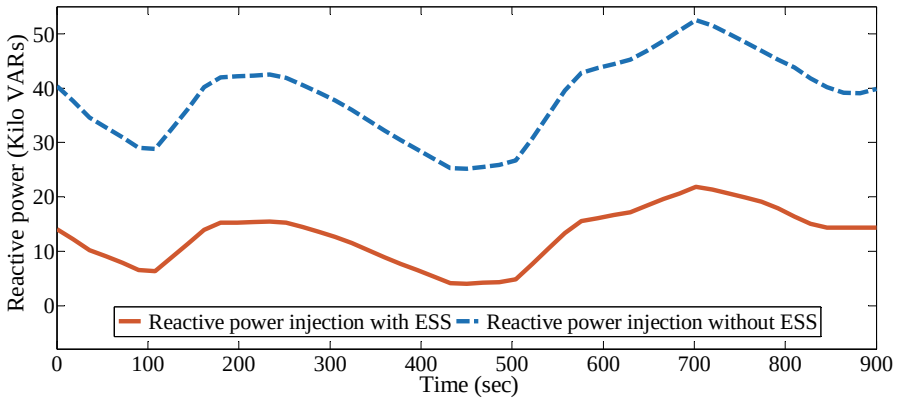

Figure 3.14. Reactive power injected by PV inverter for voltage regulation during evening peak load with and without cooperative BESS.

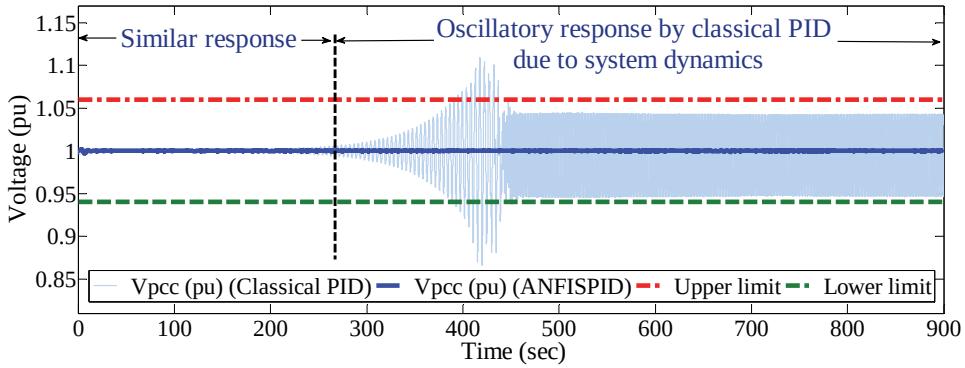

(a)

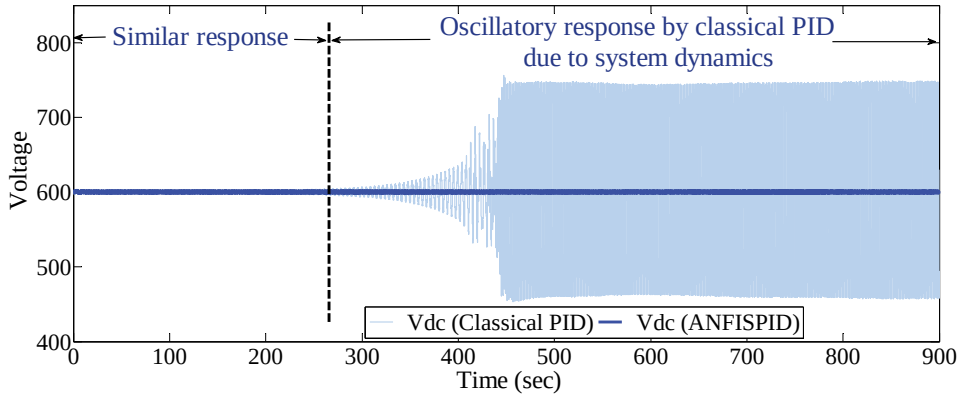

(b)

Figure 3.15. Comparison of the proposed ANFISPID-based PV inverter control scheme with classic PID-based PV inverter control scheme for (a) PCC and (b) dc-bus voltage regulation during evening.

Now, the comparison of the proposed ANFISPID-based control scheme with classic PID-based control scheme is illustrated in figure 3.15. If a classic PID with constant control parameters is applied on the system for voltage regulation, it starts to provide oscillatory response when the control parameters get obsolete with respect to system dynamics. In figure 3.15, we can see that, classic PID starts to provide oscillation from time= 261 seconds while ANFISPID-based control scheme is keeping the PCC and DC bus voltage around its nominal value with damped oscillations.

3.7.3 Case 3: Sudden voltage fluctuations due to cloud passing or large load start

The cooperative performance of the ANFISPID-based PV inverter control scheme and ANFIS-based supervisory EMS has been assessed for sudden voltage fluctuations at PCC during momentary incidents like cloud passing, large load starts etc. Impact of these momentary incidents has been depicted in Figure 3.16 where sudden PCC voltage fluctuations caused by these issues have been illustrated.

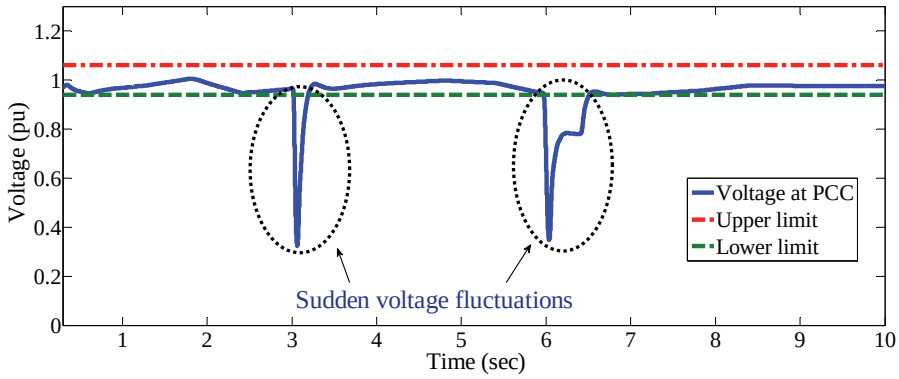

Figure 3.16. Sudden voltage fluctuations at PCC

Figure 3.17 (a) shows that the PCC voltage is being regulated around nearly the nominal voltage because of the application of cooperative ANFISPID-based PV inverter control scheme and ANFIS-based supervisory EMS. Figure 3.17 (b) depicts the power exchanges of the system during momentary incidents. Figure 18 shows the reactive power injection by PV inverter to mitigate the sudden voltage fluctuations both in the presence and absence of cooperative BESS.

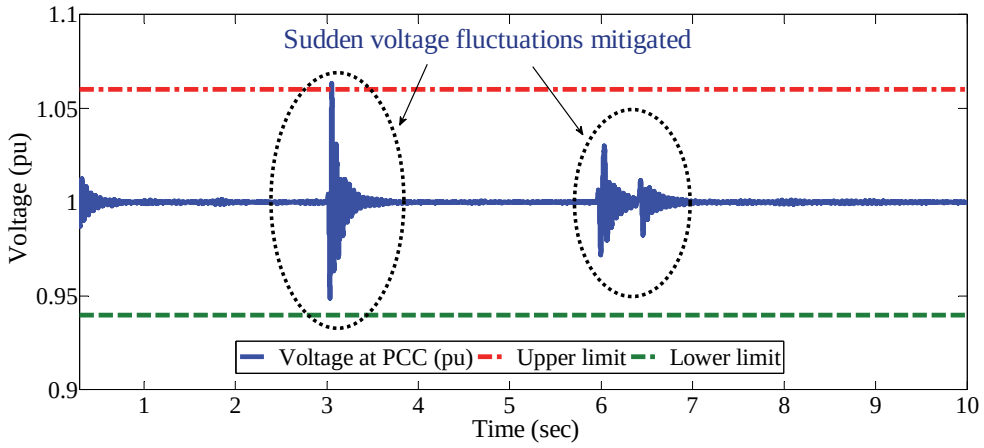

(a)

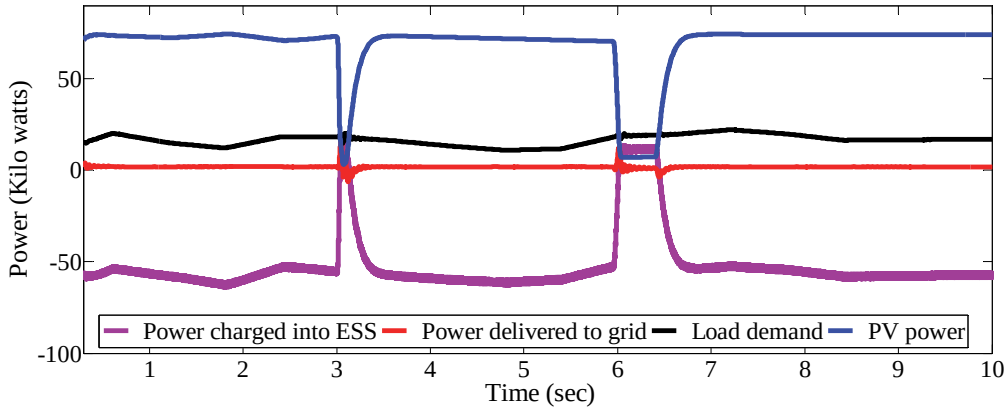

(b)

Figure 3.17. (a) Per unit voltage at PCC when applying cooperative ANFISPID-based PV inverter control scheme and ANFIS-based supervisory EMS on BESS during sudden voltage fluctuations and (b) The Power provided by PV (considering DC to AC derate factor 0.77), active power demand by dynamic loads, charged/ discharged power by BESS and power delivered to grid during momentary fluctuations.

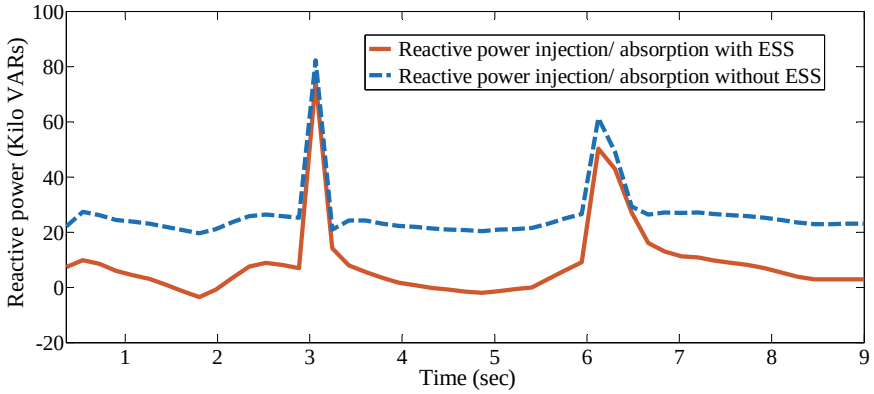

Figure 3.18. Reactive power injected by PV inverter for voltage regulation during sudden voltage fluctuations with and without cooperative BESS.

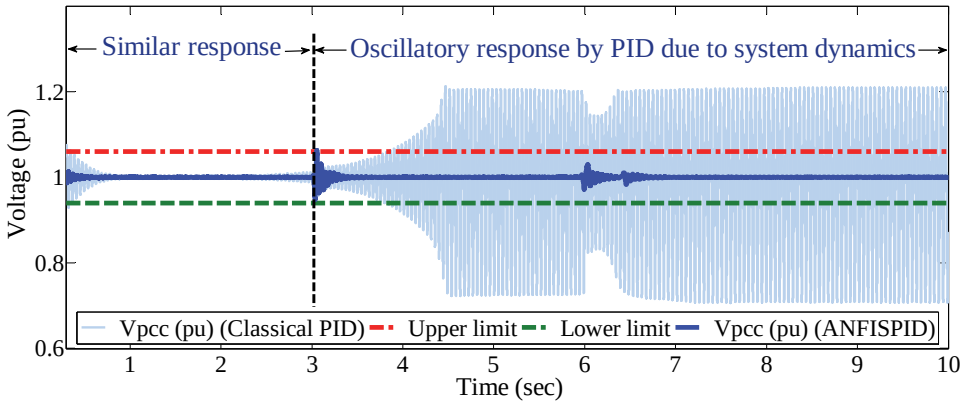

(a)

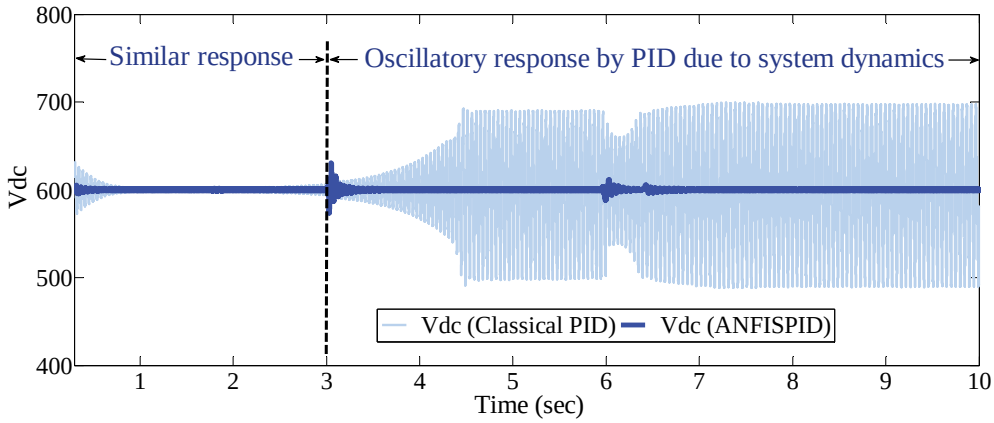

(b)

Figure 3.19. Comparison of the proposed ANFISPID-based PV inverter control scheme with classic PID-based PV inverter control scheme for (a) PCC and (b) dc-bus voltage regulation during sudden voltage fluctuations.

The comparison of the proposed ANFISPID-based control scheme with classic PID-based control scheme is illustrated in figure 3.19. If a classic PID with constant control parameters is applied on the system for voltage regulation, it starts to provide oscillatory response due to dynamic changes in operating conditions. In figure 3.19, we can see that, classic PID starts to provide oscillation from time= 298 seconds while ANFISPID-based control scheme is damping oscillations.

3.7.4 Case 4: Three-phase balanced grid-fault at PCC

In this case, the performance of the proposed cooperative voltage regulation strategy has been assessed for three-phase symmetric fault at PCC. In figure 3.20, a moderate balanced three-phase fault has been emulated at time= 1 second at PCC that sags the voltage profile near to 0.69 pu at time= 1.02 second. Then, the voltage sag gradually drops and reaches to 0.80 pu voltage at time= 1.35 second.

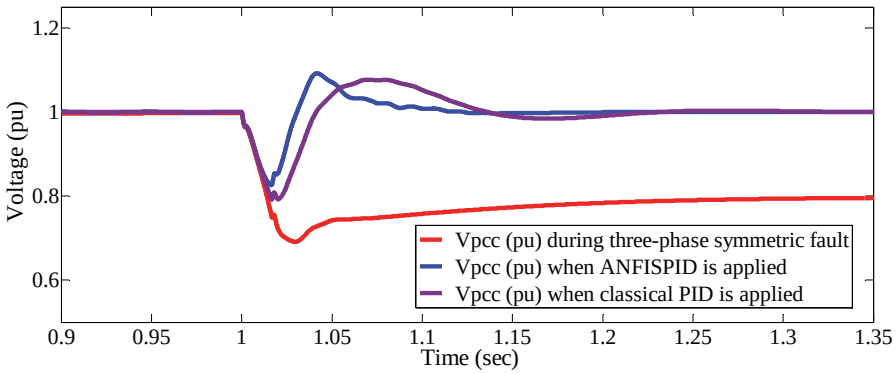

Figure 3.20. The per unit voltage at PCC when a three-phase symmetric fault occurs and when ANFISPID-based PV inverter control scheme and classic PID-based PV inverter control scheme are applied with corresponding EMS on BESS.

Here, we can see that, LVRT capability augmentation is provided by the proposed strategy. When the ANFISPID-based PV inverter control scheme is applied, PCC voltage falls downs to 0.82 (pu) at time= 1.017 seconds, then rises up to 1.092 pu at time= 1.04 seconds. Then, the PCC voltage settles down to nominal value at time= 1.1 second. The total fault clearing time of proposed ANFISPID-based control scheme is 0.1 second. On the other hand, the PCC voltage falls down to 0.79 (pu) at time= 1.01 second and rises up to 1.07 (pu) at time= 1.07 seconds when classic PID-based PV inverter control scheme is applied. After that PCC voltage settles down to nominal voltage at time= 1.35 seconds. The total fault clearing time for the

classic PID is 0.35 second which is more than the fault clearing time when ANFISPID-based PV inverter control scheme is applied (0.1 second).

Table 3.II shows the index values of the ANFISPID-based PV inverter control scheme and classic PID-based PV inverter control scheme for discussed case studies.

TABLE 3.II. INDEX VALUES OF THE PV INVERTER CONTROL SCHEMES

Case		**control index**	**ANFISPID**	**PID**
Case 1	ITSE	Active power control	0.81	2156.4
	ITAE	Active power control	0.18	24.98
	ITSE	Reactive power control	0.16	136.08
	ITAE	Reactive power control	0.01	6.51
	THD	PCC voltage	3.41%	5.17%
	THD	DC bus voltage	4.80%	15.15%
Case 2	ITSE	Active power control	0.65	3020
	ITAE	Active power control	0.25	27.78
	ITSE	Reactive power control	0.07	22.66
	ITAE	Reactive power control	0.01	2.48
	THD	PCC voltage	2.70%	4.85%
	THD	DC bus voltage	4.43%	17.13%
Case 3	ITSE	Active power control	2.2	1471.1
	ITAE	Active power control	0.3	19.97
	ITSE	Reactive power control	0.55	466.31
	ITAE	Reactive power control	0.12	11.07
	THD	PCC voltage	3.82%	18.43%
	THD	DC bus voltage	5.06%	14.21%
Case 4	ITSE	Active power control	2.79	3.26
	ITAE	Active power control	0.07	0.06
	ITSE	Reactive power control	0.82	0.84
	ITAE	Reactive power control	0.03	0.031
	THD	PCC voltage	10.98%	9.85%
	THD	DC bus voltage	11.88%	15.13%

It shows that, the proposed ANFISPID-based control scheme provides overall superior performance over the classic PID-based control scheme in all the cases. The integral time absolute error (ITAE), integral time square error (ITSE) and total harmonic distortion (THD) values for the classic PID-based control scheme are much larger than the proposed ANFISPID-based control scheme because of the oscillatory response that the classic PID-based control scheme starts to provide and all the deviated PCC voltages from reference values (errors) and square of those deviated PCC voltages (square of errors) during oscillations get integrated all through the experiment time. Besides, the simulation results show that the oscillatory response provided by the classic PID-based control scheme may cause the PCC voltage to exceed the permissible voltage range (figure 3.11 (a), 3.15 (a), 3.19 (a)). This will result in disconnection of consumers and will arise several critical power system contingencies which are expensive to recover. The results also show that the proposed ANFISPID-based intelligent PV inverter control scheme provides robust response under any system nonlinearities and fluctuations and damps oscillations which prevents these contingencies from arising and ensures better power system security.

3.7.5 Comparison between ANFIS-based supervisory energy management system and classic state-based energy management system

Simulations have been performed to assess both the ANFIS-based supervisory energy management system and state-based energy management system for a week long time-frame and the comparison result has been shown in figure 3.21.

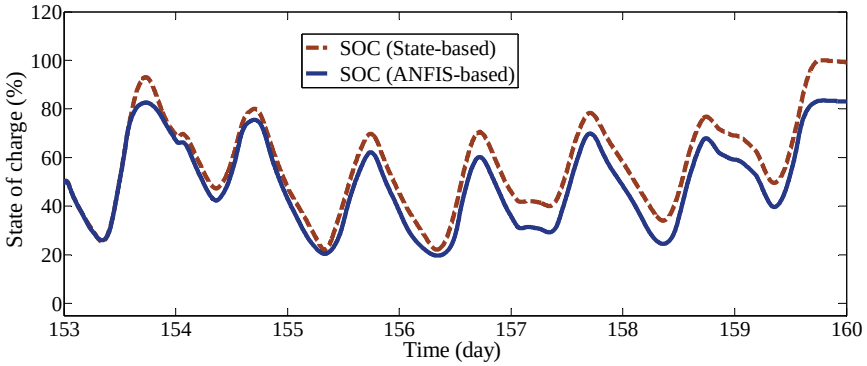

Figure 3.21. Comparison of BESS state of charge (%) when ANFIS-based supervisory energy management system and state-based energy management system are applied for one week time-frame.

In figure 3.21, we can see that the state-based energy management system charges and discharges more than ANFIS-based supervisory energy management system that reduces the battery lifetime and increases expense. Both of the EMS control strategies protect the battery from being over-charged and over-discharged and BESS in not allowed to discharge more than 20% and charging stops when SOC reaches 100%. Depending on the available PV power and the dynamic load demand, the charging and discharging rates vary all over the day and all through the year. Comparison of the battery efficiency when each of the energy management systems is implemented is depicted in table 3.III.

TABLE 3.III. Battery efficiency

Parameter		ANFIS-based	State-based
$\boldsymbol{\eta_{bat}}$	Battery efficiency (%)	78.0	74.64

Table 3.III shows that proposed ANFIS-based supervisory energy management system ensures better battery efficiency than classic state-based energy management system.

3.8 Conclusion

Voltage regulation issue is one of the most significant issues that needs to be taken care of for ensuring system stability. A two-stage cooperative operation of ANFISPID-based PV inverter control scheme and ANFIS-based supervisory EMS has been implemented in this chapter in real time to regulate the PCC voltage of weak distribution networks interconnected with large-scale PVs. Case studies showed that the ANFIS-based supervisory EMS cooperates with ANFISPID-based PV inverter control scheme by reducing PCC voltage deviation thus reducing necessary reactive power injection/ absorption by the inverter for voltage regulation. This reduces line losses through the system and overall expenses. Besides, simulation studies showed that ANFIS-based supervisory EMS ensures longer BESS life span and better BESS efficiency which increases economic feasibility. Unlike conventional PID, the ANFISPID-based PV inverter control scheme damps oscillations and provides robust response while regulating PCC voltage under any worst-case scenarios and three-phase faults. This prevents many critical power system contingencies which are expensive to recover. Moreover, it eliminates the necessity of expensive manual trial-and-error method for tuning conventional PID parameters at a regular basis and provides ‘plug-and-play’ feature for automatic tuning

once implemented. The simulation results were obtained from a realistic model replicating an actual weak distribution network integrated with large-scale of solar PVs. Actual customer load profile data, actual solar irradiance and ambient temperature data had been used to evaluate the performances of the proposed cooperative voltage regulation strategy in real scenarios.

References

[1] Zhang, B., Lam, A. Y., Domínguez-García, A. D., & Tse, D. (2015). An optimal and distributed method for voltage regulation in power distribution systems. *IEEE Transactions on Power Systems*, *30*(4), 1714-1726.

[2] Masters, C. L. (2002). Voltage rise: the big issue when connecting embedded generation to long 11 kV overhead lines. *Power engineering journal*, *16*(1), 5-12.

[3] Quezada, V. M., Abbad, J. R., & Roman, T. G. S. (2006). Assessment of energy distribution losses for increasing penetration of distributed generation. *IEEE Transactions on power systems*, *21*(2), 533-540.

[4] Lopes, J. P., Hatziargyriou, N., Mutale, J., Djapic, P., & Jenkins, N. (2007). Integrating distributed generation into electric power systems: A review of drivers, challenges and opportunities. *Electric power systems research*, *77*(9), 1189-1203.

[5] Chiradeja, P., & Ramakumar, R. (2004). An approach to quantify the technical benefits of distributed generation. *IEEE Transactions on energy conversion*, *19*(4), 764-773.

[6] Mahmud, N., & Zahedi, A. (2016). Review of control strategies for voltage regulation of the smart distribution network with high penetration of renewable distributed generation. *Renewable and Sustainable Energy Reviews*, *64*, 582-595.

[7] Zahedi, A. (2011). A review of drivers, benefits, and challenges in integrating renewable energy sources into electricity grid. *Renewable and Sustainable Energy Reviews*, *15*(9), 4775-4779.

[8] Carvalho, P. M., Correia, P. F., & Ferreira, L. A. (2008). Distributed reactive power generation control for voltage rise mitigation in distribution networks. *IEEE transactions on Power Systems*, *23*(2), 766-772.

[9] Chen, Z., & Kong, W. (2007, January). Protection Coordination Based on a Multi-agent for Distribution Power System with Distribution Generation Units. In *International Workshop on Next Generation Regional Energy System Development*.

[10] Kouro, S., Leon, J. I., Vinnikov, D., & Franquelo, L. G. (2015). Grid-connected photovoltaic systems: An overview of recent research and emerging PV converter technology. *IEEE Industrial Electronics Magazine*, *9*(1), 47-61.

[11] García, P., García, C. A., Fernández, L. M., Llorens, F., & Jurado, F. (2014). ANFIS-based control of a grid-connected hybrid system integrating renewable energies, hydrogen and batteries. *IEEE Transactions on Industrial Informatics*, *10*(2), 1107-1117.

[12] Akcayol, M. A. (2004). Application of adaptive neuro-fuzzy controller for SRM. *Advances in Engineering software*, *35*(3), 129-137.

[13] Han, Y., Young, P. M., Jain, A., & Zimmerle, D. (2015). Robust control for microgrid frequency deviation reduction with attached storage system. *IEEE Transactions on Smart Grid*, *6*(2), 557-565.

[14] Li, H., Li, F., Xu, Y., Rizy, D. T., & Kueck, J. D. (2010). Adaptive voltage control with distributed energy resources: Algorithm, theoretical analysis, simulation, and field test verification. *IEEE Transactions on Power Systems*, *25*(3), 1638-1647.

[15] Yacoubi, L., Al-Haddad, K., Dessaint, L. A., & Fnaiech, F. (2006). Linear and nonlinear control techniques for a three-phase three-level NPC boost rectifier. *IEEE Transactions on Industrial Electronics*, *53*(6), 1908-1918.

[16] Yang, S., Lei, Q., Peng, F. Z., & Qian, Z. (2011). A robust control scheme for grid-connected voltage-source inverters. *IEEE Transactions on Industrial Electronics*, *58*(1), 202-212.

[17] Espi, J. M., Castello, J., Garcia-Gil, R., Garcera, G., & Figueres, E. (2011). An adaptive robust predictive current control for three-phase grid-connected inverters. *IEEE Transactions on Industrial Electronics*, *58*(8), 3537-3546.

[18] Li, H., Shi, K. L., & McLaren, P. G. (2005). Neural-network-based sensorless maximum wind energy capture with compensated power coefficient. *IEEE transactions on industry applications*, *41*(6), 1548-1556.

[19] Jang, J. S. (1993). ANFIS: adaptive-network-based fuzzy inference system. *IEEE transactions on systems, man, and cybernetics*, *23*(3), 665-685.

[20] Smith, J. W., Sunderman, W., Dugan, R., & Seal, B. (2011, March). Smart inverter volt/var control functions for high penetration of PV on distribution systems. In *Power Systems Conference and Exposition (PSCE), 2011 IEEE/PES* (pp. 1-6). IEEE.

[21] Rizy, D. T., Xu, Y., Li, H., Li, F., & Irminger, P. (2011, July). Volt/Var control using inverter-based distributed energy resources. In *Power and Energy Society General Meeting, 2011 IEEE* (pp. 1-8). IEEE.

[22] Jahangiri, P., & Aliprantis, D. C. (2013). Distributed Volt/VAr control by PV inverters. *IEEE Transactions on power systems*, *28*(3), 3429-3439.

[23] Camacho, A., Castilla, M., Miret, J., Vasquez, J. C., & Alarcón-Gallo, E. (2013). Flexible voltage support control for three-phase distributed generation inverters under grid fault. *IEEE transactions on industrial electronics*, *60*(4), 1429-1441.

[24] Miret, J., Camacho, A., Castilla, M., de Vicuña, L. G., & Matas, J. (2013). Control scheme with voltage support capability for distributed generation inverters under voltage sags. *IEEE Transactions on Power Electronics*, *28*(11), 5252-5262.

[25] Li, H., Li, F., Xu, Y., Rizy, D. T., & Adhikari, S. (2013). Autonomous and adaptive voltage control using multiple distributed energy resources. *IEEE Transactions on Power Systems*, *28*(2), 718-730.

[26] Reid, D. (2015, April). DQ rotating frame PI control algorithm for power inverter voltage regulation modelling and simulation using the OpenModelica platform. In *SoutheastCon 2015* (pp. 1-4). IEEE.

[27] Khan, O., & Xiao, W. (2016). An efficient modeling technique to simulate and control submodule-integrated PV system for single-phase grid connection. *IEEE Transactions on Sustainable Energy*, *7*(1), 96-107.

[28] Chakraborty, C., Iu, H. H. C., & Lu, D. D. C. (2015). Power converters, control, and energy management for distributed generation. *IEEE Transactions on Industrial Electronics*, *62*(7), 4466-4470.

[29] Miñambres-Marcos, V., Guerrero-Martínez, M. Á., Romero-Cadaval, E., & González-Castrillo, P. (2014). Grid-connected photovoltaic power plants for helping node voltage regulation. *IET Renewable Power Generation*, *9*(3), 236-244.

[30] Meza, J. L., Santibáñez, V., Soto, R., & Llama, M. A. (2012). Fuzzy self-tuning PID semiglobal regulator for robot manipulators. *IEEE Transactions on industrial electronics*, *59*(6), 2709-2717.

[31] Youness, H., Moness, M., & Khaled, M. (2014). MPSoCs and multicore microcontrollers for embedded PID control: A detailed study. *IEEE Transactions on Industrial Informatics*, *10*(4), 2122-2134.

[32] Yu, J., & Liu, C. (2015, August). Design of self-tuning PID controller with fuzzy variable parameters based on LabView. In *Information and Automation, 2015 IEEE International Conference on* (pp. 2586-2591). IEEE.

[33] Dehghani, A., & Khodadadi, H. (2015, October). Fuzzy Logic Self-Tuning PID control for a single-link flexible joint robot manipulator in the presence of uncertainty. In *Control, Automation and Systems (ICCAS), 2015 15th international conference on* (pp. 186-191). IEEE.

[34] Altin, N., & Sefa, İ. (2012). dSPACE based adaptive neuro-fuzzy controller of grid interactive inverter. *Energy Conversion and Management*, *56*, 130-139.

[35] Kabir, M. N., Mishra, Y., Ledwich, G., Dong, Z. Y., & Wong, K. P. (2014). Coordinated control of grid-connected photovoltaic reactive power and battery energy storage systems to improve the voltage profile of a residential distribution feeder. *IEEE Transactions on industrial Informatics*, *10*(2), 967-977.

[36] SolarHub, "PV Module SPR-305-WHT Details," (2016) [On-line]. Available: http://www.solarhub.com/solarhub_products/776-SPR-305-WHT-SunPower

[37] System Advisor Model (SAM) (2010) [On-line] Website: https://sam.nrel.gov/

[38] Australia, Bureau of Meteorology, 2016. Website: www.bom.gov.au

[39] De Brito, M. A., Sampaio, L. P., Luigi, G., e Melo, G. A., & Canesin, C. A. (2011, June). Comparative analysis of MPPT techniques for PV applications. In *Clean Electrical Power (ICCEP), 2011 International Conference on* (pp. 99-104). IEEE.

[40] Tremblay, O., & Dessaint, L. A. (2009). Experimental validation of a battery dynamic model for EV applications. *World Electric Vehicle Journal*, *3*(1), 1-10.

[41] Fullriver, "*DC Series:* AGM Batteries for Deep Cycle Service," (2016) [On-line]. Available*:* http://www.fullriver.com/products/admin/upfile/DC80-12.pdf

[42] SimPowerSystems, T. M. "Reference, Hydro-Québec and the MathWorks." *Inc., Natick, MA* (2010).

[43] "Residential active and reactive power demand data" (2015): Ergon energy, Queensland, Australia. Website: https://www.ergon.com.au

[44] Milosevic, M. (2003). Decoupling control of d and q current components in three-phase voltage source inverter. *Tech. Rep., Technical Report, ETH Zurich*.

[45] Teodorescu, R., Liserre, M., & Rodriguez, P. (2011). *Grid converters for photovoltaic and wind power systems* (Vol. 29). John Wiley & Sons.

[46] Taher, A. (2010). Adaptive Neuro-Fuzzy Systems. In *Fuzzy Systems*. Intech.

[47] Singh, M., & Chandra, A. (2013). Real-time implementation of ANFIS control for renewable interfacing inverter in 3P4W distribution network. *IEEE Transactions on Industrial Electronics*, *60*(1), 121-128.

[48] Bebic, J., Walling, R., O'Brien, K., & Kroposki, B. (2009). The sun also rises. *IEEE Power and Energy Magazine*, *7*(3).

[49] Hennessy, T., & Kuntz, M. (2005, June). The multiple benefits of integrating electricity storage with wind energy. In *Power Engineering Society General Meeting, 2005. IEEE* (pp. 1952-1954). IEEE.

[50] Rahman, S., & Bhatnagar, R. (1988). An expert system based algorithm for short term load forecast. *IEEE Transactions on Power Systems*, *3*(2), 392-399.

[51] Alam, M. J. E., Muttaqi, K. M., & Sutanto, D. (2012, July). Distributed energy storage for mitigation of voltage-rise impact caused by rooftop solar PV. In *Power and Energy Society General Meeting, 2012 IEEE* (pp. 1-8). IEEE.

[52] Rahman, M. S., Hossain, M. J., & Lu, J. (2015, September). Utilization of parked EV-ESS for power management in a grid-tied hybrid AC/DC microgrid. In *Power Engineering Conference (AUPEC), 2015 Australasian Universities* (pp. 1-6). IEEE.

[53] Rahman, M. S., Hossain, M. J., & Lu, J. (2016). Coordinated control of three-phase AC and DC type EV–ESSs for efficient hybrid microgrid operations. *Energy Conversion and Management*, *122*, 488-503.

[54] Hara, R., Kita, H., Tanabe, T., Sugihara, H., Kuwayama, A., & Miwa, S. (2009). Testing the technologies. *IEEE Power and energy magazine*, *7*(3).

[55] Yoshimoto, K., Nanahara, T., Koshimizu, G., & Uchida, Y. (2006, October). New control method for regulating state-of-charge of a battery in hybrid wind power/battery energy storage system. In *Power Systems Conference and Exposition, 2006. PSCE'06. 2006 IEEE PES* (pp. 1244-1251). IEEE.

[56] Mahmud, M. A., Hossain, M. J., & Pota, H. R. (2014). Voltage variation on distribution networks with distributed generation: Worst case scenario. *IEEE Systems Journal*, *8*(4), 1096-1103.

[57] Castañeda, M., Cano, A., Jurado, F., Sanchez, H., & Fernandez, L. M. (2013). Sizing optimization, dynamic modeling and energy management strategies of a stand-alone PV/hydrogen/battery-based hybrid system. *International journal of hydrogen energy*, *38*(10), 3830-3845.

Chapter 4

A Novel Event-triggered Communication-Based Distributed Cooperative Voltage Control Strategy For Large Grid-tied PV System

"Mahmud, N., Zahedi, A., & Jacob. M. (2017) A novel event-triggered communication-based distributed cooperative voltage control strategy for large grid-tied PV system *IEEE Transactions on Industrial Informatics*. (Under review)"

Abstract

In this chapter, the voltage regulation problem of low-voltage distribution network with large-scale penetration of solar photovoltaics (PVs) has been addressed. A discrete event-triggered communication-based distributed cooperative control strategy has been proposed to control Battery Energy Storage Systems (BESSs) and PV interfacing inverters for feeder voltage regulation that requires minimal communication. The distributed cooperative voltage control strategy has been separated into two different control layers (distributed control layer and cooperative control layer). Discrete event-triggered communication mechanism has been implemented among neighbour agents in each layer and appropriate triggering conditions have been designed that dramatically reduces the amount of communication and relax the real-time information exchange requirement among agents. A realistic radial distribution feeder has been designed in MATLAB/ Simulink environment to show that the proposed discrete event-triggered distributed cooperative voltage control strategy requires lower communication rates while preserving the desired voltage control performance.

4.1 Introduction

Large-scale penetration of solar PVs into conventional power system is becoming a popular tradition rapidly. This tradition arises several technical challenges among which voltage regulation challenge is the most significant. Voltage regulation problem mainly results from the reverse power flow caused by excess PV power, generated during high solar irradiation period and this problem tends to limit the amount of PV penetration into grid [1], [2].

Various sorts of strategies have been proposed to mitigate the voltage regulation problem that include network reconfiguration [3-5], power curtailment [6], reactive power injection/ absorption [7], utilization of energy storage systems [8] etc. Active power curtailment reduces the efficiency of solar PVs and causes wastage of generated power [9]. The reactive power capability of PV inverters is limited and injection/ absorption of reactive power increases the line loss through the system. Moreover, the impact of injected/ absorbed reactive power on the voltage profile of low-voltage distribution feeder is minimal because of the higher R/X ratio. Therefore, the solo-implementation of PV inverter reactive power will require inverters with higher power rating, which is expensive. Utilizing energy storage system (e.g. BESS) is another effective strategy to regulate the feeder voltage [10]. This strategy is more effective in system with higher R/X ratio as it stores/ discharges active power for voltage control. However, frequent charge/ discharge reduces the life span of BESS and solo-implementation of BESS for voltage regulation needs very large BESS capacity, which is expensive and unfeasible. In this scenario, a cooperative operation of BESS and PV inverter for feeder voltage regulation is advantageous [11], [12]. In this chapter, a cooperative operation among neighbour BESSs and PV inverters will be proved advantageous to regulate the feeder voltage with reduced inverter power rating, power loss through system and BESS capacity.

Since PV generators are located in a heterogeneous and distributed fashion through low-voltage feeders, distributed control strategies are required to improve the stability, scalability and security of the system. Distributed control strategy has become popular nowadays in controlling BESSs and PV inverters [13-21] due to its robustness to individual agent errors, scalability with respect to increased number of agents and reduced computational load. A distributed algorithm has been proposed in [13] to regulate output power of dispersed energy storage system. A distributed cooperative control strategy has been proposed in [14] to maintain supply-demand balance. However, [13], [14] did not consider the technical limitations of energy storage system, which are storage capacity and SOC. [15] has proposed a distributed

energy management system for SOC balancing in DC micro grids. An improved distributed cooperative control has been developed in [16] that performs dynamic energy level balancing between BESSs for islanded micro grids. A distributed cooperative control strategy has been employed in [17] to coordinate power sharing among heterogeneous energy storage devices. A consensus-based distributed voltage control strategy has been proposed in [18] that guarantees a desired reactive power distribution in steady state and requires distributed communication among inverters. [19] proposed a weighted average consensus protocol to synchronize the average voltage to a reference value assuming varying communication topologies and time delays. A coordinated control method composed of local and distributed control has been proposed in [20] for distributed BESSs where an identical capacity has been assumed for batteries and a similar reference waveform is considered to control the SOC of all batteries. In [10], combination of a local droop-based control method and a distributed cooperative control algorithm has been proposed to utilize BESS capacity efficiently for voltage regulation. All of the existing results on distributed cooperative voltage control of low-voltage distribution feeder interconnected with DGs including the ones mentioned above have been based on an explicit assumption that data communication among agents is performed continually at every instant of time or periodically at equidistant sampling instants. However, the communication network of a distribution grid usually has limited bandwidth and therefore, an efficient use of the communication infrastructure is desirable [21]. In this scenario, introducing the need-based aperiodic communication scheme, such as self-triggered or event triggered communication can significantly reduce those unnecessary sample-state transmissions and make effective use of the communication network [22]-[24]. In the event-triggered communication scheme, a sample-state transmission between agents is triggered when a state-measurement error exceeds a given threshold while in the self-triggered communication scheme, the next triggering time instant is determined by the previous received data and knowledge on plant dynamics. Most recently, a self-triggered communication-based consensus approach has been applied for distributed generation control in microgrids [25]. However, in self-triggered communication scheme, the next triggering time is precomputed depending upon previously received data. That is not an appropriate approach in a stochastic system (like grid-tied PV system) because an emergency triggering situation may appear any time before the precomputed triggering instant. In that case, implementing event-triggered communication-based control scheme ensures better performance as the triggering instants are executed depending upon the dynamic state measurements of the stochastic system. In this chapter, a discrete event-triggered communication-based distributed cooperative control scheme has been proposed to save the

limited network resource while preserving the desired voltage control performance. It is 'discrete' as state measurements and error computations are performed in discrete time instants to determine whether the measured state should be transmitted. Therefore, extra hardware for continuous measurement and computation is not necessary like it is for continuous event-triggered communication schemes [26], [27].

In the proposed distributed cooperative voltage control strategy, the distributed voltage control and the cooperative voltage control have been separated into two different control layers. In the distributed voltage control layer, a leader-following consensus-based distributed voltage control strategy has been implemented on BESSs, connected with each bus through the feeder. Unlike [13], [14], the technical limitations of BESSs have been considered in this chapter and the cooperative voltage control layer is initiated for each bus when BESS of that bus reaches its technical limit (during distributed voltage control layer). The cooperative voltage control layer is implemented on BESSs and PV inverters in two different stages to provide cooperative voltage support when distributed voltage control is unavailable. Then, discrete event-triggered communication scheme has been introduced among neighbour agents for information transmission in both the control layers. Simulation results will show that separating the distributed cooperative control strategy into different layers and implementing the discrete event-triggered communication scheme for data transmission reduce the amount of communication among agents while preserving the voltage control performance. To the authors' knowledge, this is the first time that a distributed cooperative voltage control, separated into two different layers and introduced with discrete event-triggered communication scheme, has been implemented to regulate the voltage through low-voltage distribution feeder with highly penetrated solar PVs.

This chapter is organized as follows. Section 4.2 describes and analyses the voltage control issue of large grid-tied PV system. Section 4.3 details the proposed event-triggered distributed cooperative control strategy for voltage regulation. Section 4.4 details the case studies and simulation results and section 4.5 establishes the conclusion derived from the work.

4.2 Problem description and analysis

4.2.1 Distribution network model

A low-voltage radial distribution feeder has been adopted to evaluate the performance of the discrete event-triggered communication-based distributed cooperative voltage control strategy. Figure 4.1 depicts the low-voltage radial test distribution feeder.

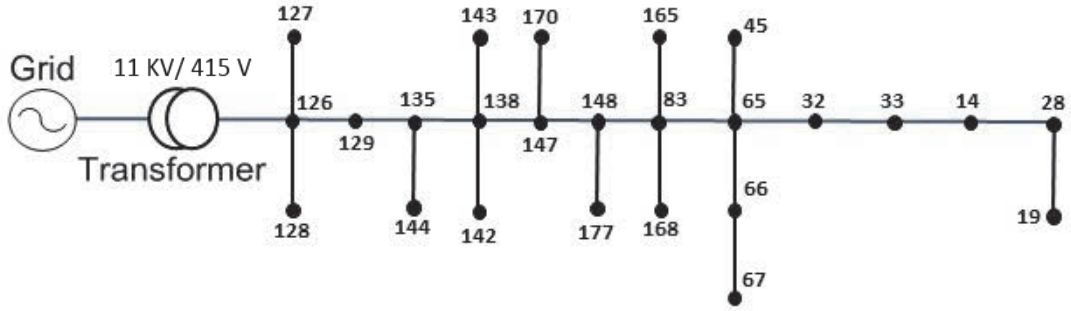

Figure 4.1. Radial test distribution feeder.

In each bus, a solar PV, a BESS and a residential load are connected and it has been considered that a solar PV and a BESS form a distributed generator (DG). Each DG is connected with the distribution feeder through a 3-phase DC/ AC inverter. A maximum power point tracking (MPPT) controller controls the DC-DC boost converter to maximize the PV power output implementing "perturb and observe" algorithm. A BESS is connected to the DC-bus through a bidirectional DC-DC buck-boost converter. Rooftop solar PVs, connected to the feeder in this study, are heterogeneously distributed and solar panel sizing is not proportional to the amount of load through the feeder.

Figure 4.2 illustrates a detailed diagram of a low-voltage radial distribution feeder. If the power generated by rooftop PV is more than the power consumed by load and power charged into BESS together, the excess complex power at bus m, S_m is injected into distribution feeder.

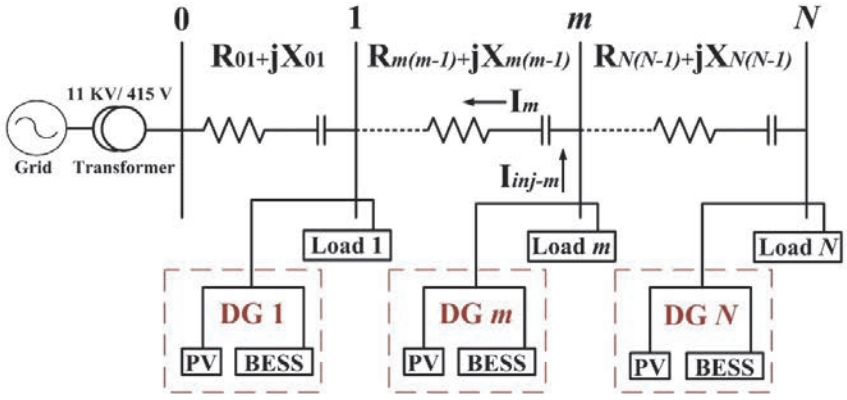

Figure 4.2. Radial distribution feeder with PV, BESS and load.

Therefore, the complex power injected into bus m is,

$$S_m = V_m I_{inj-m}^* \tag{4.1}$$

$$P_m + jQ_m = V_m I_{inj-m}^* \tag{4.2}$$

So, (4.2) can be re-written as,

$$I_{inj-m} = \frac{P_m - jQ_m}{V_m^*}$$

Therefore, the reverse current flow through the feeder at bus *m* is,

$$I_m = \sum_{l=m}^{N} I_{inj-l} = \sum_{l=m}^{N} \frac{P_l - jQ_l}{V_l^*} \tag{4.3}$$

Let us consider, $R_{m(m-1)} + jX_{m(m-1)}$ is the impedance between node m and node $(m-1)$ and I_m is the current flow from node m to node $(m-1)$. Therefore, voltage at bus m can be expressed as,

$$V_m = V_{m-1} + I_m(R_{m(m-1)} + jX_{m(m-1)}) \tag{4.4}$$

Therefore, the voltage deviation between node *m* and node $(m-1)$ can be expressed as,

$$\Delta V_m = V_m - V_{m-1} = \sum_{l=m}^{N} \frac{P_l - jQ_l}{V_l^*} (R_{m(m-1)} + jX_{m(m-1)}) \tag{4.5}$$

$$= \sum_{l=m}^{N} \frac{P_l R_{m(m-1)} + Q_l X_{m(m-1)}}{V_m^*} + j \frac{P_l X_{m(m-1)} - Q_l R_{m(m-1)}}{V_m^*} \quad (4.6)$$

The voltage drop across the feeder is approximately equal to the real part of the voltage drop as the angle between the DG bus voltage and the sending end voltage is very small. If we consider the DG bus voltage as reference bus, the angle of DG bus voltage is 0. As a result, equation (4.6) can be approximated as,

$$\Delta V_m = V_m - V_{m-1} = \sum_{l=m}^{N} \frac{P_l R_{m(m-1)} + Q_l X_{m(m-1)}}{V_m} \quad (4.7)$$

From (4.4), one can see that, both active power (P) and reactive power (Q) have influence on bus voltage deviations. For a low-voltage distribution feeder with high R/X ratio, active power has more impact on bus voltages than reactive power. Besides, the active power charged into BESS for voltage control can be utilized for power supply when there is no solar available [28]. In contrast, injection/ absorption of reactive power for voltage control causes higher power losses through the feeder and lower power factor. Therefore, in this chapter, active power control has been implemented first to regulate the feeder voltage. When BESSs are unavailable for voltage support after reaching their technical limits, the reactive power capability of three phase DC/ AC inverters has been utilized to regulate the voltage.

4.2.2 Communication network model

Consider a system of a group of N interacting agents. The communication connections among the agents can be represented by an undirected communication graph, $\mathcal{g} = \{\nu, \varepsilon\}$. Here, $\nu = \{1, 2, 3\ldots N\}$ is the index set of N agents and ε is the edge set of paired agents where, $\varepsilon \subseteq \nu \times \nu$. $\mathcal{A} = [a_{mn}] \in \mathbb{R}^{N \times N}$ is the weighted adjacency matrix. If nodes m and n can communicate with each other, then there is communication link between them. Therefore, $(m,n) \in \varepsilon$ and $a_{mn} > 0$. In this chapter, agents only from neighbour buses have communication link between them. The communication neighbour set of node m is represented as, $N_m = \{n \in \nu | (m,n) \in \varepsilon\}$. The adjacency matrix, $\mathcal{A} = [a_{mn}]$ can be defined as,

$$\begin{cases} a_{mn} > 0, & \text{if } n \in N_m \\ a_{mn} = 0, & \text{otherwise} \end{cases} \quad (4.8)$$

Here, self-loops are not included. For all $m \in \nu$, $a_{mm} = 0$. The in-degree of node m is defined as $deg_{in}(m) = \sum_{n=1}^{N} a_{mn}$, for any $\in \nu$. The degree matrix is represented as, $\mathcal{D}$ = diag ($deg_{in}(1)$, $deg_{in}(2)$,…… $deg_{in}(N)$). The laplacian matrix of graph $\mathcal{g}$ is given by, $\mathcal{L} = \mathcal{D} - \mathcal{A}$. If

and only if the graph $\mathcal{G}$ is connected, $\mathcal{L}$ has a zero eigenvalue and the corresponding eigenvector is the vector of ones. For an undirected graph, all the eigenvalues are nonnegative and they can be ordered sequentially in an ascending order as, $0 = \lambda_1(\mathcal{G}) \leq \lambda_2(\mathcal{G}) \leq \cdots \leq \lambda_N(\mathcal{G})$. If $\mathcal{G}$ is connected, then $\lambda_2(\mathcal{G}) > 0$.

4.3 Proposed discrete event-triggered distributed cooperative voltage control strategy

The proposed discrete event-triggered communication-based distributed cooperative voltage control strategy is implemented on BESSs and PV inverters from adjacent buses of a low-voltage radial distribution network. This distributed cooperative control is implemented in two separated layers. Which are: 1) Distributed control layer, 2) Cooperative control layer. In distributed control layer, an event-triggered distributed voltage control strategy is implemented among the BESSs to keep the voltages of all the buses within allowable zone. A leader-following consensus algorithm has been developed to control the bus voltages through the feeder in a distributed coordinated fashion. However, voltage support from a BESS is limited as its capacity is limited and BESS stops to charge/ discharge when the state-of-charge (SOC) reaches the upper/ lower limit. Once BESS of any bus reaches its capacity limit during distributed control layer, the cooperative control layer is initiated. In the cooperative control layer, a two-stage cooperative control algorithm has been developed. The two-stage cooperative control is stated below:

Stage 1: The first-stage of cooperative control layer is implemented on BESSs. An event-triggered cooperation algorithm is initiated in the incident of adjacent BESSs being unavailable for voltage control (when SOC reaches limit) and voltage of that adjacent bus exceeding the allowable zone. This algorithm does not require an expensive continuous communication among adjacent BESSs to be operated.

Stage 2: The second-stage of cooperative control layer is implemented on the PV interfacing inverters to provide voltage support if first-stage of cooperative voltage support by adjacent BESSs is no longer available (when BESSs from adjacent buses reach their SOC limit too). The control steps are discussed in details below:

4.3.1 Leader-following consensus algorithm for BESS for distributed voltage control (Distributed control layer)

A distributed coordinated voltage control among BESSs is implemented to keep the bus voltages within allowable zone. In this layer, the BESSs coordinate with immediate adjacent BESSs utilizing limited communication links and decide their respective share of participation (P_m^{ref}) to control the overall feeder voltage in distributed fashion. The share of participation of BESS at the last bus (P_N^{ref}) of radial feeder has been considered as the virtual leader of the distributed control algorithm as the last bus has highest/ lowest voltage in the system [20]. Initially, the share of participation of BESS at last bus (P_N^{ref}) is determined considering equation 4.9. Afterwards, this information is conveyed to other buses through the feeder by communication links between adjacent neighbours. Figure 4.3 depicts the control structure of proposed event-triggered distributed cooperative voltage control implemented on BESS at bus *m*.

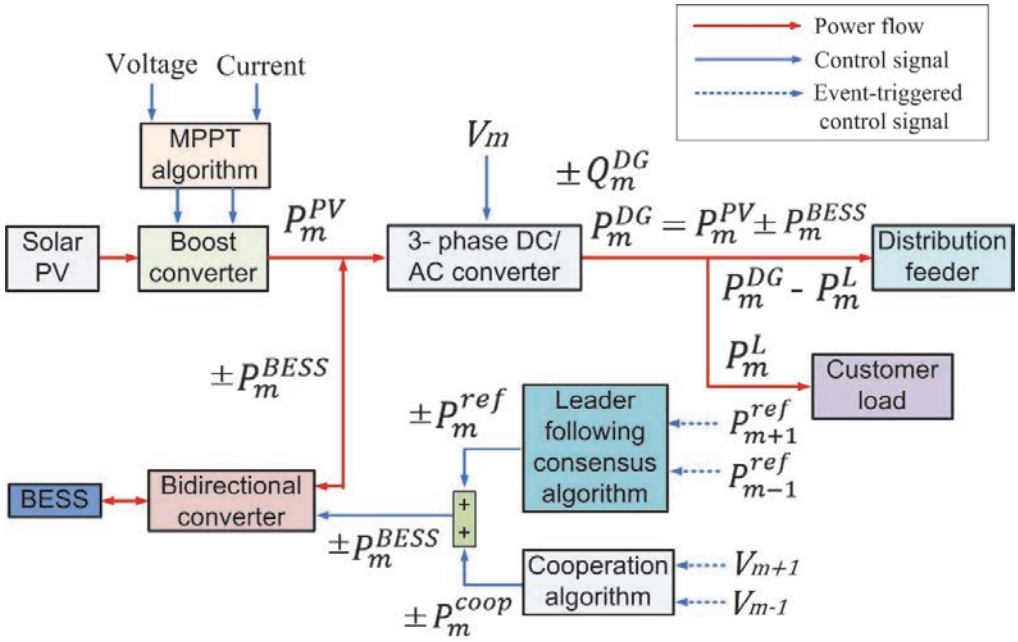

Figure 4.3. Control structure of event-triggered distributed cooperative voltage control implemented on BESS at bus m.

In this chapter, the allowable voltage zone is considered as $\pm 6\%$ of the nominal bus voltage, which means the upper voltage limit (V_{up}) is 1.06 p.u. and lower voltage limit (V_{low}) is 0.94

p.u. The proposed leader-following consensus-based distributed control algorithm will be activated when bus voltages enter into 'critical zone' that is from 1.055 p.u. ($V_{cric\text{-}up}$) to 1.06 p.u. (V_{up}) and from 0.94 p.u. (V_{low}) to 0.945 p.u. ($V_{cric\text{-}low}$). P_N^{ref} can be defined as,

$$P_N^{ref}(t) = \begin{cases} k_1\left(V_{cric-up} - V_N(t)\right), \ when\ V_N(t) > V_{cric-up} \\ 0, \ when\ V_{cric-low} < V_N(t) < V_{cric-up} \\ k_2\left(V_{cric-low} - V_N(t)\right), \ when\ V_N(t) < V_{cric-low} \end{cases} \quad (4.9)$$

Here, coefficients k_1 and k_2 are control gains that determine the accuracy and convergence speed of the control algorithm. P_N^{ref} is then conveyed down through the feeder via communication links between adjacent BESSs.

The share of participation of BESS at bus m can be represented as follows:

$$P_m^{ref}(t) = \sum_{n=1}^{N-1} s_{mn} P_n^{ref}(t) + s_{mN} P_N^{ref}(t), \quad (4.10)$$

Where, $n = 1, 2, 3, \ldots N-1$

When, $V_m(t) > V_{cric-up}$

Or, $V_m(t) < V_{cric-low}$

Where, s_{mn} is the (m, n) entry of a row stochastic matrix $\mathcal{S}$, which can be expressed as,

$$S_{mn} = \frac{a_{mn}}{\sum_{k=1}^{N} a_{mk}} \quad (4.11)$$

In order to implement the distributed voltage control at bus m, BESS at bus m needs to monitor the share of participation of adjacent neighbour BESSs at bus n (considering, $n \in \nu$ and $(m,n) \in \varepsilon$) to generate the distributed voltage control reference, $P_m^{ref}(t)$. Traditionally, signal transmission between adjacent BESSs takes place periodically with a constant sampling period, which requires large real-time information exchange requirements. Event-triggered communication scheme can significantly reduce the occupancy of limited bandwidth while preserving the satisfactory distributed voltage control performance. In this chapter, in the proposed discrete event-triggered communication scheme, the state measurement and error computation are performed only at constant sampling period *h* (at discrete time steps). The measured sampled state is transmitted to neighbour control agents only when the computed error between the measured sampled state and last transmitted state violates a predefined threshold. Let's assume that each bus n transmits the share of participation of $BESS_n$ at time instants denoted by,

$$t_0^n = 0 < t_1^n < \cdots < t_i^n < \cdots, i \in \mathbb{N} \tag{4.12}$$

Let's consider, the transmitted share of participation of $BESS_n$ at event-triggering time instant t_i^n is $P_n^{ref}(t_i^n)$. The computed error at event-triggering time instant t_i^n for distributed voltage control can be defined as,

$$e_n^{dis}(t_i^n) = P_n^{ref}(t_i^n) - P_n^{ref}(t_{i-1}^n) \tag{4.13}$$

If the computed error between the current measured sampled state $P_n^{ref}(t)$ and the last transmitted sampled state $P_n^{ref}(t_{i-1}^n)$ is more than a predefined threshold then the measured state $P_n^{ref}(t)$ is transmitted to the neighbour control agents and $t = t_i^n$. Therefore, considering event-triggered communication scheme, (4.10) can be rewritten as,

$$P_m^{ref}(t) = \sum_{n=1}^{N-1} s_{mn} P_n^{ref}(t_i^n) + s_{mN} P_N^{ref}(t_i^N) \tag{4.14}$$

Where, $n = 1, 2, 3, \ldots, N-1$, $i \in \mathbb{N}$ and $t \in [t_i^n, t_{i+1}^n)$

When, $V_m(t) > V_{cric-up}$ or, $V_m(t) < V_{cric-low}$

By properly controlling the magnitude of computed error, the data transmission frequency between adjacent buses can be significantly reduced while implementing the distributed voltage control through the feeder.

4.3.2 Cooperation algorithm for BESS (first-stage of cooperative control layer)

Initial SOC of BESSs can be different to one another that can be caused by technical problems, uneven charge/ discharge or temporary outages. As a result, BESS can be unavailable for voltage control when SOC reaches its limit and this may cause the bus voltage to exceed the allowable zone. An event-triggered cooperation algorithm has been proposed and its performance has been analysed in this chapter where BESSs from adjacent buses provide voltage support when BESS of a particular bus reaches its SOC limit. If $BESS_n$ reaches its SOC limit during distributed voltage control layer and V_n exceeds the allowable zone, the cooperative control formula for BESS at bus m is:

$$P_m^{coop}(t) = \sum_{n=1}^{N} K_{m3} a_{mn} \left(V_{cric-up} - V_n(t) \right), \tag{4.15}$$

And, $P_m^{coop}(t) = \sum_{n=1}^{N} K_{m4} a_{mn} \left(V_{cric-low} - V_n(t) \right)$ (4.16)

When, $V_n(t) > V_{cric-up}$ and $SOC_n\ (t) > 80$

Or, $V_n(t) < V_{cric-low}$ and $SOC_n\ (t) <\ 20$

Here, coefficients K_{m3} and K_{m4} are the cooperative control gains for bus m, which determine the control accuracy and convergence speed. To implement the cooperative control formula illustrated in (4.15) and (4.16), data transmission between control agent of $BESS_m$ and voltage measurement agent at bus n is required. Voltage measurement at bus n takes place at discrete time steps with a sampling period h and the measured voltage is transmitted to control agent of $BESS_m$ only when the computed error exceeds a predefined threshold. Let's assume that bus n transmits the voltage measurements at time instants denoted by,

$$t_0^n = 0\ < t_1^n < \cdots < t_j^n < \cdots,\ j\ \in\ \mathbb{N} \tag{4.17}$$

The computed error can be defined as,

$$e_n^{coop}(t_j^n) = V_n\left(t_j^n\right) - V_n\left(t_{j-1}^n\right) \tag{4.18}$$

Here, $V_n\left(t_j^n\right)$ is the transmitted sampled voltage of bus n at event-triggering instant t_j^n. Considering event-triggered communication scheme, (4.15) and (4.16) can be rewritten as,

$$P_m^{coop}(t)=\sum_{n=1}^{N} K_{m3} a_{mn}\left(V_{cric-up} - V_n\left(t_j^n\right)\right), \tag{4.19}$$

$$\text{And, } P_m^{coop}(t) =\sum_{n=1}^{N} K_{m4} a_{mn}\left(V_{cric-low} - V_n\left(t_j^n\right)\right) \tag{4.20}$$

This event-triggered communication-based cooperative control is initiated only when SOC_n reaches its limit considering, $N_m = \{n \in v \mid (m,n) \in \varepsilon\}$. This cooperative control from bus m is added with the share of distributed control at bus m and provides voltage support to both the buses until the voltage deviation is mitigated or SOC_m reaches limit. So, the power charge/ discharge reference for $BESS_m$ is,

$$P_m^{BESS}(t) = P_m^{ref}(t) +\ P_m^{coop}(t) \tag{4.21}$$

4.3.3 Cooperation algorithm for PV inverter (second-stage of cooperative control layer)

If SOC of both $BESS_m$ and $BESS_n$ reach their limits (considering, $(m,n) \in \varepsilon$) and voltage at bus m gets out of allowable zone, reactive power support from PV inverter at bus m is initiated. Figure 4.4 depicts the control structure of PV inverter at bus m.

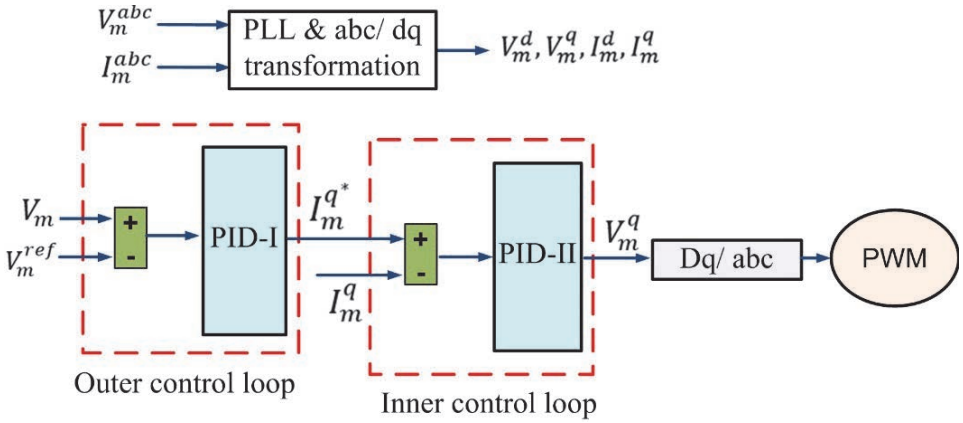

Figure 4.4. Control structure of PV inverter at bus m.

In this study, PV inverter control scheme has been implemented based on dq reference frame theory. The three-phase active power (P) and reactive power (Q), generated by PV inverter at bus m are:

$$P_m(t) = \frac{3}{2}(V_m^d(t)I_m^d(t) + V_m^q(t)I_m^q(t)) \quad (4.22)$$

$$Q_m(t) = \frac{3}{2}(V_m^q(t)I_m^d(t) - V_m^d(t)I_m^q(t)) \quad (4.23)$$

Assuming that the d-axis component is perfectly aligned with the grid voltage V_m^q = 0, the active power and the reactive power will therefore be proportional to I_m^d and I_m^q respectively:

$$P_m(t) = \frac{3}{2}V_m^d(t)I_m^d(t) \quad (4.24)$$

$$Q_m(t) = -\frac{3}{2}V_m^d(t)I_m^q(t) \quad (4.25)$$

The current q component I_m^q is controlled by generating reference $I_m^{q\,*}$ to manage appropriate reactive power injection/ absorption by the PV inverter. The control algorithm for reactive power support by PV inverter at bus m can be formulated as:

$$I_m^{q\,*}(t) = K_{p1}\left(V_{ref} - V_m(t)\right) + K_{i1}\int\left(V_{ref} - V_m(t)\right)dt + K_{d1}\frac{d\left(V_{ref} - V_m(t)\right)}{dt} \quad (4.26)$$

$$V_m^q(t) = K_{p2}\left(I_m^{q\,*}(t) - I_m^q(t)\right) + K_{i2}\int\left(I_m^{q\,*}(t) - I_m^q(t)\right)dt + K_{d2}\frac{d\left(I_m^{q\,*}(t) - I_m^q(t)\right)}{dt} \quad (4.27)$$

When, $V_m(t) > V_{cric-up}$, $SOC_m > 80$ and $SOC_n > 80$

Or, $V_m(t) < V_{cric-low}$, $SOC_m < 20$ and $SOC_n < 20$

This way, PV inverter mitigates the voltage deviation from allowable limit at the second-stage of cooperative control layer.

4.4 Application of the proposed discrete event-triggered distributed cooperative control

The performance of the proposed discrete event-triggered communication-based distributed cooperative voltage control strategy has been analysed in a low-voltage radial test distribution feeder (illustrated in figure 4.1). The radial distribution feeder has been designed and simulated in Matlab/ Simulink environment. The solar irradiance (W/m^2) and ambient temperature (°C) data have been collected from Australian Bureau of Meteorology (BOM) and network data and residential customer load data have been collected from local DNO. The capacity of BESSs through the feeder is not proportional to PV capacities like it is in [10] to provide realistic test environment. Figure 4.5 illustrates the voltages of critical buses of the test distribution feeder in 24-hour timeframe.

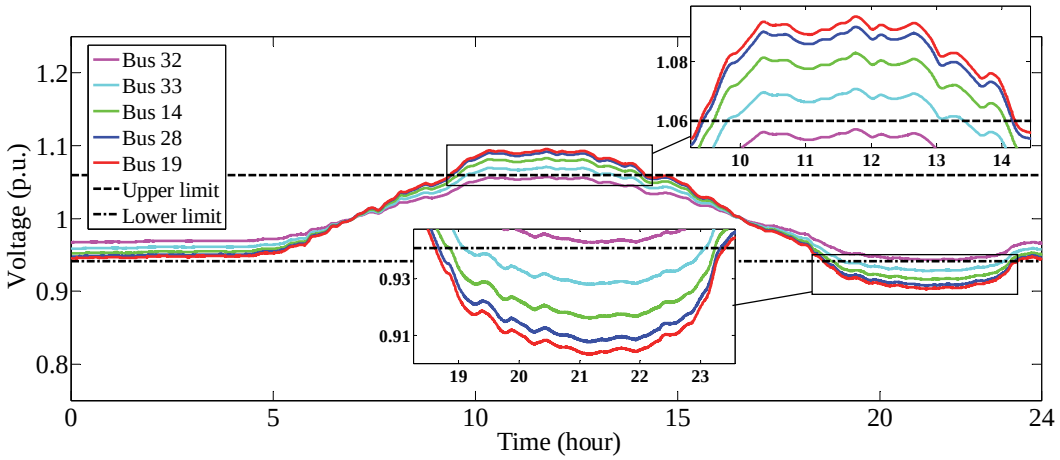

Figure 4.5. 24-hour voltage profile of the critical buses.

For a radial distribution feeder, the buses at the end of the feeder (furthest from substation) are considered as critical buses as the bus voltages tend to exceed the allowable zone. Here, one can see that bus voltages increase during high PV generation period and the voltages of bus 19, bus 28, bus 14 and bus 33 exceed upper allowable limit. Later on the day, during evening, bus voltages show voltage sags due to peak load demand and voltages of bus 19, bus 28, bus 14 and bus 33 exceed the lower allowable limit. Three test cases have been analysed to evaluate the performance of each control layer and a comparative analysis has been carried out on the reduction of communication instants while implementing event-triggered communication scheme. Case studies will also show that the required BESS capacity and injected/ absorbed reactive power for voltage control in case of cooperative operation is lesser than the case of solo-operation of each of them. The index that has been used to compare total reactive power injection/ absorption per day is:

Integral reactive power injection/ absorption,

$$\text{IRPI/ IRPA} = \int_0^T Q_m dt, \quad \text{where } m \in v \tag{4.28}$$

4.4.1 Distributed voltage control for BESS without cooperation (only distributed control layer)

In the first test case, the performance of the proposed leader-following consensus-based distributed voltage control algorithm has been analysed without any cooperation among adjacent BESSs and PV inverters.

In the distributed voltage control layer, BESSs from the critical buses ($BESS_{19}$, $BESS_{28}$, $BESS_{14}$ and $BESS_{33}$) participate in distributed voltage control. $BESS_{32}$ has not participated in the leader-following consensus-based distributed voltage control as V_{32} is within the allowable zone. The initial SOC of all the BESSs is considered at the lower SOC limit which is 20%. In figure 4.6, one can see that the voltages of all critical buses are being regulated within allowable zone till time t = 11.55 hours. At time t = 11.55 hours, the SOC of $BESS_{19}$ reaches its upper limit (90% SOC) and not available anymore for voltage control. As a consequence, at t = 11.55 hours, V_{19} exceeds the upper voltage limit. $BESS_{28}$, $BESS_{14}$ and $BESS_{33}$ keep participating in feeder voltage control by charging in the excess generated PV power in distributed fashion. $BESS_{28}$ becomes unavailable for voltage control as its SOC reaches its upper limit (90% SOC) at time t = 12.12 hours. As a consequence, V_{28} exceeds the allowable voltage limit at t = 12.12

hours. $BESS_{14}$ and $BESS_{33}$ continue to provide distributed voltage control until they reach their upper SOC limits at t = 12.32 hours and t = 13.03 hours respectively. After t = 13.03 hours, all V_{19}, V_{28}, V_{14} and V_{33} are outside of the allowable zone as all the BESSs are out of capacity.

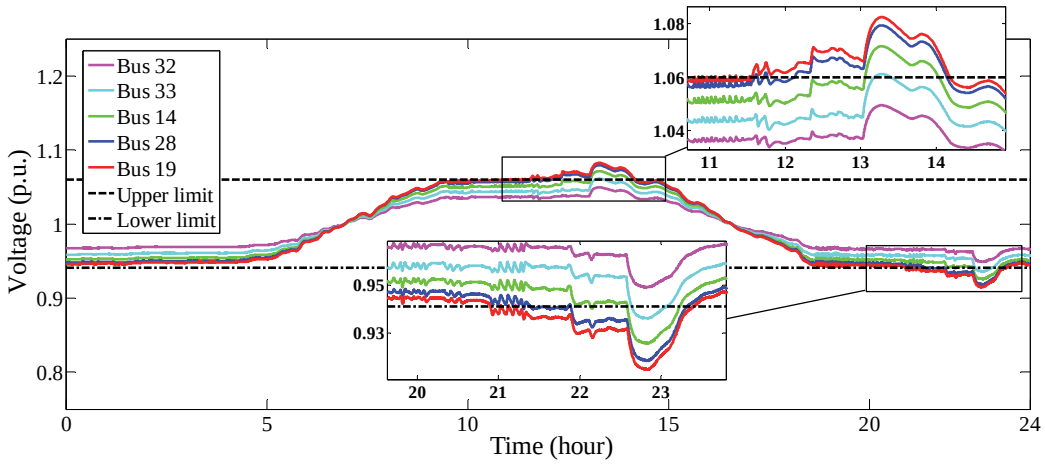

(a)

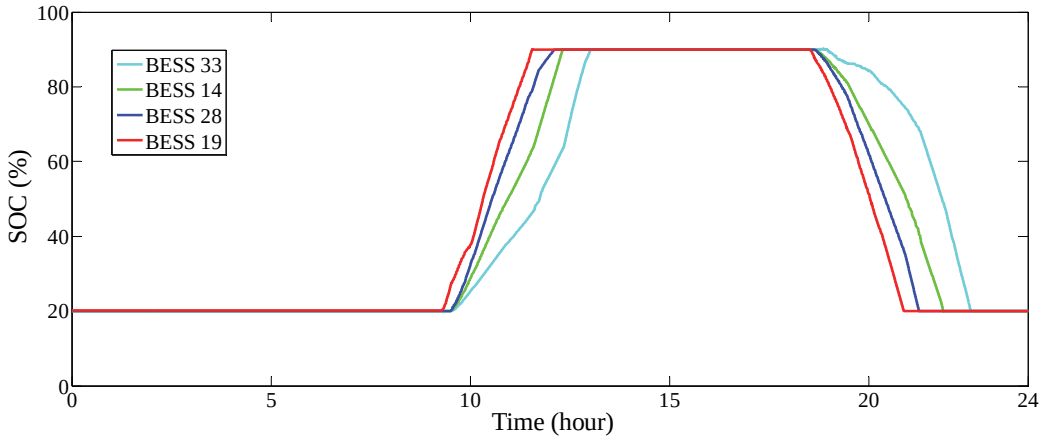

(b)

Figure 4.6. (a) 24-hour voltage profile and (b) SOC of BESSs when distributed voltage control is implemented without any cooperation.

During evening period, voltage sag occurs and V_{19}, V_{28}, V_{14} and V_{33} exceed the lower allowable voltage limit. $BESS_{19}$, $BESS_{28}$, $BESS_{14}$ and $BESS_{33}$ have been fully charged during day time and are ready to discharge to provide voltage support during evening. The leader-following consensus algorithm controls the bus voltages in a distributed fashion and keeps

them within lower allowable limit until the BESSs reach their lower SOC limit (20% SOC). $BESS_{19}$, $BESS_{28}$, $BESS_{14}$ and $BESS_{33}$ reach their lower SOC limit at time t = 20.89, t = 21.27, t = 21.88 and t = 22.56 hours respectively. Voltages at one or more critical buses exceed lower allowable limit with time with the unavailability of one or more BESSs for distributed voltage control.

4.4.2 Distributed voltage control for BESS with cooperation among adjacent BESSs (only distributed control layer and first-stage of cooperative control layer)

In the previous section, one could see that $BESS_{19}$, $BESS_{28}$, $BESS_{14}$ and $BESS_{33}$ reach their upper SOC limit at time t = 11.55, t = 12.12, t = 12.32 and t = 13.03 hours. Due to unavailability of one or more BESSs for participating in distributed voltage control, voltage of one or more buses exceed allowable limit. Figure 4.7 shows the 24-hour voltage profile of critical buses when distributed voltage control with cooperation among adjacent BESSs is implemented. During midday, when $BESS_{19}$ reaches its SOC limit and V_{19} exceeds the allowable zone (at t = 11.55 hour), the cooperation algorithm of the control structure of $BESS_{28}$ gets activated and provides cooperative voltage support for V_{19} and regulates it within limit. $BESS_{28}$ keeps providing the cooperative voltage support for V_{19} until its SOC reaches its upper limit. When $BESS_{28}$ reaches its limit (at t = 11.71 hours), V_{19} and V_{28} both exceed the allowable zone. This initiates the cooperation algorithm of $BESS_{14}$ and $BESS_{19}$. $BESS_{14}$ provides cooperative voltage support for V_{28} and keeps it within upper limit (another neighbour, $BESS_{19}$ is unavailable for cooperation as it has already reached its upper SOC limit). This also initiates the cooperation algorithm of PV-$inverter_{19}$ and it starts to absorb reactive power to regulate V_{19} within limit. However, PV inverter support will be discussed in the next section and is not implemented in this section. Therefore, V_{19} exceeds upper allowable voltage limit from t = 11.71 hour.

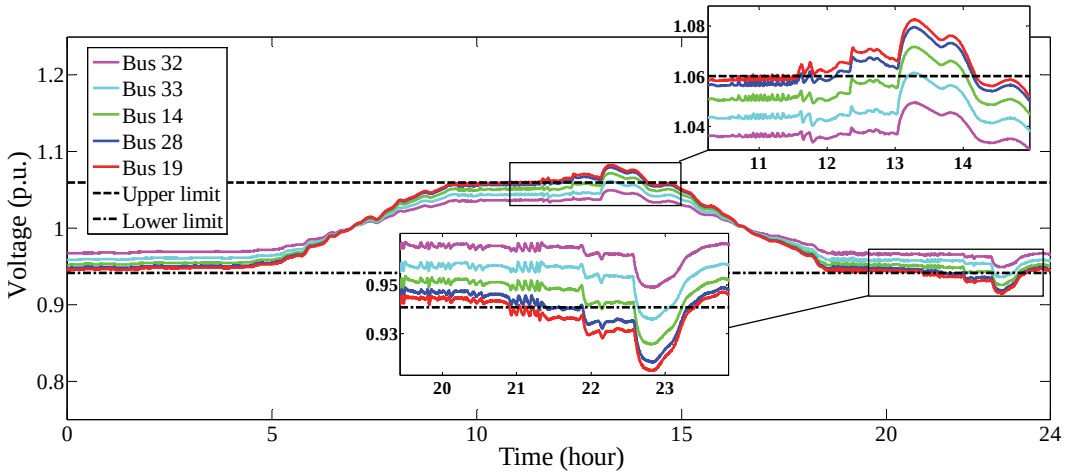

(a)

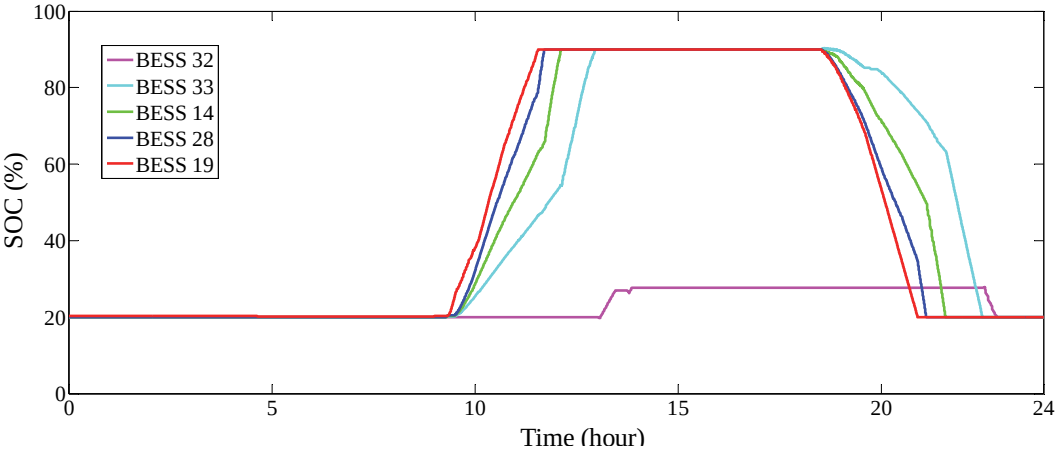

(b)

Figure 4.7. (a) 24-hour voltage profile and (b) SOC of BESSs when distributed voltage control with cooperation among adjacent BESSs is implemented.

$BESS_{14}$ reaches its upper SOC limit at time t = 12.12 hour and this initiates the cooperative operation of $BESS_{33}$ and PV-$inverter_{28}$. Another adjacent neighbour $BESS_{28}$ is unavailable for cooperative voltage support as its SOC has already reached its limit. As PV inverter support is not considered in this section, V_{28} gets out of allowable zone from t = 12.12 hour. $BESS_{33}$ reaches its upper SOC limit at t = 12.97 hours. The cooperation algorithm of the control structure of $BESS_{32}$ gets initiated at t = 13.26 hours when V_{33} enters into critical zone.

During evening, $BESS_{19}$ reaches lower SOC limit (20% SOC) at t = 20.9 hours and $BESS_{28}$ provides cooperative voltage support to keep V_{19} within limit. In this way, $BESS_{14,}$ $BESS_{33}$ and $BESS_{32}$ provide cooperative voltage support when $BESS_{28}$, $BESS_{14}$ and $BESS_{33}$ reach their lower SOC limits respectively.

4.4.3 Distributed voltage control for BESS with cooperation among adjacent BESSs and PV inverters (complete distributed and cooperative control layer together)

In Figure 4.8., one can see that, $BESS_{19}$ reaches its SOC limit at t = 11.55 hours and $BESS_{28}$ reaches its limit at t = 11.71 hours during day time. After t = 11.71 hours, $BESS_{14}$ provides cooperative voltage support for V_{28} as adjacent neighbour. However, V_{19} exceeds the upper allowable voltage limit as $BESS_{19}$ and $BESS_{28}$ both are unavailable. This initiates the cooperation algorithm of PV $inverter_{19}$ to regulate V_{19} within allowable zone by absorbing appropriate reactive power. By the time $BESS_{14}$ reaches its upper SOC limit, $BESS_{33}$ provides voltage support to V_{14} and PV-$inverter_{28}$ provides voltage support to V_{28} when it exceeds the upper voltage limit (from t = 12.12 hours). This is how PV-$inverter_{14}$ provides voltage support to V_{14} when $BESS_{33}$ reaches its upper SOC limit and V_{14} exceeds upper allowable voltage limit (from t = 13.27 hours). V_{33} does not require cooperative reactive power support from PV-$inverter_{33}$ as $BESS_{32}$ does not reach its upper SOC limit during cooperation.

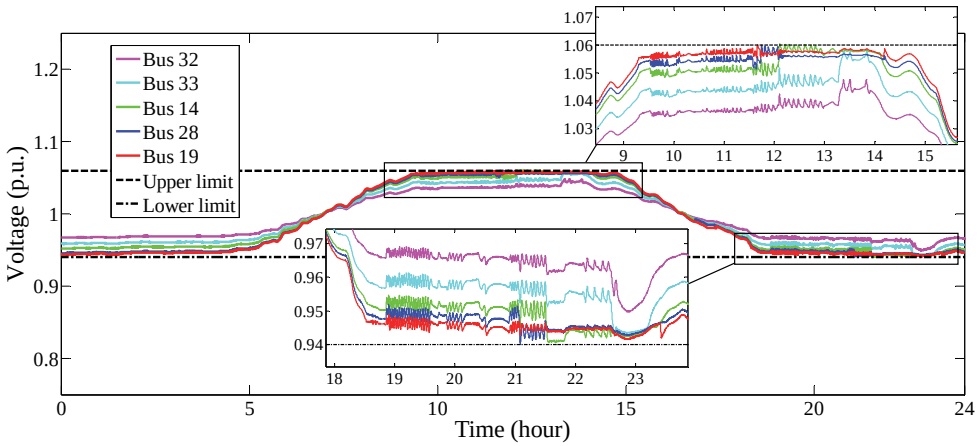

(a)

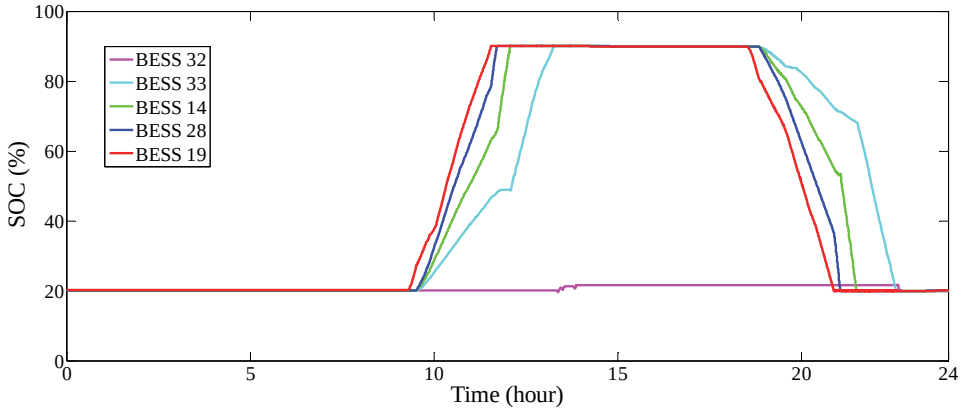

(b)

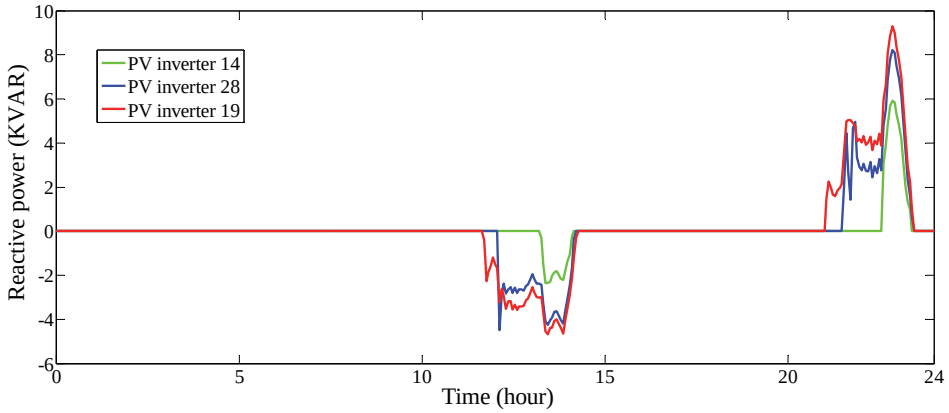

(c)

Figure 4.8. (a) 24-hour voltage profile, (b) SOC of BESSs and (C) reactive power injection/ absorption by PV inverters when distributed voltage control with cooperation among adjacent BESSs and PV inverters is implemented.

During evening, PV inverters inject appropriate reactive power to raise the bus voltages if BESS of a particular bus and adjacent buses reach lower SOC limit and voltage of those buses exceed lower voltage limit. From figure 4.8, one can see that, PV-inverter$_{19}$, PV-inverter$_{28}$ and PV-inverter$_{14}$ get initiated at t = 21.06 hours, t = 21.54 hours and t = 22.62 hours respectively and inject reactive power to regulate V_{19}, V_{28}, and V_{14} within allowable limit. Figure 4.9 illustrates the distributed control input from bus 19 during a part of the day.

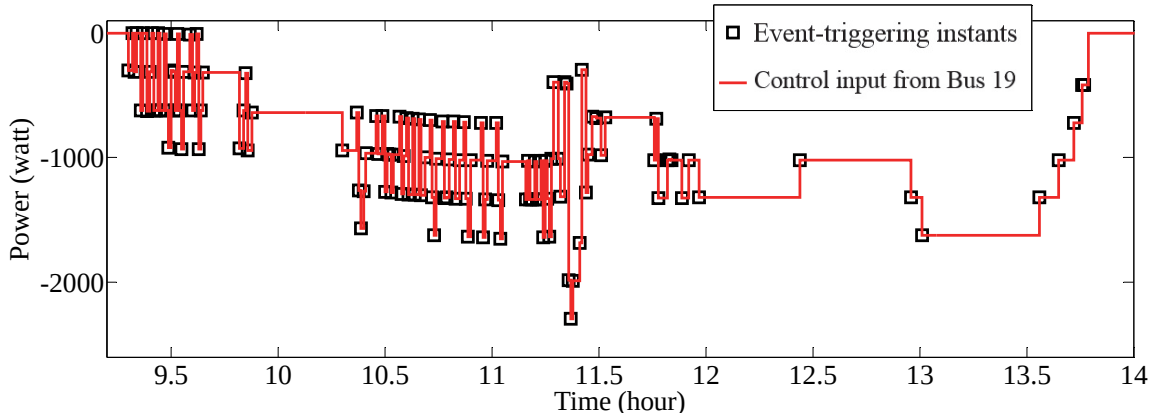

Figure 4.9. A part of distributed control input from bus 19 with event-triggered communication scheme.

In this figure, one can see that the agent at bus 19 performs state measurement and error computation at each discrete time step and transmits the measured state when the computed error exceeds a defined threshold. The threshold for computed error in the distributed control layer has been considered as 300 watts. Each time the error between last transmitted data and current measured data reaches the threshold- an event is triggered, the discrete transmission data changes to a new value and the distributed control input to neighbour control agent is updated.

Figure 4.10 illustrates the evaluation of computed errors, $e_{19}^{dis}(t)$ under the event-triggered communication scheme. Once an event is triggered, the computed error goes back to zero as the last transmitted data has been updated.

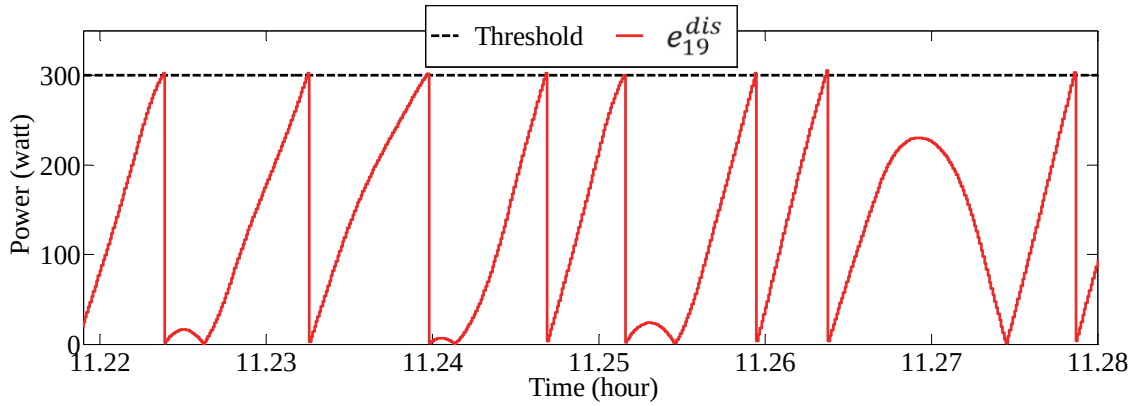

(a)

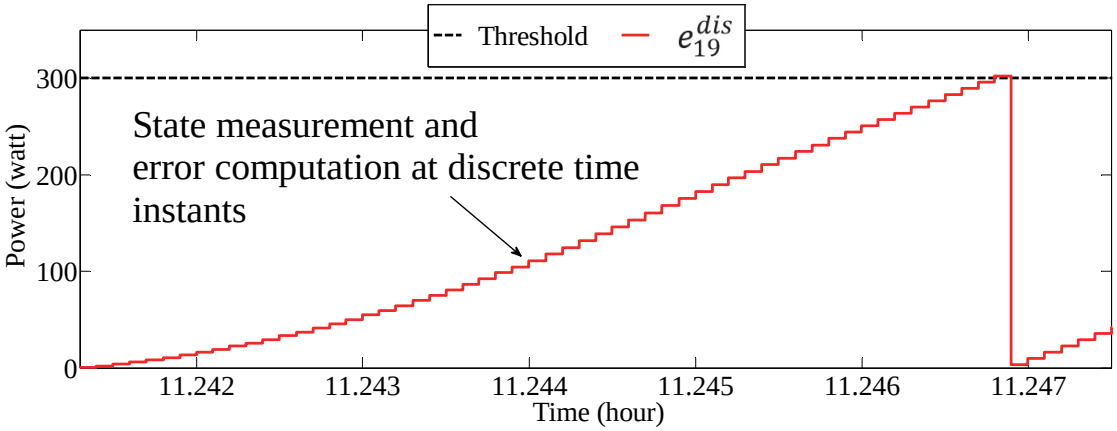

(b)

Figure 4.10. (a) Evolution of computed errors, $e_{19}^{dis}(t)$ during a part of the day (b) one event generation process for $e_{19}^{dis}(t)$.

Figure 4.11 shows event-triggering time instants at each critical bus in distributed voltage control layer during a part of the day.

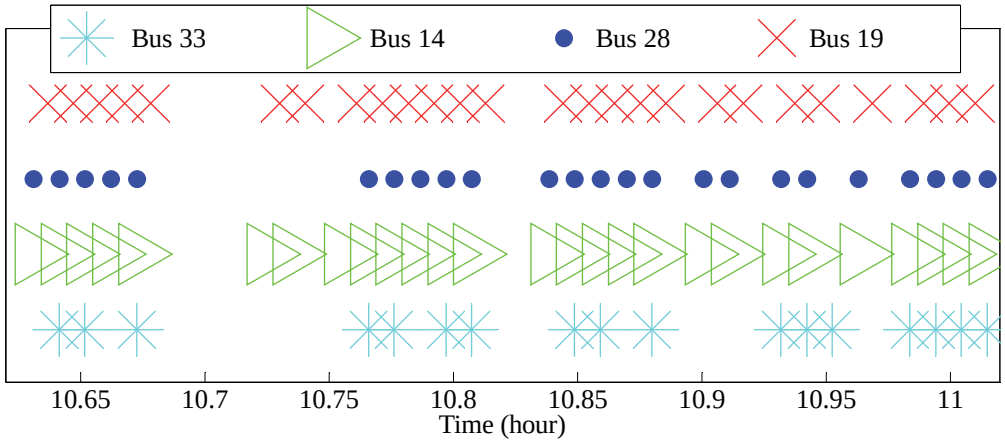

Figure 4.11. A part of event-triggering time instants in distributed voltage control layer.

In the first-stage of cooperative voltage control layer, the voltage measurement at each critical bus (with BESS that has reached its limit) is transmitted to its neighbour buses as cooperative control input. Figure 4.12 illustrates the cooperative control input from each critical bus under event-triggered communication scheme.

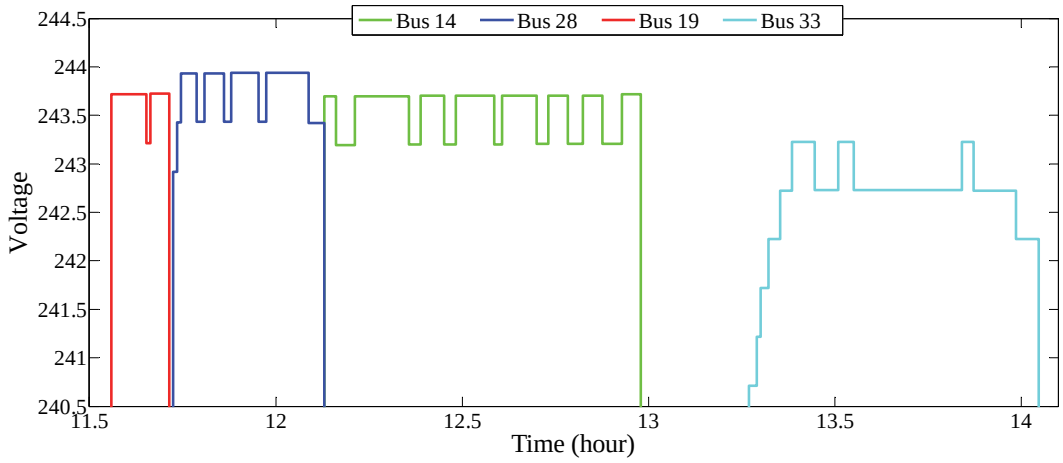

Figure 4.12. Cooperative control inputs from critical buses (to neighbor buses) under event-triggered communication scheme.

In figure 4.13, one can see the evolution of computed errors in voltage measurement at bus 14 under event-triggered communication scheme.

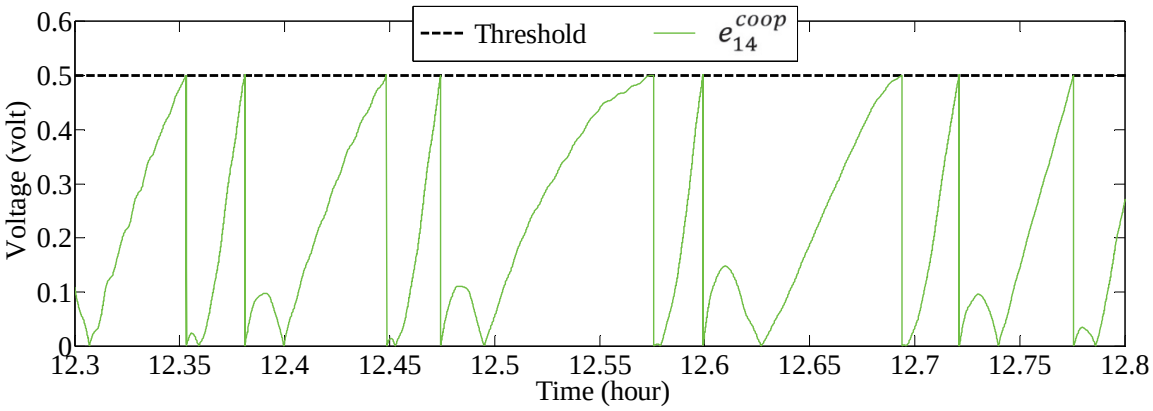

(a)

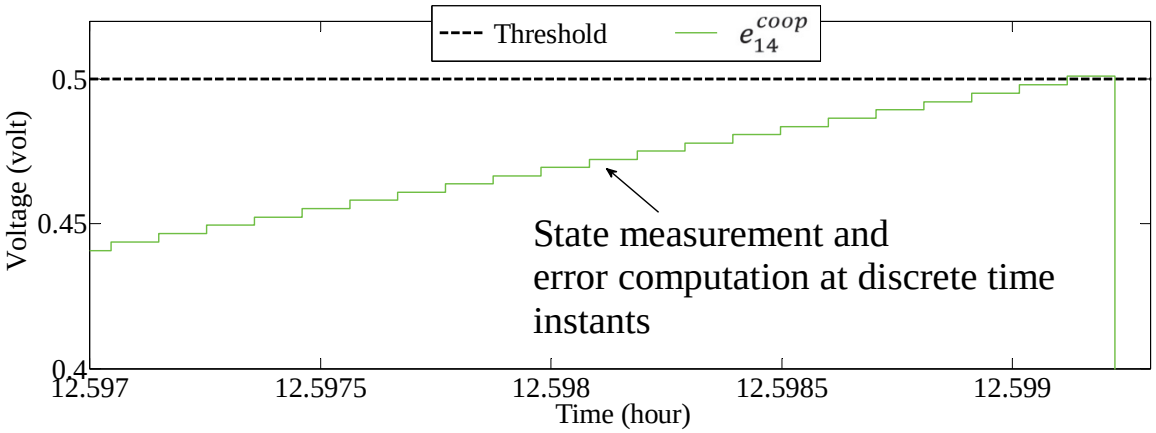

(b)

Figure 4.13. (a) Evolution of computed errors, $e_{14}^{coop}(t)$ during a part of the day (b) one event generation process for $e_{14}^{coop}(t)$.

Agent at bus 14 performs state measurement and error computation at each discrete time step and transmits the measured state when the computed error exceeds a defined threshold. The threshold value for voltage measurement error has been considered as 0.5 Volt. Figure 4.14 shows a part of event-triggering time instants at critical buses in cooperative voltage control layer.

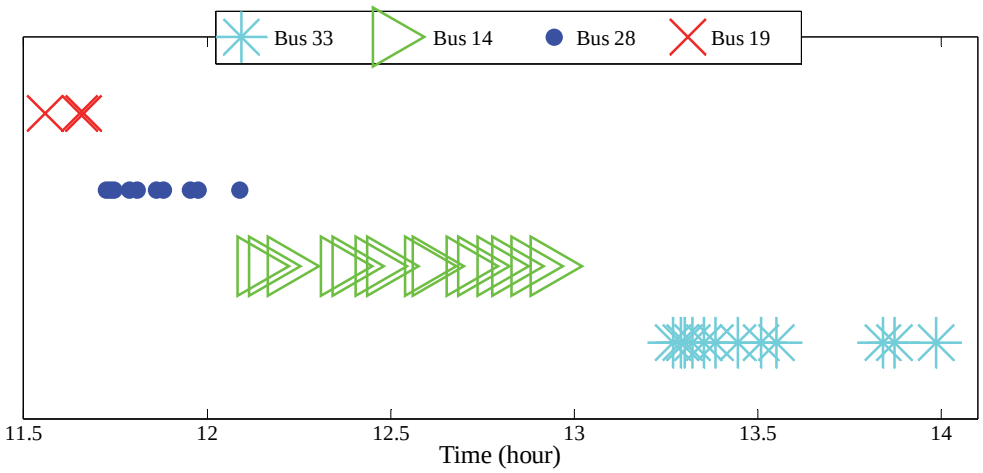

Figure 4.14. A part of event-triggering time instants in cooperative voltage control layer.

To evaluate the advantage of event-triggered communication over periodic communication, the number of data transmission instants under both the communication schemes have been illustrated in Table 4.I. The data from Table 4.I and the results from our case studies show that the event-triggered communication scheme can significantly reduce the communication amount without any notable performance loss in voltage regulation. Table 4.I also illustrates the significance of separating the distributed cooperative control into two different layers. For comparison purpose, a non-separated distributed cooperative control has been considered that has been proposed in [10]. In [10], each bus requires to transmit two parameters to neighbours, which are: share of participation of BESSs and SOC. The average SOC estimation algorithm would keep the energy level of BESSs close together as far as possible. This will require each BESS to transmit its SOC level to neighbours till the average time of all BESSs reaching their limit. However, in this chapter, due to separated control layer, the transmission of bus voltage level (second parameter to transmit) is only required from the time instant when the BESS of that bus reaches its limit to the time instant when the neighbour BESSs also reach their limit. This significantly reduces the necessary data transmission between neighbours while implementing cooperative voltage control.

TABLE 4.I. NUMBER OF DATA TRANSMISSION INSTANTS

Scheme	Bus 19	Bus 28	Bus 14	Bus 33
Event-triggered communication (separated layer)	276	287	329	251
Event-triggered communication (non-separated layer)	613	611	615	575
Periodic communication	81,700	86,300	1,01,100	95,400

Table 4.II depicts the coefficients of control algorithms of the distributed cooperative voltage control scheme.

TABLE 4.II. SYSTEM COEFFICIENTS

Coefficients for share of participation of leader for distributed control		
$K_1 = 1.5$		$K_2 = 2.3$
Coefficients for cooperation algorithm for BESS		**Coefficients for cooperation algorithm for PV inverters**
$K_{19\,3} = 7.5$	$K_{19\,4} = 6.5$	$g_{19} = 1$
$K_{28\,3} = 6.0$	$K_{28\,4} = 7.0$	$g_{28} = 2$
$K_{14\,3} = 6.5$	$K_{14\,4} = 7.5$	$g_{14} = 2$
$K_{33\,3} = 5.5$	$K_{33\,4} = 5.5$	$g_{33} = 2$
$K_{32\,3} = 4.5$	$K_{32\,4} = 9.5$	$g_{32} = 2$

Table 4.III illustrates the comparison between the cooperative operation of BESSs and PV inverters and the solo-implementation of each of them. It shows that, BESS sizing needs to be much larger when implemented alone to control the voltage. On the other hand, it needs excessive amount of injection/ absorption of reactive power to control the bus voltages if PV inverters are implemented alone.

TABLE 4.III. COMPARISON BETWEEN COOPERATIVE OPERATION AND SOLO-IMPLEMENTATION OF BESSS AND PV INVERTERS

Bus	**Cooperative operation of BESS and PV inverters**			**Only BESS**	**Only PV inverter**	
	BESS (kWh)	**IRPA/ IRPI (MVAR)**		**BESS (kWh)**	**IRPA/ IRPI (MVAR)**	
		IRPA	**IRPI**		**IRPA**	**IRPI**
19	3.6	265.1	352.3	10.2	1049.5	1371.7
28	4.6	205.9	254.1	9.3	924.63	1120.9
14	6.5	42.3	62.9	12.2	630.3	924.5
33	10.8	-	-	15.7	267.1	418.5
32	8.1	-	-	8.1	-	-

4.5 Conclusion

A novel discrete event-triggered communication-based distributed cooperative voltage control strategy implemented on BESSs and PV inverters has been proposed in this chapter. The proposed distributed cooperative voltage control scheme efficiently utilizes the storage capacity of neighbour BESSs and reactive power capacity of PV inverters and it has been separated into two different control layers that reduces necessary communication between neighbour agents. Then, discrete event-triggered communication scheme has been implemented in each control layer that dramatically reduces data transmission between agents and significantly releases communication bandwidth. Three case studies have shown the significance of each control layer for feeder voltage regulation throughout the day. They have

shown that the cooperation among neighbour BESSs and PV inverters reduces the BESS sizing requirement and reactive power injection/ absorption requirement at each bus, which eventually reduces capital costs and power losses through the system. Case studies have also proved that separating the distributed cooperative control into different layers and implementing discrete event-triggered communication scheme between agents decrease communication instants in remarkable extent. This significantly reduces the occupancy of limited communication bandwidth and prevents communication bottleneck. The simulation test results were obtained from a realistic low-voltage distribution network model interconnected with large-scale PVs and actual network data, load profile data, solar irradiance and ambient temperature data have been used to evaluate the performance of proposed control strategy in realistic environment.

References

[1] Mohammadi, P., & Mehraeen, S. (2017). Challenges of PV integration in low-voltage secondary networks. *IEEE Transactions on Power Delivery*, *32*(1), 525-535.

[2] Mahmud, N., & Zahedi, A. (2016). Review of control strategies for voltage regulation of the smart distribution network with high penetration of renewable distributed generation. *Renewable and Sustainable Energy Reviews*, *64*, 582-595.

[3] Masters, C. L. (2002). Voltage rise: the big issue when connecting embedded generation to long 11 kV overhead lines. *Power engineering journal*, *16*(1), 5-12.

[4] Ranamuka, D., Agalgaonkar, A. P., & Muttaqi, K. M. (2014). Online voltage control in distribution systems with multiple voltage regulating devices. *IEEE Transactions on Sustainable Energy*, *5*(2), 617-628.

[5] Todorovski, M. (2014). Transformer voltage regulation—Compact expression dependent on tap position and primary/secondary voltage. *IEEE Transactions on Power Delivery*, *29*(3), 1516-1517.

[6] Ghosh, S., Rahman, S., & Pipattanasomporn, M. (2017). Distribution voltage regulation through active power curtailment with PV inverters and solar generation forecasts. *IEEE Transactions on Sustainable Energy*, *8*(1), 13-22.

[7] Li, P., Ji, H., Wang, C., Zhao, J., Song, G., Ding, F., & Wu, J. (2017). A Coordinated Control Method of Voltage and Reactive Power for Active Distribution Networks Based on Soft Open Point. *IEEE Transactions on Sustainable Energy*.

[8] Jayasekara, N., Masoum, M. A., & Wolfs, P. J. (2016). Optimal operation of distributed energy storage systems to improve distribution network load and generation hosting capability. *IEEE Transactions on Sustainable Energy*, *7*(1), 250-261.

[9] Olivier, F., Aristidou, P., Ernst, D., & Van Cutsem, T. (2016). Active management of low-voltage networks for mitigating overvoltages due to photovoltaic units. *IEEE Transactions on Smart Grid*, *7*(2), 926-936.

[10] Zeraati, M., Golshan, M. E. H., & Guerrero, J. (2016). Distributed Control of Battery Energy Storage Systems for Voltage Regulation in Distribution Networks with High PV Penetration. *IEEE Transactions on Smart Grid*.

[11] Kabir, M. N., Mishra, Y., Ledwich, G., Dong, Z. Y., & Wong, K. P. (2014). Coordinated control of grid-connected photovoltaic reactive power and battery energy storage systems to improve the voltage profile of a residential distribution feeder. *IEEE Transactions on industrial Informatics*, *10*(2), 967-977.

[12] Mahmud, N., Zahedi, A., & Mahmud, A. (2017). A cooperative operation of novel PV inverter control scheme and storage energy management system based on ANFIS for voltage regulation of grid-tied PV system. *IEEE Transactions on Industrial Informatics*.

[13] Xin, H., Zhang, M., Seuss, J., Wang, Z., & Gan, D. (2013). A real-time power allocation algorithm and its communication optimization for geographically dispersed energy storage systems. *IEEE Transactions on Power Systems*, *28*(4), 4732-4741.

[14] Xu, Y., Zhang, W., Hug, G., Kar, S., & Li, Z. (2015). Cooperative control of distributed energy storage systems in a microgrid. *IEEE Transactions on smart grid*, *6*(1), 238-248.

[15] Oliveira, T. R., Silva, W. W. A. G., & Donoso-Garcia, P. F. (2016). Distributed secondary level control for energy storage management in dc microgrids. *IEEE Transactions on Smart Grid*.

[16] Morstyn, T., Hredzak, B., & Agelidis, V. G. (2015). Distributed cooperative control of microgrid storage. *IEEE transactions on power systems*, *30*(5), 2780-2789.

[17] Morstyn, T., Hredzak, B., & Agelidis, V. G. (2016). Cooperative multi-agent control of heterogeneous storage devices distributed in a DC microgrid. *IEEE Transactions on Power Systems*, *31*(4), 2974-2986.

[18] Schiffer, J., Seel, T., Raisch, J., & Sezi, T. (2016). Voltage stability and reactive power sharing in inverter-based microgrids with consensus-based distributed voltage control. *IEEE Transactions on Control Systems Technology*, *24*(1), 96-109.

[19] Lai, J., Zhou, H., Lu, X., Yu, X., & Hu, W. (2016). Droop-based distributed cooperative control for microgrids with time-varying delays. *IEEE Transactions on Smart Grid*, *7*(4), 1775-1789.

[20] Wang, Y., Tan, K. T., Peng, X. Y., & So, P. L. (2016). Coordinated control of distributed energy-storage systems for voltage regulation in distribution networks. *IEEE Transactions on Power Delivery*, *31*(3), 1132-1141.

[21] Yang, Q., Barria, J. A., & Green, T. C. (2011). Communication infrastructures for distributed control of power distribution networks. *IEEE Transactions on Industrial Informatics*, *7*(2), 316-327.

[22] Li, C., Yu, X., Yu, W., Huang, T., & Liu, Z. W. (2016). Distributed event-triggered scheme for economic dispatch in smart grids. *IEEE Transactions on Industrial Informatics*, *12*(5), 1775-1785.

[23] Zhang, X. M., Han, Q. L., & Zhang, B. L. (2017). An overview and deep investigation on sampled-data-based event-triggered control and filtering for networked systems. *IEEE Transactions on Industrial Informatics*, *13*(1), 4-16.

[24] Henriksson, E., Quevedo, D. E., Peters, E. G., Sandberg, H., & Johansson, K. H. (2015). Multiple-loop self-triggered model predictive control for network scheduling and control. *IEEE Transactions on Control Systems Technology*, *23*(6), 2167-2181.

[25] Tahir, M., & Mazumder, S. K. (2015). Self-triggered communication enabled control of distributed generation in microgrids. *IEEE Transactions on Industrial Informatics*, *11*(2), 441-449.

[26] Wang, X., & Lemmon, M. D. (2011). Event-triggering in distributed networked control systems. *IEEE Transactions on Automatic Control*, *56*(3), 586-601.

[27] Tabuada, P. (2007). Event-triggered real-time scheduling of stabilizing control tasks. *IEEE Transactions on Automatic Control*, *52*(9), 1680-1685.

[28] García, P., García, C. A., Fernández, L. M., Llorens, F., & Jurado, F. (2014). ANFIS-based control of a grid-connected hybrid system integrating renewable energies, hydrogen and batteries. *IEEE Transactions on Industrial Informatics*, *10*(2), 1107-1117.

Chapter 5

An Event-triggered Distributed Cooperative Voltage Control With Communication Link Failures On A Partly Cloudy Day

"Mahmud, N., Zahedi, A., & Jacob. M. (2017) An event-triggered distributed cooperative voltage control on a partly cloudy day with communication link failures *IEEE Transactions on Energy Conversion*. (Under review)"

Abstract

In this chapter, the issues with event-triggered communication-based distributed cooperative voltage control of low-voltage distribution network with large-scale penetration of solar photovoltaics (PVs) with imperfect communication have been addressed. The performance of a discrete event-triggered communication-based distributed cooperative control strategy for feeder voltage regulation has been analysed on a partly cloudy day with highly fluctuating solar irradiation. As reliable and resilient communication network plays a vital role in the performance of distributed cooperative control in highly fluctuating operating conditions, the performance of the discrete event-triggered communication-based distributed cooperative voltage controller has been evaluated in events of random communication link failures on a partly cloudy day. An alternate path routing algorithm has been adopted for data dissemination to provide resiliency to communication network and to provide robustness to proposed distributed cooperative voltage control strategy. A realistic radial distribution feeder has been designed in MATLAB/ Simulink environment to analyse the impact of random communication link failures on the operability of discrete event-triggered communication-based distributed cooperative voltage control strategy on a partly cloudy day and to evaluate the performance of proposed alternate path routing algorithm in providing robustness to imperfect communication scheme.

5.1 Introduction

The practice of interconnecting solar PVs with low-voltage distribution network is accelerating at a rapid pace throughout the world. Since 2010, significantly increased amount of solar PVs have been penetrated into distribution grid worldwide comparing to the previous four decades [1]. As the percentage of penetration of solar PVs grows, the low-voltage distribution system experiences more challenges. Violation of allowable feeder voltage limit is one of the most crucial challenges from network operation standpoint in a low-voltage distribution network due to high PV penetration [2].

To address this issue of voltage limit violations, various sorts of mitigation strategies have been proposed which can be performed by either utilities or customers. Utilities need to reconfigure the network structure (such as increasing conductor size [3], installing voltage regulators [4], changing the set-points of transformers [5] etc.) frequently to cope up with fast increasing PV integration which is very expensive. The traditional voltage regulators like on-load tap changers (OLTC), switched capacitors (SC), step voltage regulators (SVR) are not efficient enough to regulate the voltage in the fast nonlinear dynamics when large-scale stochastic PVs are integrated [6]. On the other hand, the strategies that can be followed by the customers to regulate the voltage within allowable limits include power curtailment [7], reactive power injection/ absorption [8] and utilization of energy storage systems [9]. Active power curtailment reduces the efficiency of solar PVs and causes wastage of generated power. Reactive power compensation by the power electronic converters (e.g. solar PV inverters) increases the line loss through the system. Besides, the impact of injected/ absorbed reactive power on the voltage profile of the low-voltage distribution feeder is minimal because of the higher R/X ratio. Utilizing energy storage system (e.g. BESS) is more effective in systems with higher R/X ratio as it stores/ discharges active power for voltage control. However, implementation of BESS for voltage regulation needs very large BESS capacity which is expensive and unfeasible. In this chapter, a performance evaluation of cooperative operation of both BESSs and PV inverters from neighbour buses has been performed to regulate the feeder voltage with highly penetrated PVs on a partly cloudy day (fluctuating operating conditions).

These control strategies mentioned above can be implemented in several structures, such as: centralized control structure, decentralized control structure and distributed control structure. Authors of [10] have proposed a centralized control strategy for energy storage system to

control the voltage in distribution network. This kind of centralized controller requires significant investment on extensive communication assets and the controller itself undergoes excessive computational burden. This is not feasible for modern large interconnected system and a communication failure can affect the entire system operation. Authors of [11] have implemented decentralized cooperative control between PV inverter and battery energy storage system to control the PCC voltage. This kind of control strategy does not require communication links to operate and works on local measurements. However, there is no coordination and cooperation among neighbour controllers in this strategy which may cause system oscillation and unbalanced conditions. Besides, capacity of many controllers can be left unused which could be utilized to cooperate with neighbour controllers to enhance the global control performance. The third category, distributed control, does not operate only on local measurements and does not require large communication infrastructure. The control devices communicate and coordinate with neighbour control devices which makes it advantageous than the other two as it needs minimal communication for sharing information. Besides, communication failure affects only a small zone in this strategy.

Since PV generators are located in a heterogeneous and distributed fashion through low-voltage feeders, distributed control strategies are more suitable for the system. Distributed control strategy has become popular nowadays in controlling BESSs and PV inverters [12-20] due to its robustness to individual agent errors, its scalability with respect to increased number of agents and reduced computational load. However, the communication network of a distribution grid usually has limited bandwidth and therefore, an efficient use of the communication infrastructure is necessary [21]. Therefore, performing communication among agents continually at every instant of time or periodically at equidistant sampling instants as it has been assumed in [12-20] is seldom feasible. To relax the occupancy for limited communication bandwidth, implementing need-based aperiodic communication scheme, such as event triggered communication can significantly reduce those unnecessary sample-state transmissions and make effective use of the communication network [22]-[24]. In the event-triggered communication scheme, a sample-state transmission between agents is triggered when a state-measurement error exceeds a given threshold. In this chapter, a discrete event-triggered communication-based distributed cooperative control scheme has been designed and implemented to save the limited network resource while preserving the desired voltage control performance on a partly cloudy day. In this event-triggered communication scheme, a measured sampled state is transmitted to neighbour control agents only when the computed

error between the measured sampled state and last transmitted state violates a predefined threshold. This threshold is defined in such a way that the communication instants between agents are reduced as much as possible without affecting the performance of the distributed controller. Therefore, if there is a failure of data transmission during a discrete event-triggered communication instant between agents in an event-triggered communication scheme, it can significantly affect the performance of the distributed controller. Besides, on a partly cloudy day, fast variation of solar irradiation associated with cloud transients causes rapid voltage variation through the distribution feeder with highly penetrated PVs [25], [26]. This phenomenon will trigger very frequent and increased number of communication instants which requires highly reliable and resilient communication network for stable distributed voltage control operation. However, communication networks are usually subjected to numbers of disturbances and challenges in normal operation due to attacks, large-scale disasters, mobility and characteristics of wireless communication channels [27]. Attacks against the communication network is very frequent and it is practically impossible to achieve fully resilient network because of cost constraints and design flaws. Therefore, it is necessary to evaluate the dependability and performability of the discrete event-triggered communication-based distributed cooperative voltage control strategy when subjected to communication disruptions such as, communication link failures.

Various sorts of strategies have been proposed in different literatures for recovery from communication failures, such as forward error correction (FEC), acknowledgement (ACK), multipath routing etc. Among them, multipath routing has received considerable research interest recently to assure quality of service (QoS) with better reliability and resilience to data transmission [28-30]. In multipath routing protocol, it establishes more than one path to ensure reliable data transmission from source to sink. It utilizes link redundancy to enhance the system delivery rate and reduces control cost and end-to-end delay. There are several multipath routing discovery mechanisms such as, partially disjoint or braided multipath routing [31-34], disjoint multipath routing [35-37], dynamical jumping real-time fault-tolerant (DMRF) routing protocol [38] etc. A desirable goal of multipath routing is to deliver data along more than one path to provide resilience against any random communication link or node failure. In disjoint multipath routing, paths can be long because of the impact of using multiple hops. Therefore, significantly more energy is expended. Besides, some nodes on main paths may be used for many times, which leads to more energy consumption. On the other hand, braided multipath

increases the number of paths implicitly and all the nodes on main paths may be used equally by turns, which leads to less energy consumption and makes overall network load balancing.

If failure on certain path happens, flooding the network for path rediscovery is necessary for disjoint multipath. However, braided multipath constructs a small number of alternate paths that can recover from this kind of failure without flooding the network for rediscovery. For each node on the main path, the construction mechanism of such alternate path is to find the best path from the source to the destination that does not contain that node [39]. In our paper, for the radial communication network topology, each node (at each bus) selects their back-up node on the network so that if there is a communication link failure from the node upstream, an alternate path can be constructed without that node. The constructed alternate path will be disjoint with the failed communication link. The main novelties of this chapter are:

1) Performance evaluation of the discrete event-triggered communication-based distributed cooperative voltage control strategy for large grid-tried solar PV system under fluctuating operating condition (on a partly cloudy day).
2) Evaluation of reliability and performability of discrete event-triggered communication scheme for distributed feeder voltage control with highly penetrated solar PVs when subjected to random communication link failures under fluctuating operating condition (on a partly cloudy day).
3) Design, implementation and performance evaluation of an alternate path routing algorithm to provide robustness against random communication link failures under fluctuating operating condition (on a partly cloudy day) while implementing discrete event-triggered communication-based distributed cooperative feeder voltage control strategy.

This chapter is organized as follows. Section 5.2 describes and analyses the voltage control issue of large grid-tied PV system on a partly cloudy day. Section 5.3 details the proposed event-triggered distributed cooperative control strategy for voltage regulation. Section 5.4 details the design and implementation of alternate path routing algorithm to provide robustness against communication link failures. Section 5.5 details the case studies and simulation results and section 5.6 establishes the conclusion derived from the work.

5.2 Problem description and analysis

5.2.1 Distribution network model

A low-voltage radial distribution feeder has been adopted to evaluate the performance of the proposed discrete event-triggered communication-based distributed cooperative voltage control strategy on a partly cloudy day. Figure 5.1 depicts the low-voltage radial test distribution feeder.

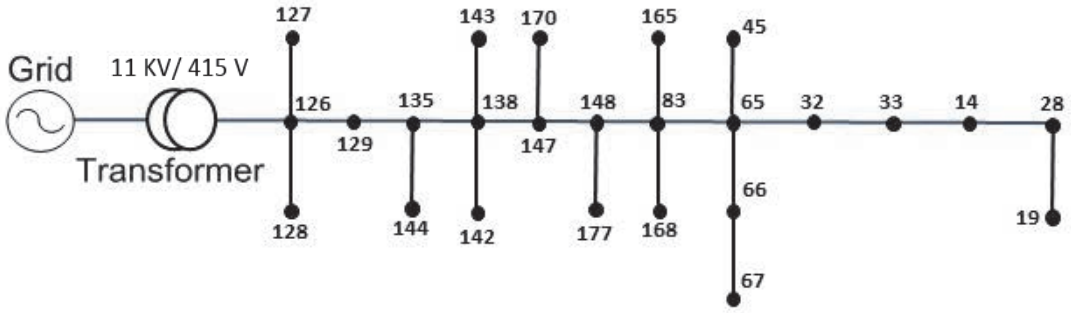

Figure 5.1. Radial test distribution feeder.

A solar PV, a BESS and a residential load are connected with each bus through the feeder. Each solar PV is connected with the distribution feeder through a 3-phase DC/ AC inverter. A BESS is connected to the DC-bus through a bidirectional DC-DC buck-boost converter. Figure 5.2 illustrates a detailed diagram of a low-voltage radial distribution feeder.

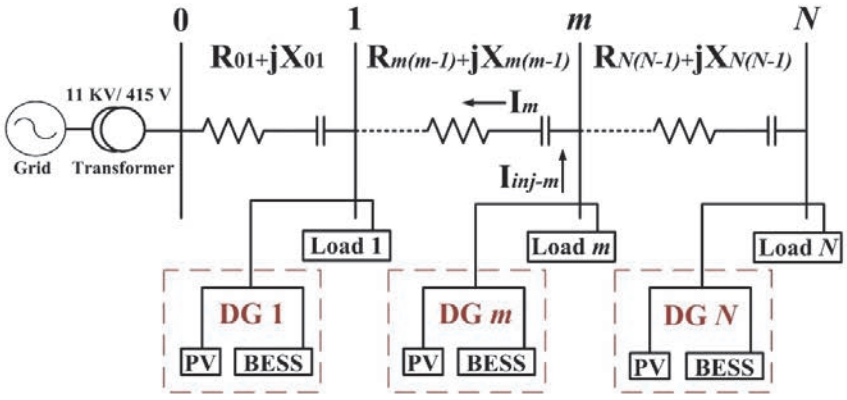

Figure 5.2. Radial distribution feeder with PV, BESS and load.

From previous chapter, the voltage deviation between node m and node $(m-1)$ can be expressed as,

$$\Delta V_m = V_m - V_{m-1} = \sum_{l=m}^{N} \frac{P_l R_{m(m-1)} + Q_l X_{m(m-1)}}{V_m} \quad (5.1)$$

Figure 5.3 illustrates the characterization of cloud transients with solar irradiation profile on a typical clear sunny day and a partly cloudy day. It shows that on a partly cloudy day, the solar irradiation fluctuates significantly higher comparing to a clear sunny day.

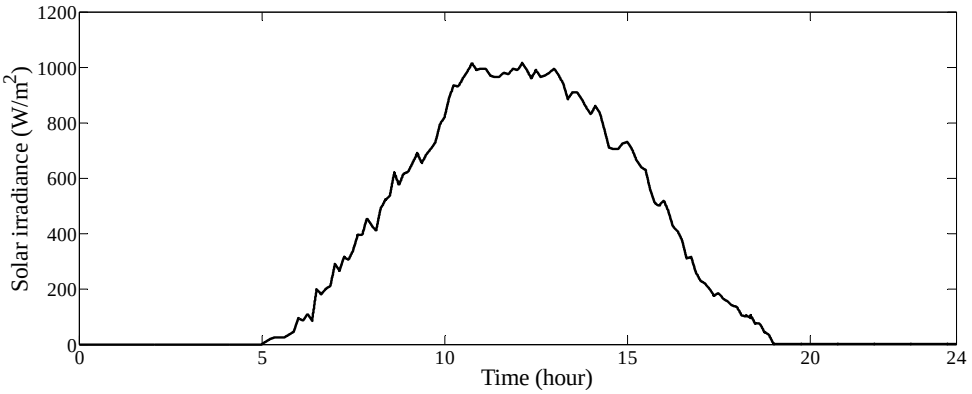

(a)

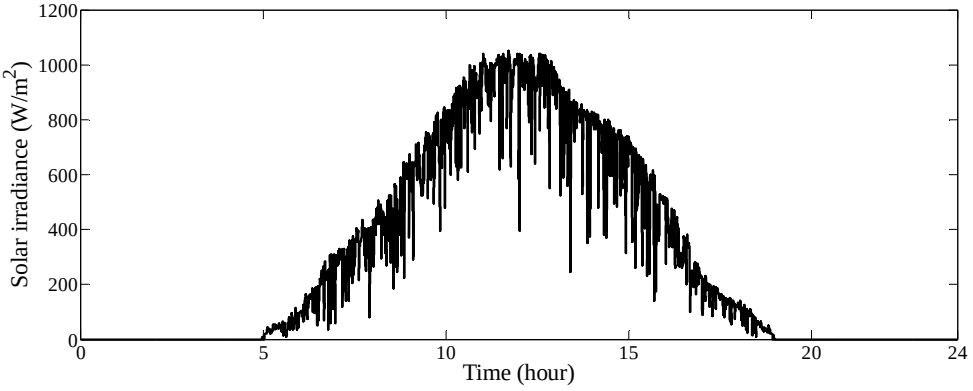

(b)

Figure 5.3. Solar irradiation profile (a) clear sunny day (b) partly cloudy day

Figure 5.4 illustrates the impact of cloud transients on the voltage profile along the distribution feeder.

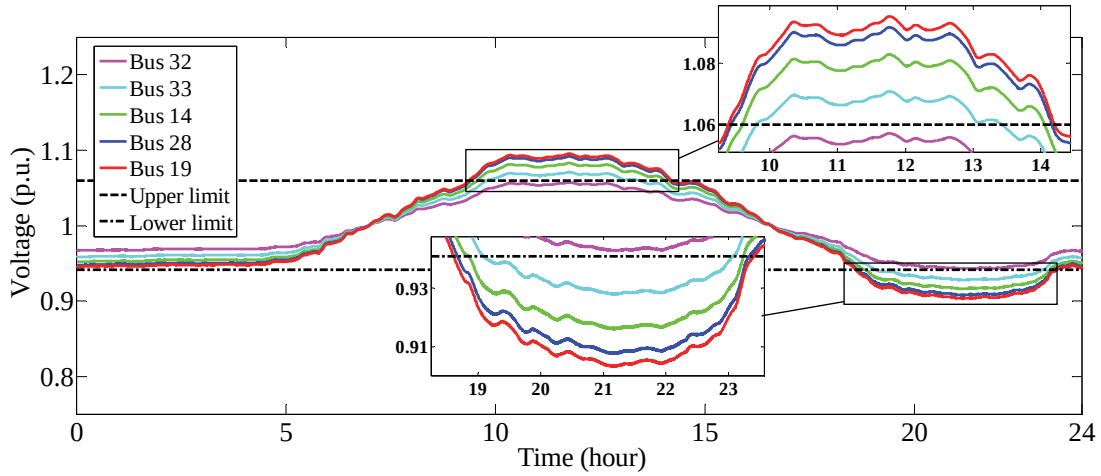

(a)

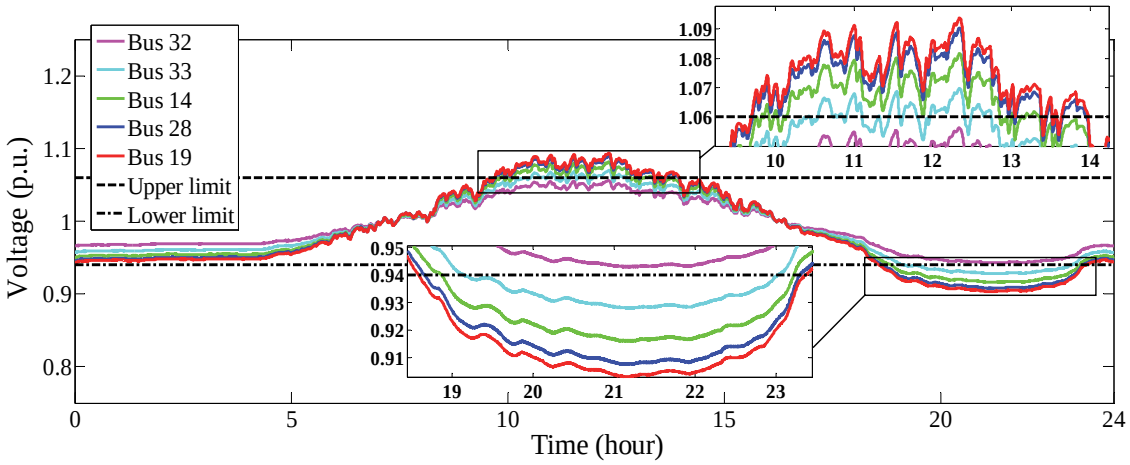

(b)

Figure 5.4. 24-hour voltage profile of the critical buses (a) clear sunny day (b) partly cloudy day

When a cloud sweeps over a PV site, the fast variation in power output can be as high as 80% and can last a few seconds. During partly cloudy days, the period from the instant a cloud reaches the coverage area of the PV generator until it leaves that area lasts between 0.5 to 8 minutes [40].

5.2.2 Communication network model

Consider a system of a group of N interacting agents. The communication connections among the agents can be represented by an undirected communication graph, $\mathcal{g} = \{\nu, \varepsilon\}$. Here, $\nu = \{1, 2, 3\ldots N\}$ is the index set of *N* agents and ε is the edge set of paired agents where, $\varepsilon \subseteq \nu \times \nu$. $\mathcal{A} = [a_{mn}] \epsilon \mathbb{R}^{N\times N}$ is the weighted adjacency matrix. If nodes m and n can communicate with each other, then there is communication link between them. Therefore, $(m,n) \in \varepsilon$ and $a_{mn} > 0$. In this paper, agents only from neighbour buses have communication link between them. The communication neighbour set of node m is represented as, $N_m = \{n \in \nu | (m,n) \in \varepsilon\}$. The adjacency matrix, $\mathcal{A} = [a_{mn}]$ can be defined as,

$$\begin{cases} a_{mn} > 0, \text{ if } n \in N_m \\ a_{mn} = 0, \quad \text{otherwise} \end{cases} \tag{5.2}$$

Here, self-loops are not included. For all $m \in \nu$, $a_{mm} = 0$. The in-degree of node *m* is defined as $deg_{in}(m) = \sum_{n=1}^{N} a_{mn}$, for any $\in \nu$. The degree matrix is represented as, $\mathcal{D}$ = diag (deg_{in} (1), deg_{in} (2),…… deg_{in} (N)). The laplacian matrix of graph $\mathcal{g}$ is given by, $\mathcal{L} = \mathcal{D} - \mathcal{A}$. If and only if the graph $\mathcal{g}$ is connected, $\mathcal{L}$ has a zero eigenvalue and the corresponding eigenvector is the vector of ones. For an undirected graph, all the eigenvalues are nonnegative and they can be ordered sequentially in an ascending order as, $0 = \lambda_1(\mathcal{g}) \leq \lambda_2(\mathcal{g}) \leq \cdots \leq \lambda_N(\mathcal{g})$. If $\mathcal{g}$ is connected, then $\lambda_2(\mathcal{g}) > 0$.

5.3 Proposed discrete event-triggered distributed cooperative voltage control strategy on a partly cloudy day

The event-triggered distributed cooperative control is implemented on the system in two layers. Which are: 1) Distributed control layer, 2) Cooperative control layer. In distributed control layer, an event-triggered distributed voltage control strategy is implemented among all the BESSs to keep the voltages of all the buses within allowable zone. A leader-following consensus algorithm has been proposed to control the bus voltages through the feeder in a distributed coordinated fashion. However, voltage support from a BESS is limited as its capacity is limited and BESS stops to charge/ discharge when the state-of-charge (SOC) reaches the upper/ lower limit. Once BESS of any bus reaches its capacity limit during distributed control layer, the cooperative control layer is initiated. In the cooperative control layer, a two-stage event-triggered cooperative control algorithm has been proposed. The two-stage cooperative control is stated below:

Stage 1: The first-stage of event-triggered cooperative control is implemented on BESSs. An event-triggered cooperation algorithm is initiated in the incident of adjacent BESSs being unavailable for voltage control (when SOC reaches limit) and voltage of that adjacent bus exceeding the allowable zone. This algorithm does not require an expensive continuous communication among adjacent BESSs to be operated.

Stage 2: The second-stage of event-triggered cooperative control is implemented on the PV interfacing inverters to provide voltage support if first-stage of cooperative voltage support by adjacent BESSs is no longer available (when BESSs from adjacent buses reach their SOC limit too). The control steps are discussed in details below:

5.3.1 Leader-following consensus algorithm for BESS for distributed voltage control (Distributed control layer)

The BESSs coordinate with immediate adjacent BESSs utilizing limited communication links and decide their respective share of participation (P_m^{ref}) to control the overall feeder voltage in distributed fashion. The share of participation of BESS at the last bus $\left(P_N^{ref}\right)$ of radial feeder has been considered as the virtual leader of the distributed control algorithm as the last bus has highest/ lowest voltage in the system [19]. Initially, the share of participation of BESS at last bus $\left(P_N^{ref}\right)$ is determined considering equation 5.3. Afterwards, this information is conveyed to other buses through the feeder by communication links between adjacent neighbours. Figure 5.5 depicts the control structure of proposed event-triggered distributed cooperative voltage control implemented on BESS at bus *m*.

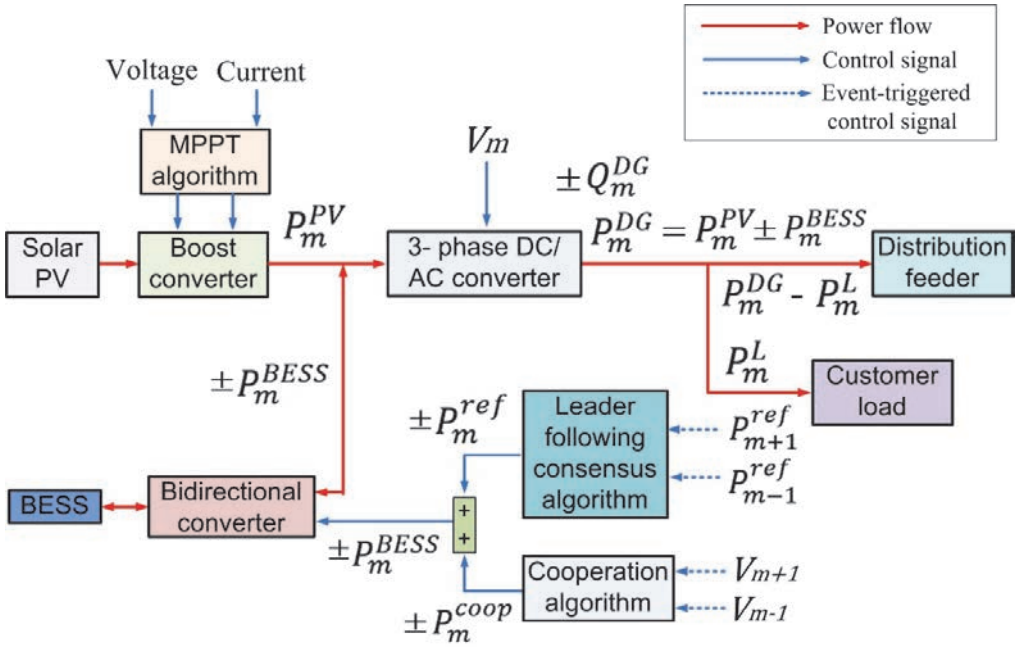

Figure 5.5. Control structure of event-triggered distributed cooperative voltage control implemented on BESS at bus m.

The allowable voltage zone is considered as $\pm 6\%$ of the nominal bus voltage, which means the upper voltage limit (V_{up}) is 1.06 p.u. and lower voltage limit (V_{low}) is 0.94 p.u. The proposed leader-following consensus-based distributed control algorithm will be activated when bus voltages enter into 'critical zone' that is from 1.055 p.u. ($V_{cric\text{-}up}$) to 1.06 p.u. (V_{up}) and from 0.94 p.u. (V_{low}) to 0.945 p.u. ($V_{cric\text{-}low}$). P_N^{ref} can be defined as,

$$P_N^{ref}(t) = \begin{cases} k_1\left(V_{cric-up} - V_N(t)\right), & when\ V_N(t) > V_{cric-up} \\ 0, & when\ V_{cric-low} < V_N(t) < V_{cric-up} \\ k_2\left(V_{cric-low} - V_N(t)\right), & when\ V_N(t) < V_{cric-low} \end{cases} \quad (5.3)$$

Here, coefficients k_1 and k_2 are control gains that determine the accuracy and convergence speed of the control algorithm. P_N^{ref} is then conveyed down through the feeder via communication links between adjacent BESSs.

The share of participation of BESS at bus m can be represented as follows:

$$P_m^{ref}(t) = \sum_{n=1}^{N-1} s_{mn} P_n^{ref}(t) + s_{mN} P_N^{ref}(t), \quad (5.4)$$

Where, $n = 1, 2, 3, \ldots N-1$

When, $V_m(t) > V_{cric-up}$

Or, $V_m(t) < V_{cric-low}$

Where, s_{mn} is the (m, n) entry of a row stochastic matrix $\mathcal{S}$, which can be expressed as,

$$S_{mn} = \frac{a_{mn}}{\sum_{k=1}^{N} a_{mk}} \tag{5.5}$$

In order to implement the distributed voltage control at bus m, BESS at bus m needs to monitor the share of participation of adjacent neighbour BESSs at bus n (considering, $n \in \nu$ and $(m,n) \in \varepsilon$) to generate the distributed voltage control reference, $P_m^{ref}(t)$. Traditionally, signal transmission between adjacent BESSs takes place periodically with a constant sampling period, which requires large real-time information exchange requirements. Event-triggered communication scheme can significantly reduce the occupancy of limited bandwidth while preserving the satisfactory distributed voltage control performance. In our paper, in the proposed discrete event-triggered communication scheme, the state measurement and error computation are performed only at constant sampling period h (at discrete time steps). The measured sampled state is transmitted to neighbour control agents only when the computed error between the measured sampled state and last transmitted state violates a predefined threshold. Let's assume that each bus n transmits the share of participation of $BESS_n$ at time instants denoted by,

$$t_0^n = 0 < t_1^n < \cdots < t_i^n < \cdots, i \in \mathbb{N} \tag{5.6}$$

Let's consider, the transmitted share of participation of $BESS_n$ at event-triggering time instant t_i^n is $P_n^{ref}(t_i^n)$. The computed error at event-triggering time instant t_i^n for distributed voltage control can be defined as,

$$e_n^{dis}(t_i^n) = P_n^{ref}(t_i^n) - P_n^{ref}(t_{i-1}^n) \tag{5.7}$$

If the computed error between the current measured sampled state $P_n^{ref}(t)$ and the last transmitted sampled state $P_n^{ref}(t_{i-1}^n)$ is more than a predefined threshold then the measured state $P_n^{ref}(t)$ is transmitted to the neighbour control agents and $t = t_i^n$. Therefore, considering event-triggered communication scheme, (5.7) can be rewritten as,

$$P_m^{ref}(t) = \sum_{n=1}^{N-1} s_{mn} P_n^{ref}(t_i^n) + s_{mN} P_N^{ref}(t_i^N) \tag{5.8}$$

Where, $n = 1, 2, 3, \ldots, N-1$, $i \in \mathbb{N}$ and $t \in [t_i^n,\ t_{i+1}^n)$

When, $V_m(t) > V_{cric-up}$ or, $V_m(t) < V_{cric-low}$

By properly controlling the magnitude of computed error, the data transmission frequency between adjacent buses can be significantly reduced while implementing the distributed voltage control through the feeder.

5.3.2 Cooperation algorithm for BESS (first-stage of cooperative control layer)

Initial SOC of BESSs can be different to one another that can be caused by technical problems, uneven charge/ discharge or temporary outages. As a result, BESS can be unavailable for voltage control when SOC reaches its limit and this may cause the bus voltage to exceed the allowable zone. An event-triggered cooperation algorithm has been proposed and its performance has been analysed where BESSs from adjacent buses provide voltage support when BESS of a particular bus reaches its SOC limit. If $BESS_n$ reaches its SOC limit during distributed voltage control layer and V_n exceeds the allowable zone, the cooperative control formula for BESS at bus m is:

$$P_m^{coop}(t)=\sum_{n=1}^{N} K_{m3} a_{mn} \left(V_{cric-up} - V_n(t)\right), \tag{5.9}$$

$$\text{And, } P_m^{coop}(t) = \sum_{n=1}^{N} K_{m4} a_{mn} \left(V_{cric-low} - V_n(t)\right) \tag{5.10}$$

$$\text{When, } V_n(t) > V_{cric-up} \text{ and } SOC_n\ (t) > 80$$

$$\text{Or, } V_n(t) < V_{cric-low} \text{ and } SOC_n\ (t) < 20$$

Here, coefficients K_{m3} and K_{m4} are the cooperative control gains for bus m, which determine the control accuracy and convergence speed. To implement the cooperative control formula illustrated in (5.9) and (5.10), data transmission between control agent of $BESS_m$ and voltage measurement agent at bus n is required. Voltage measurement at bus n takes place at discrete time steps with a sampling period h and the measured voltage is transmitted to control agent of $BESS_m$ only when the computed error exceeds a predefined threshold. Let's assume that bus n transmits the voltage measurements at time instants denoted by,

$$t_0^n = 0 < t_1^n < \cdots < t_j^n < \cdots,\ j \in \mathbb{N} \tag{5.11}$$

The computed error can be defined as,

$$e_n^{coop}(t_j^n) = V_n\left(t_j^n\right) - V_n\left(t_{j-1}^n\right) \tag{5.12}$$

Here, $V_n(t_j^n)$ is the transmitted sampled voltage of bus n at event-triggering instant t_j^n. Considering event-triggered communication scheme, (5.9) and (5.10) can be rewritten as,

$$P_m^{coop}(t)=\sum_{n=1}^{N} K_{m3} a_{mn} \left(V_{cric-up} - V_n(t_j^n)\right), \tag{5.13}$$

And, $$P_m^{coop}(t) =\sum_{n=1}^{N} K_{m4} a_{mn} \left(V_{cric-low} - V_n(t_j^n)\right) \tag{5.14}$$

This event-triggered communication-based cooperative control is initiated only when SOC_n reaches its limit considering, $N_m = \{n \in v \mid (m,n) \in \varepsilon\}$. This cooperative control from bus m is added with the share of distributed control at bus m and provides voltage support to both the buses until the voltage deviation is mitigated or SOC_m reaches limit. So, the power charge/ discharge reference for $BESS_m$ is,

$$P_m^{BESS}(t) = P_m^{ref}(t) + P_m^{coop}(t) \tag{5.15}$$

5.3.3 Cooperation algorithm for PV inverter (second-stage of cooperative control layer)

If SOC of both $BESS_m$ and $BESS_n$ reach their limits (considering, $(m,n) \in \varepsilon$) and voltage at bus m gets out of allowable zone, reactive power support from PV inverter at bus m is initiated. Figure 5.6. illustrates the control structure of PV inverter at bus m.

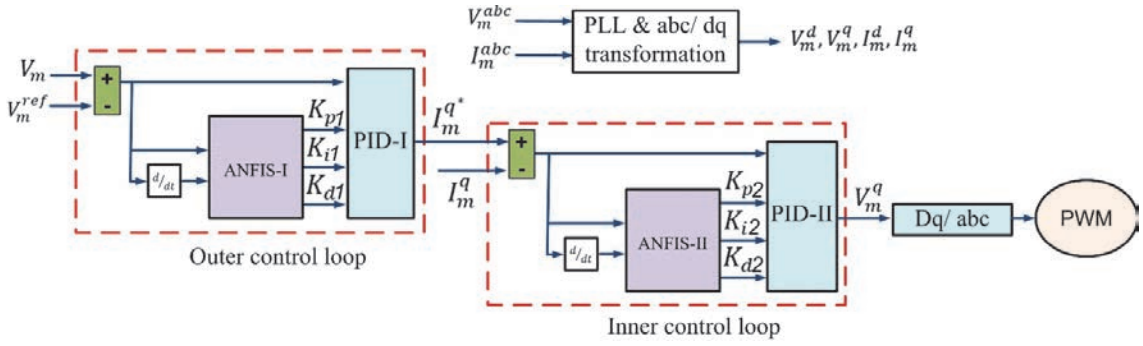

Figure 5.6. Control structure of PV inverter at bus m.

As the cloud transients cause rapid voltage variations through the feeder, classic PID controllers are not efficient enough to provide stable voltage control performance in this fluctuation operating condition [11]. In this scenario, ANFISPID-based PV inverter control scheme has been adopted in this chapter to provide stable voltage control operation with damped system oscillation at the second-stage of cooperative control layer.

In this study, PV inverter control scheme has been implemented based on dq reference frame theory. The three-phase active power (P) and reactive power (Q), generated by PV inverter at bus m are:

$$P_m(t) = \frac{3}{2}\left(V_m^d(t)I_m^d(t) + V_m^q(t)I_m^q(t)\right) \tag{5.16}$$

$$Q_m(t) = \frac{3}{2}\left(V_m^q(t)I_m^d(t) - V_m^d(t)I_m^q(t)\right) \tag{5.17}$$

Assuming that the d-axis component is perfectly aligned with the grid voltage V_m^q = 0, the active power and the reactive power will therefore be proportional to I_m^d and I_m^q respectively:

$$P_m(t) = \frac{3}{2}V_m^d(t)I_m^d(t) \tag{5.18}$$

$$Q_m(t) = -\frac{3}{2}V_m^d(t)I_m^q(t) \tag{5.19}$$

The current q component I_m^q is controlled by generating reference $I_m^{q\,*}$ to manage appropriate reactive power injection/ absorption by the PV inverter. The structure of ANFIS-based PID control scheme that controls the grid interfacing PV inverter is illustrated in figure 5.6. It consists of two control loops, (1) Outer control loop, and (2) Inner control loop. The outer control loop is to generate the reference values of current q component ($I_m^{q\,*}$) to manage inverters reactive power exchange. The voltage deviation from reference and the derivative of this deviation (as a prediction of future deviations) are given as inputs into ANFISPID- I. V_{ref} is referred as the bus voltage reference (240 volts phase-to-neutral). In ANFISPID- I, intelligent ANFIS-I tunes the gains (K_{p1}, K_{i1} and K_{d1}) of PID-I controller to generate the appropriate $I_m^{q\,*}$ for regulating the voltage of bus m to its reference value.

$$I_m^{q\,*}(t) = K_{p1}\left(V_{ref} - V_m(t)\right) + K_{i1}\int\left(V_{ref} - V_m(t)\right)dt + K_{d1}\frac{d\left(V_{ref} - V_m(t)\right)}{dt} \tag{5.20}$$

When, $V_m(t) > V_{cric-up}$, $SOC_m > 80$ and $SOC_n > 80$

Or, $V_m(t) < V_{cric-low}$, $SOC_m < 20$ and $SOC_n < 20$

$I_m^{q\,*}$ is then provided to the inner control loop where the measured q-axis component current (I_m^q) is regulated by ANFIS-II to follow the corresponding reference values ($I_m^{q\,*}$).

$$V_m^q(t) = K_{p2}\left(I_m^{q\,*}(t) - I_m^q(t)\right) + K_{i2}\int\left(I_m^{q\,*}(t) - I_m^q(t)\right)dt + K_{d2}\frac{d\left(I_m^{q\,*}(t) - I_m^q(t)\right)}{dt} \tag{5.21}$$

In ANFISPID- II, ANFIS- II auto-tunes the PID- II control gains (K_{p2}, K_{i2} and K_{d2}) to control the measured q-axis component current I_m^q to follow corresponding reference $I_m^{q\,*}$.

The output of the controller is the voltage quadrature-axis component (V_m^q) that the pulse width modulation (PWM) inverter has to generate. This way, PV inverter mitigates the voltage deviation from allowable limit at the second-stage of cooperative control layer.

5.4 Proposed alternate path routing algorithm to provide robustness to random communication link failures

The resilience of a communication scheme mainly illustrates that when the primary communication path between source and sink fails, an alternate path is available to transmit the data. This can assure the ability of a system to deliver a desired level of functionality in the occurrence of faults. In this chapter, the performance of the proposed discrete event-triggered communication-based distributed cooperative voltage control strategy has been evaluated in the occurrence of random communication link failures and an alternate communication path routing algorithm has been designed and its performance has been evaluated in providing robustness to the proposed voltage controller against these failures.

To implement the distributed voltage control along the feeder, a leader following consensus-based distributed voltage control algorithm has been utilized. The performance of the leader-following consensus-based distributed control algorithm is significantly dependent upon the perfect tracking of virtual leader and any communication link failure with the leader can put significant adverse impact on the voltage control. The performability is also affected when there is a communication link failure between any other two nodes except the leader node. The communication network topology of the radial distribution feeder is stated below in Figure 5.7.:

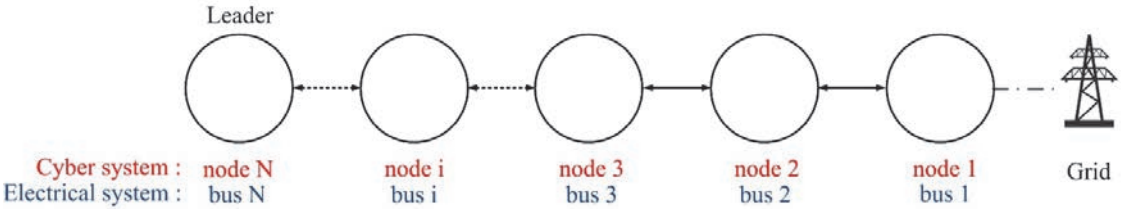

Figure 5.7. Communication graph for N-bus radial distribution feeder

The topology of the communication network has been adopted as same as the topology of the electrical system (radial). To provide robustness against random communication link failures, in this radial communication network, each node selects its back-up node so that if there is a communication link failure with the node upstream, an alternate path can be constructed without that node. This strategy will provide robustness to the downstream nodes to follow the virtual leader node in the occurrence of random communication link failures.

Figure 5.8 illustrates a 5-node radial communication network where all the communication links between adjacent nodes are fault-free. In this 5-node communication network, node-5 has been considered as the leader of the system. Therefore, the topology of the nodes from upstream to downstream has been considered as from node-5 to node-1.

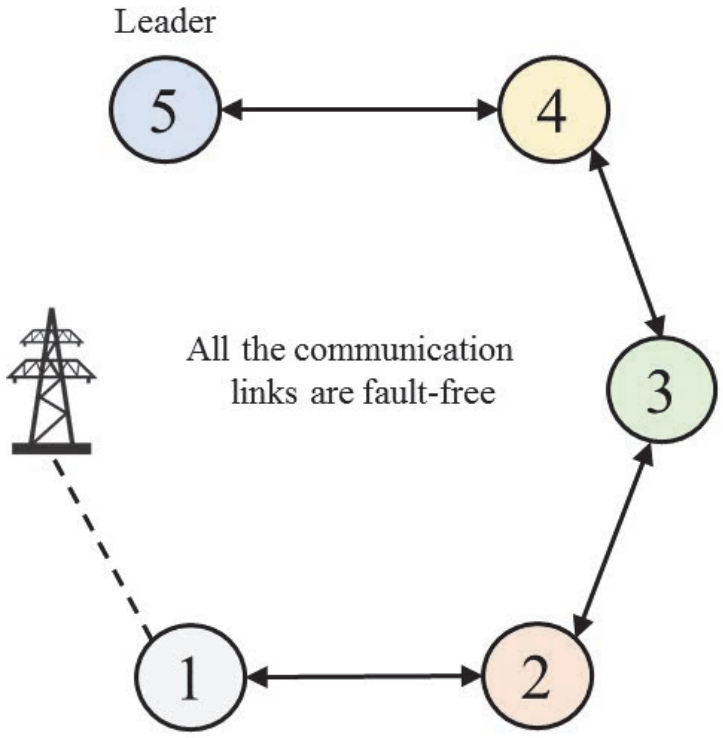

Figure 5.8. A 5-node communication network in radial topology with no fault

Figure 5.9 shows communication link failures at different locations of the 5-node communication network.

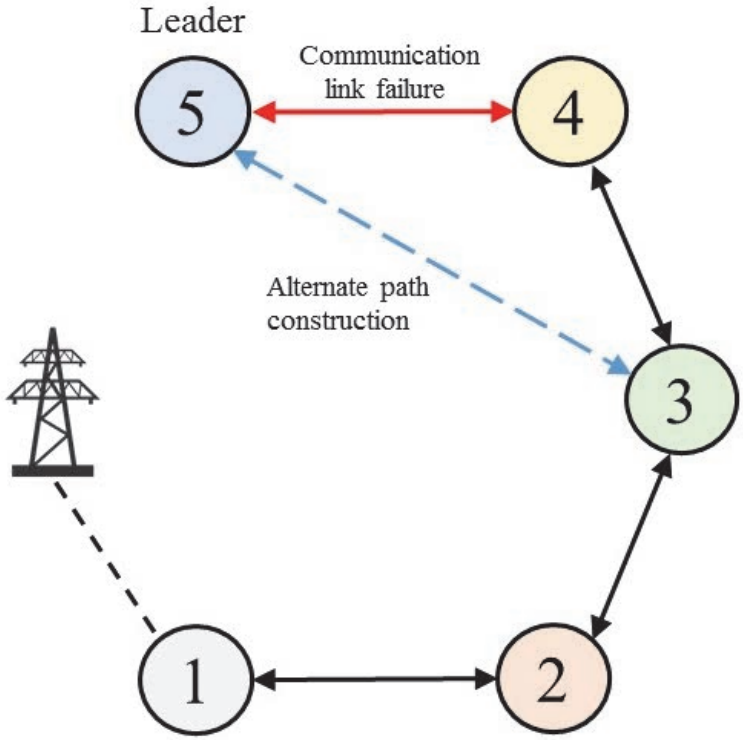
Leader
Communication
link failure
5
4
Alternate path
construction
3
1
2

(a)

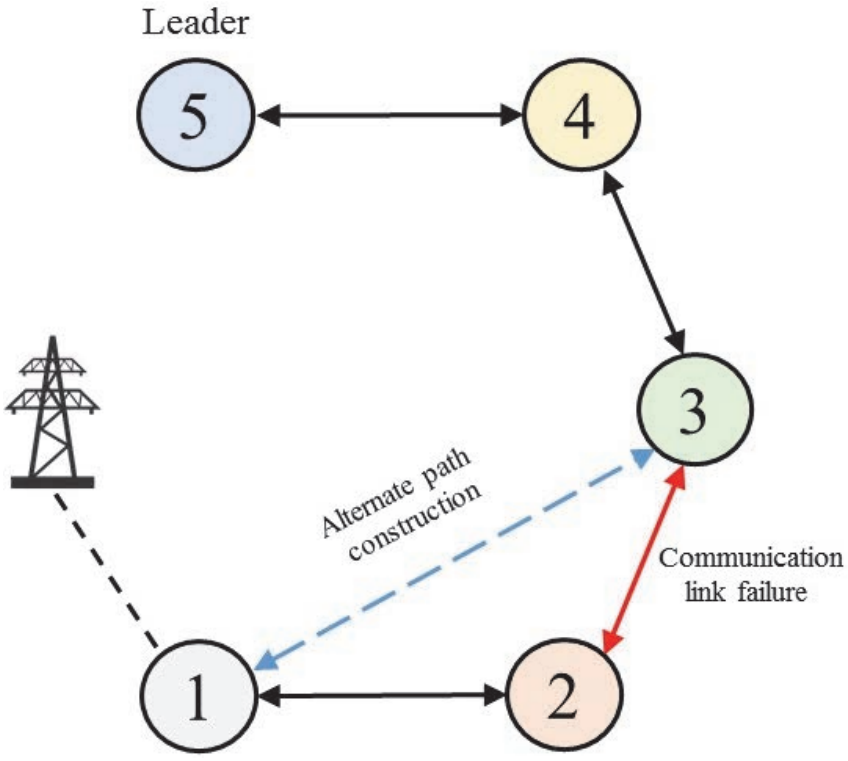
Leader
5
4
3
Alternate path
construction
Communication
link failure
1
2

(b)

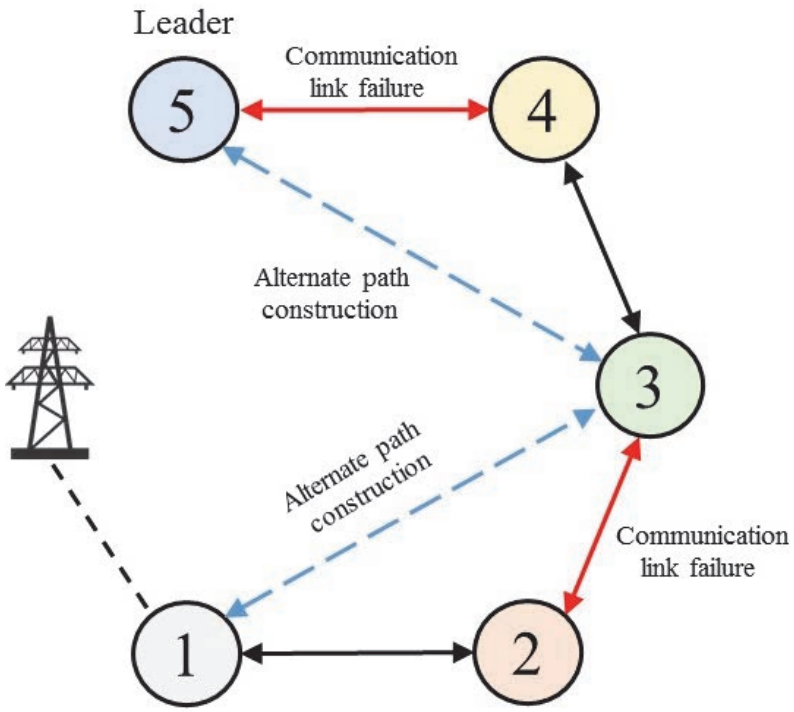

(c)

Figure 5.9. Communication link failures and construction of alternate paths (a) Leader-to-node communication link failure (b) node-to-node communication link failure (c) Leader-to-node and node-to-node communication link failures

In figure 5.9 (a), an instant has been illustrated when there is a communication link failure between the leader node (node-5) and the node immediate downstream (node-4). Therefore, there is no data transmission between node-5 and node-4 at that instant. The back-up node of any node in this network has been considered as the node immediate downstream of that node. In figure 5.9 (a), the back-up node for node-4 is node-3. Therefore, the instant when there is a communication link failure between node-5 and node-4, an alternate path gets constructed between node-5 and node-3 so that the downstream nodes through the radial network can still follow the virtual leader. In figure 5.9 (b), an instant has been illustrated when there is a communication link failure between two nodes on the network other than the leader (node-3 and node-2). The back-up node for node-2 is node-1 and the instant when the communication link failure between node-3 and node-2 takes place, an alternate path gets constructed between

node-3 and node-1 so that node-2 and node-1 still can track the leader. In figure 5.9 (c), an instant has been illustrated when there is a communication link failure between both leader-to-node and node-to-node. In this case, alternate paths are constructed for both the failures to provide robustness to the functionality of following the virtual leader.

5.5 Application of the proposed discrete event-triggered distributed cooperative voltage control on a partly cloudy day and the proposed alternate path routing algorithm during random communication link failures

The performance of the discrete event-triggered communication-based distributed cooperative voltage control strategy has been analysed on a partly cloudy day with fluctuating operating conditions. The voltage profile for the critical buses of the radial distribution network on a partly cloudy day is illustrated in figure 5.10.

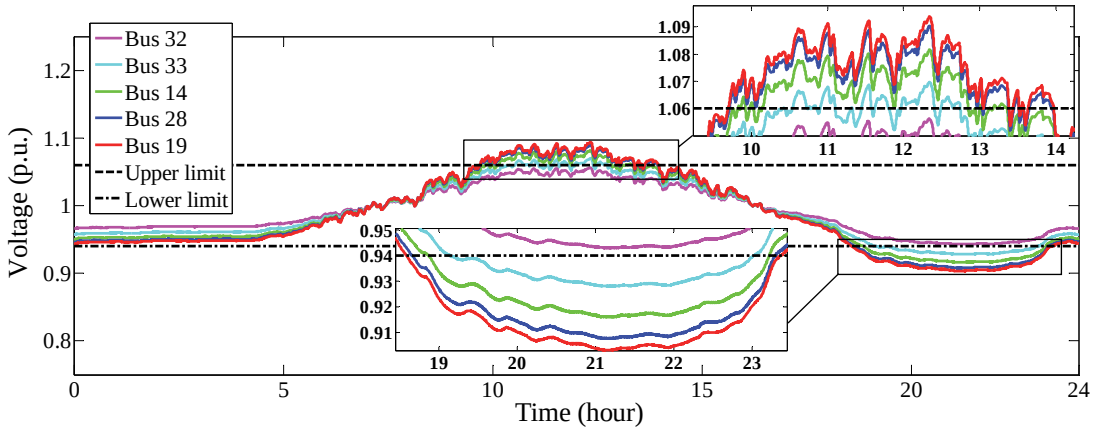

Figure 5.10. 24-hour voltage profile of the critical buses on a partly cloudy day.

For a radial distribution feeder, the buses at the end of the feeder (furthest from substation) are considered as critical buses as the bus voltages tend to exceed the allowable zone. Figure 5.10 illustrates the voltages of critical buses of the test distribution feeder in 24-hour timeframe. Here, one can see that the bus voltages tend to experience rapid variations due to the impact of cloud transients and the voltages of bus 19, bus 28, bus 14 and bus 33 exceed the allowable limits. Three test cases have been analysed to evaluate the performance of each control layer on a partly cloudy day and a comparative analysis has been carried out for the communication

instants while implementing event-triggered communication scheme on a clear day and a partly cloudy day. Another test case has been carried out to evaluate the performance of the discrete event-triggered distributed cooperative voltage control strategy in the occurrence of random communication link failures. This test case also evaluates the performance of the proposed alternate path routing algorithm to provide robustness against these failures.

5.5.1 Distributed voltage control for BESS without cooperation (only distributed control layer)

In the first test case, the performance of the proposed leader-following consensus-based distributed voltage control algorithm has been analysed without any cooperation among adjacent BESSs and PV inverters on a partly cloudy day.

In the distributed voltage control layer, BESSs from the critical buses ($BESS_{19}$, $BESS_{28}$, $BESS_{14}$ and $BESS_{33}$) participate in distributed voltage control. $BESS_{32}$ has not participated in the leader-following consensus-based distributed voltage control as V_{32} is within the allowable zone. The initial SOC of all the BESSs is considered at the lower SOC limit which is 20%. In figure 5.11, one can see that the voltages of all critical buses are being regulated within allowable zone till time t = 12.47 hours. At time t = 12.47 hours, the SOC of $BESS_{19}$ reaches its upper limit (90% SOC) and not available anymore for voltage control. Here, one can see that it takes longer time for $BESS_{19}$ to reach the upper SOC limit on a partly cloudy day comparing to a clear sunny day as the solar irradiance drops down when the cloud passes and so does the magnitude of voltage deviation. At t = 12.47 hours, V_{19} exceeds the upper voltage limit. $BESS_{28}$, $BESS_{14}$ and $BESS_{33}$ keep participating in feeder voltage control by charging in the excess generated PV power in distributed fashion. $BESS_{28}$ becomes unavailable for voltage control as its SOC reaches its upper limit (90% SOC) at time t = 13.25 hours. However, 13.25 hour is quite past the peak solar irradiation period and the magnitude of voltage deviation is not high enough at that time on a partly cloudy day. Therefore, the distributed voltage control operation of only $BESS_{14}$ and $BESS_{33}$ is enough to regulate V_{19}, $V_{28,}$ V_{14} and V_{33} within allowable limit from t = 13.25 hours. Figure 5.11 (b) shows that $BESS_{14}$ and $BESS_{33}$ do not reach their upper SOC limit on a partly cloudy day the way they did on a clear sunny day. As a consequence, they provide voltage support for comparatively shorter time during evening.

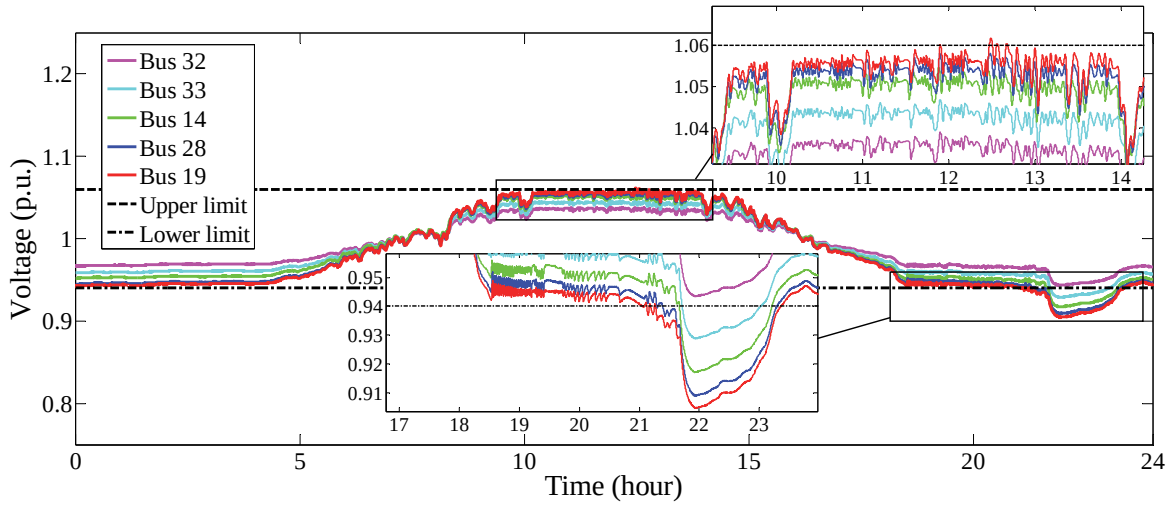

(a)

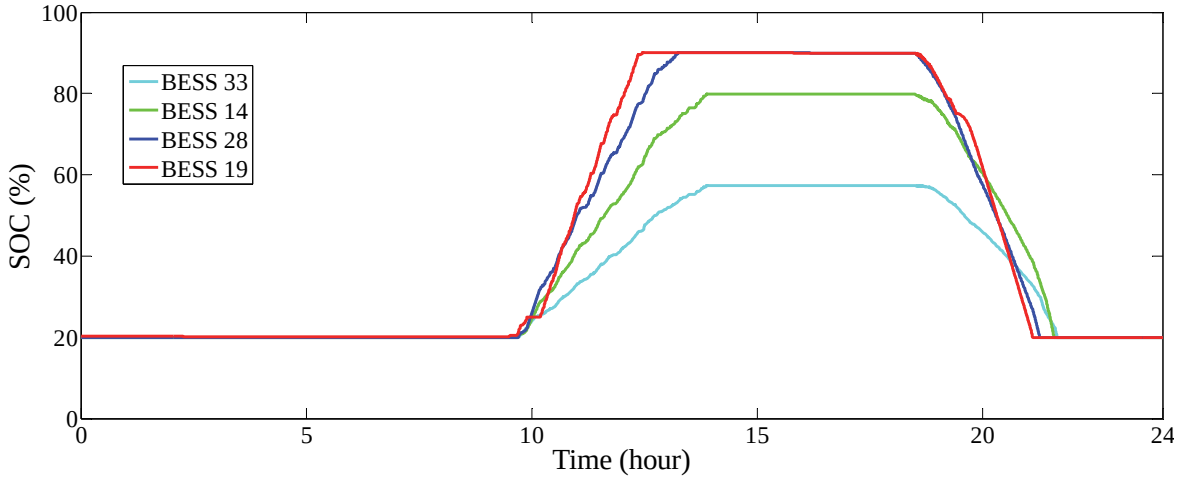

(b)

Figure 5.11. (a) 24-hour voltage profile and (b) SOC of BESSs on a partly cloudy day when distributed voltage control is implemented without any cooperation.

During evening period, voltage sag occurs and V_{19}, V_{28}, V_{14} and V_{33} exceed the lower allowable voltage limit. $BESS_{19}$ and $BESS_{28}$ have been fully charged and $BESS_{14}$ and $BESS_{33}$ have been partly charged during day time and are ready to discharge to provide voltage support

during evening. The leader-following consensus algorithm controls the bus voltages in a distributed fashion and keeps them within lower allowable limit until the BESSs reach their lower SOC limit (20% SOC). $BESS_{19}$, $BESS_{28}$, $BESS_{14}$ and $BESS_{33}$ reach their lower SOC limit at time t = 20.89, t = 21.27, t = 21.66 and t = 21.59 hours respectively. Voltages at one or more critical buses exceed lower allowable limit with time with the unavailability of one or more BESSs for distributed voltage control.

5.5.2 Distributed voltage control for BESS with cooperation among adjacent BESSs (only distributed control layer and first-stage of cooperative control layer)

In the previous section, one could see that $BESS_{19}$ and $BESS_{28}$ reached their upper SOC limit at time t = 12.47 and t = 13.25 hours. Due to unavailability of $BESS_{19}$ for participating in distributed voltage control, voltage of bus 19 exceeded allowable limit. Figure 5.12 shows the 24-hour voltage profile of critical buses when distributed voltage control with cooperation among adjacent BESSs is implemented on a partly cloudy day. During midday, when $BESS_{19}$ reaches its SOC limit and V_{19} exceeds the allowable zone (at t = 12.47 hour), the cooperation algorithm of the control structure of $BESS_{28}$ gets activated and provides cooperative voltage support for V_{19} and regulates it within limit. $BESS_{28}$ keeps providing the cooperative voltage support for V_{19} until its SOC reaches its upper limit (at t = 12.68 hours). When $BESS_{28}$ reaches its limit, V_{19} and V_{28} both exceed the allowable zone. This initiates the cooperation algorithm of $BESS_{14}$ and $BESS_{19}$. $BESS_{14}$ provides cooperative voltage support for V_{28} and keeps it within upper limit (another neighbour, $BESS_{19}$ is unavailable for cooperation as it has already reached its upper SOC limit). Therefore, V_{19} exceeds upper allowable voltage limit from t = 12.68 hour.

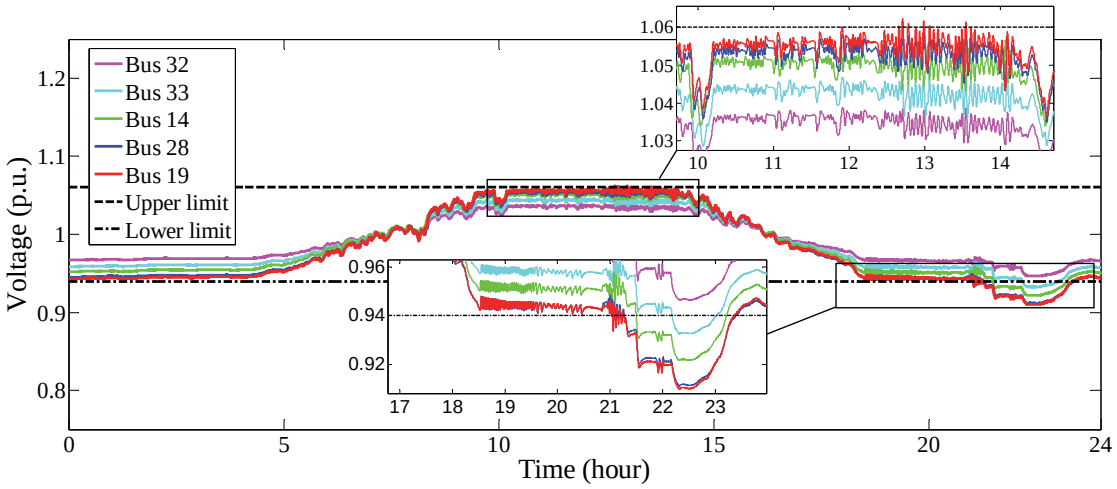

(a)

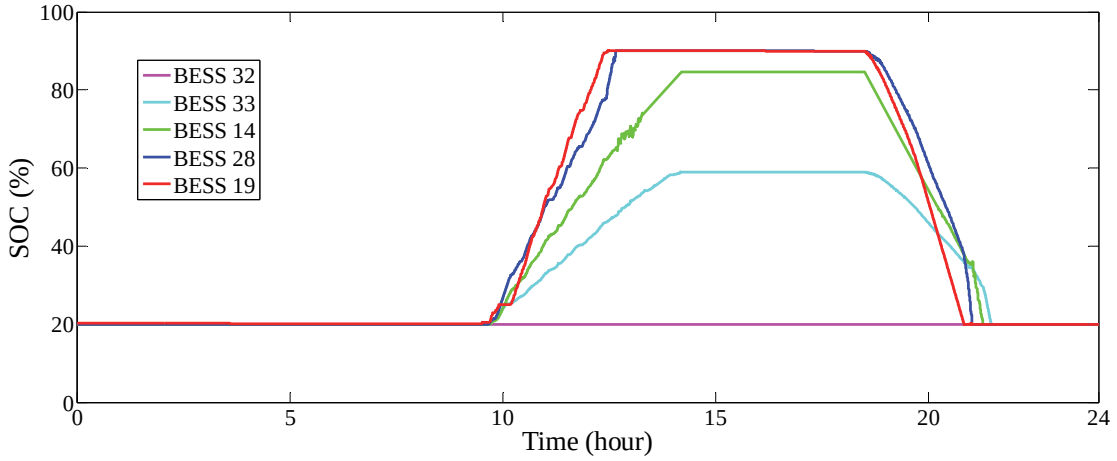

(b)

Figure 5.12. (a) 24-hour voltage profile and (b) SOC of BESSs on a partly cloudy day when distributed voltage control with cooperation among adjacent BESSs is implemented.

$BESS_{14}$ and $BESS_{33}$ provide voltage support till t = 14.21 hours. After t = 14.21 hours, all the bus voltages enter into allowable zone due to lesser solar irradiation.

During evening, $BESS_{19}$, $BESS_{28}$, $BESS_{14}$ and $BESS_{33}$ reach their lower SOC limits at t = 20.85 hours, t = 21.03 hours, t = 21.26 hours and t = 21.37 hours respectively.

5.5.3 Distributed voltage control for BESS with cooperation among adjacent BESSs and PV inverters (complete distributed and cooperative control layer together)

During day time, $BESS_{19}$ reaches its SOC limit at t = 12.47 hours and $BESS_{28}$ reaches its limit at t = 12.68 hours. After t = 12.68 hours, $BESS_{14}$ provides cooperative voltage support for V_{28} as adjacent neighbour. However, V_{19} exceeds the upper allowable voltage limit as $BESS_{19}$ and $BESS_{28}$ both are unavailable. This initiates the cooperation algorithm of PV $inverter_{19}$ to regulate V_{19} within allowable zone by absorbing appropriate reactive power. PV-$inverter_{28}$ and PV-$inverter_{14}$ do not need to initiate and provide voltage support to V_{28} and V_{14} as $BESS_{14}$ and $BESS_{33}$ do not reach their upper SOC limit on a partly cloudy day.

During evening, PV inverters inject appropriate reactive power to raise the bus voltages if BESS of a particular bus and adjacent buses reach lower SOC limit and voltage of those buses exceed lower voltage limit. From figure 5.13 (c), one can see that, PV-$inverter_{19}$, PV-$inverter_{28}$ and PV-$inverter_{14}$ gets initiated at t = 21.03 hours, t = 21.265 hours and t = 21.38 hours respectively and inject reactive power to regulate V_{19}, V_{28}, and V_{14} within allowable limit.

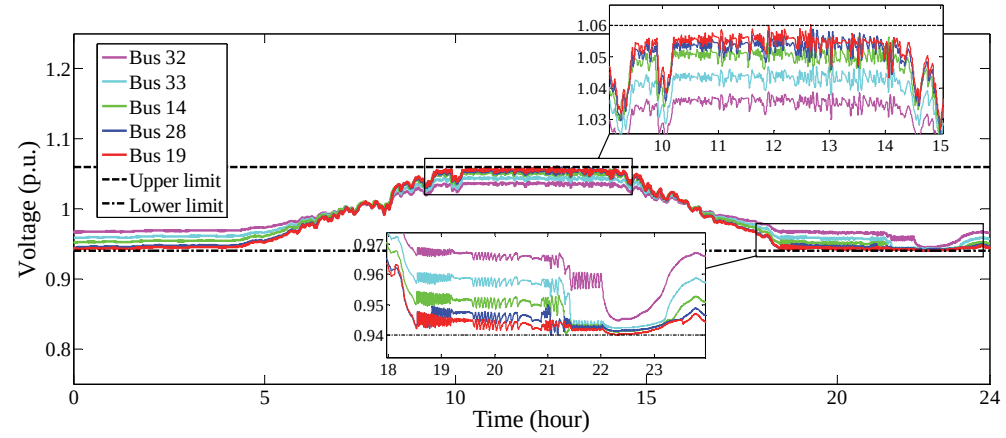

(a)

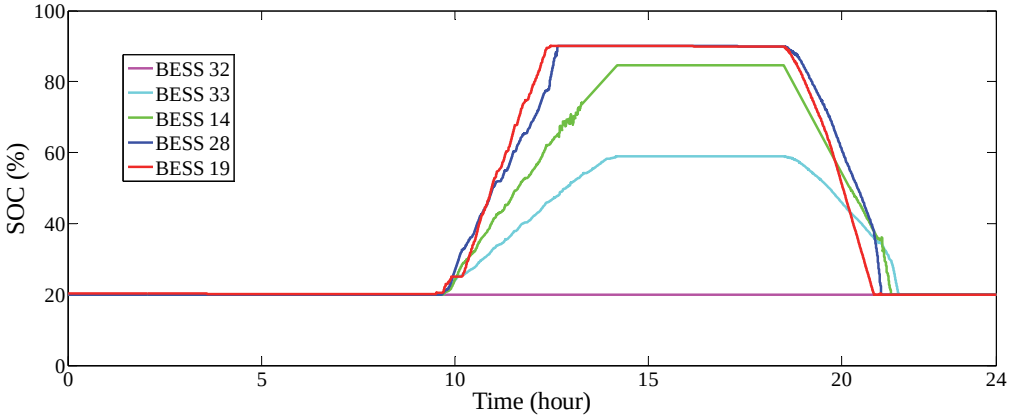

(b)

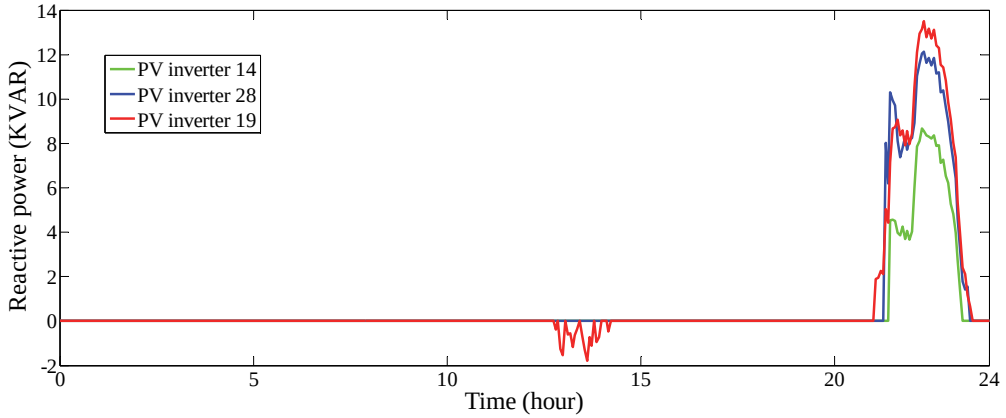

(c)

Figure 5.13. (a) 24-hour voltage profile (b) SOC of BESSs and (C) reactive power injection/ absorption by PV inverters on a partly cloudy day when distributed voltage control with cooperation among adjacent BESSs and PV inverters is implemented.

Figure 5.14 illustrates the distributed control input from bus 19 during a part of the partly cloudy day. Agent at bus 19 performs state measurement and error computation at each discrete time step and transmits the measured state when the computed error exceeds a defined threshold. In our paper, the threshold for computed error in the distributed control layer has been considered as 300 watts. Each time the error between last transmitted data and current measured data reaches the threshold- an event is triggered, the discrete transmission data changes to a new value and the distributed control input to neighbour control agent is updated.

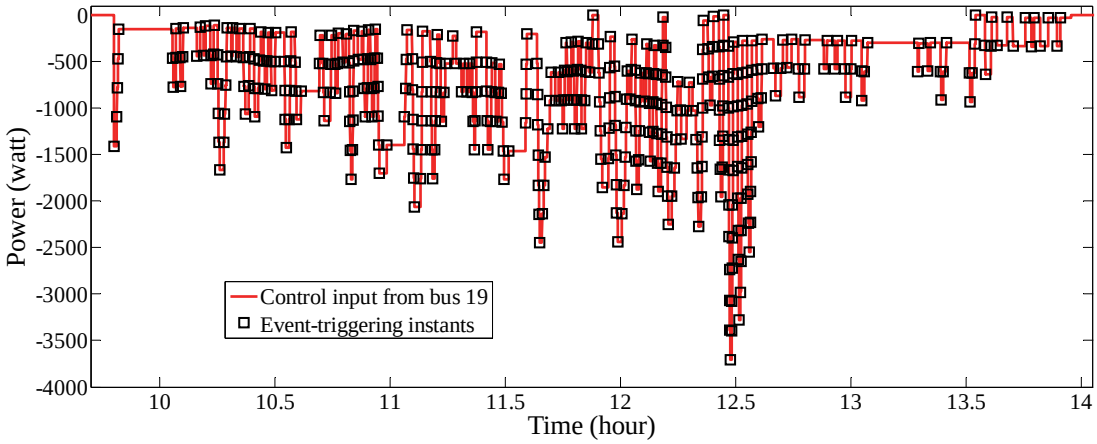

Figure 5.14. A part of distributed control input from bus 19 with event-triggered communication scheme on a partly cloudy day.

It can be seen in figure 5.14 that the frequency of event-triggered communication instants is much higher on a partly cloudy day comparing to a clear sunny day. Therefore, a reliable and resilient communication network is highly recommended to ensure the desirable distributed voltage control performance. If there is a communication link failure during one or more discrete communication instants between agents, it may put significant adverse impact on the performability of the distributed voltage control.

Figure 5.15 shows event-triggering time instants at each critical bus in distributed voltage control layer during a part of the (a) clear sunny day and (b) partly cloudy day. It illustrates that the frequency of event-triggered communication instants get highly increased on a partly cloudy day comparing to a clear sunny day.

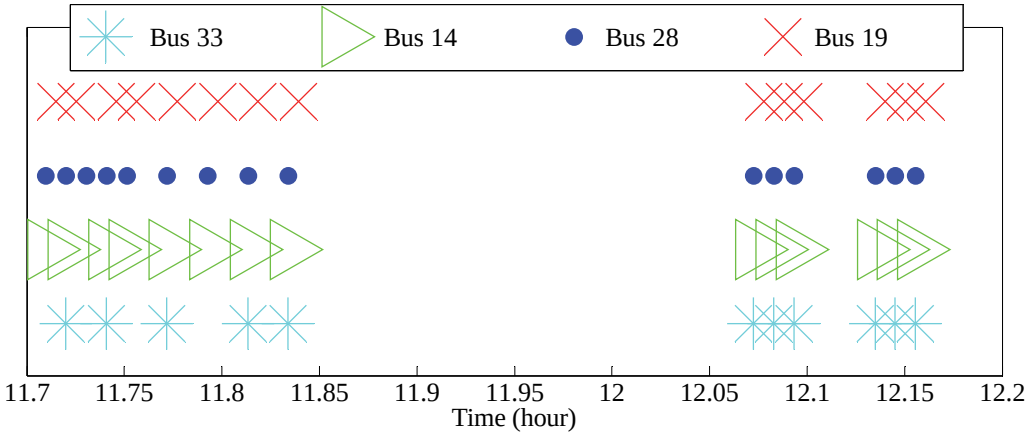

(a)

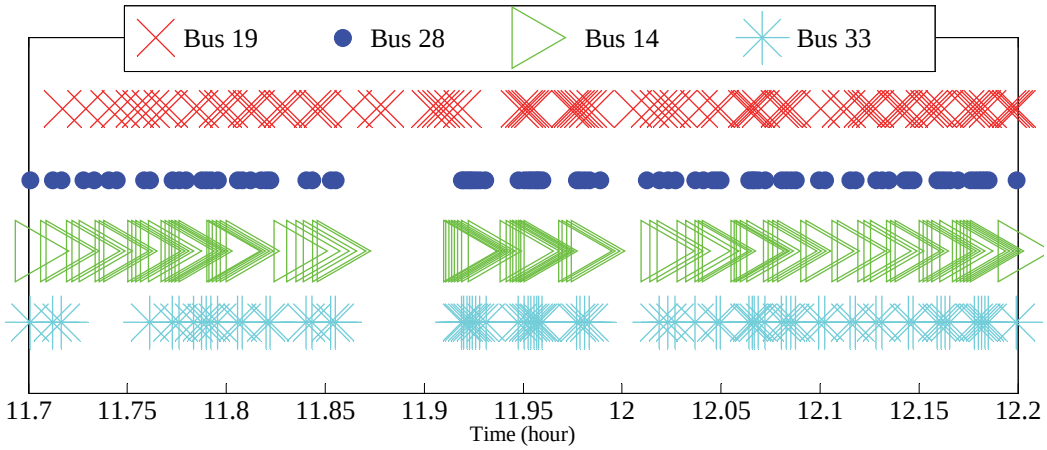

(b)

Figure 5.15. A part of event-triggering time instants in distributed voltage control layer (a) clear sunny day (b) partly cloudy day

In the first-stage of cooperative voltage control layer, the voltage measurement at each critical bus (with BESS that has reached its limit) is transmitted to its neighbour buses as cooperative control input. The threshold value for voltage measurement error has been considered as 0.5 Volt. Figure 5.16 illustrates the cooperative control input from bus 19 and bus 28 under event-triggered communication scheme.

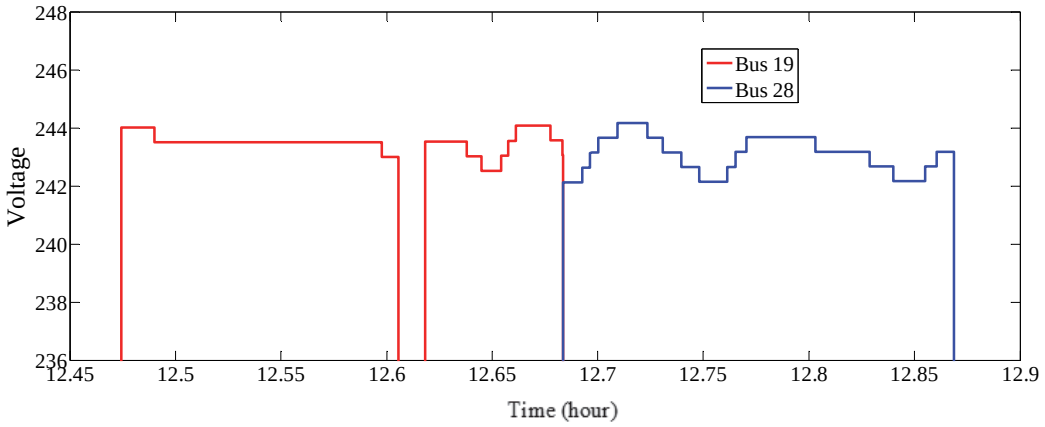

Figure 5.16. Cooperative control inputs from critical buses (to neighbor buses) under event-triggered communication scheme on a partly cloudy day.

To compare the differences of event-triggering instants between a clear sunny day and a partly cloudy day, the number of communication instants on both the days have been illustrated in Table I. The data from Table 5.I shows that the communication instants on a partly cloudy day is significantly higher than the communication instants on a clear sunny day.

TABLE 5.I. NUMBER OF DATA TRANSMISSION INSTANTS

Communication instants	**Bus 19**	**Bus 28**	**Bus 14**	**Bus 33**
Clear sunny day	276	287	329	251
Partly cloudy day	497	545	608	476

Table 5.II depicts the coefficients of control algorithms of the distributed cooperative voltage control scheme (same as clear sunny day).

TABLE 5. II. SYSTEM COEFFICIENTS

Coefficients for share of participation of leader for distributed control		
$K_1 = 1.5$		$K_2 = 2.3$
Coefficients for cooperation algorithm for BESS		**Coefficients for cooperation algorithm for PV inverters**
$K_{19\,3} = 7.5$	$K_{19\,4} = 6.5$	$g_{19} = 1$
$K_{28\,3} = 6.0$	$K_{28\,4} = 7.0$	$g_{28} = 2$
$K_{14\,3} = 6.5$	$K_{14\,4} = 7.5$	$g_{14} = 2$
$K_{33\,3} = 5.5$	$K_{33\,4} = 5.5$	$g_{33} = 2$
$K_{32\,3} = 4.5$	$K_{32\,4} = 9.5$	$g_{32} = 2$

5.5.4 Impact analysis of communication link failures and performance evaluation of the proposed alternate-path routing algorithm to provide robustness to distributed voltage controller

The main theme of discrete event-triggered communication-based distributed voltage control strategy is to reduce the communication instants as much as possible without degrading the performance of the distributed voltage controller. Therefore, a successful data transmission between neighbour agents is compulsory at each communication instant. Disruption or communication link failure during one or more communication instants can affect the controller performance in a significant way. Figure 5.17 – figure 5.26 illustrate the impact of communication link failure between bus 19 and bus 28 during a series of communication instants.

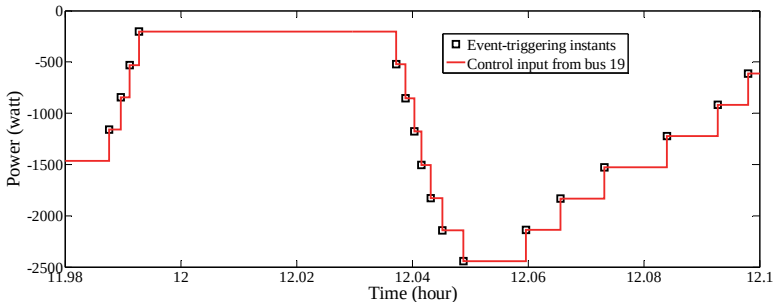

(a)

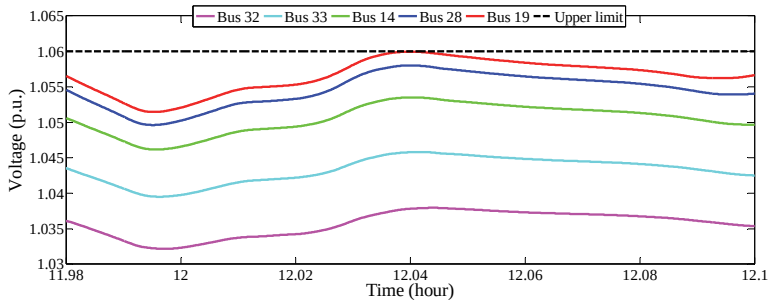

(b)

Figure 5.17. (a) Control input from bus 19 to bus 28 with no communication link failure (11.98-12.1 hours) (b) Critical bus voltages are controlled with desirable performance.

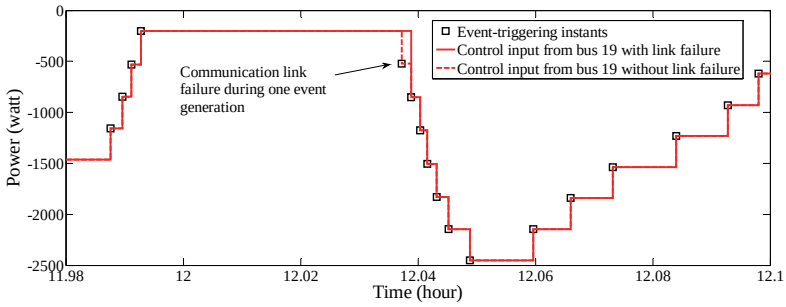

(a)

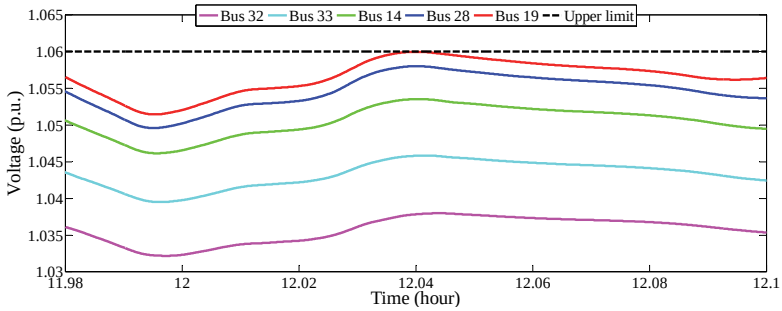

(b)

Figure 5.18. (a) Control input from bus 19 to bus 28 with communication link failure for one communication instant (11.98-12.1 hours) (b) V19 tends to exceed the allowable limit.

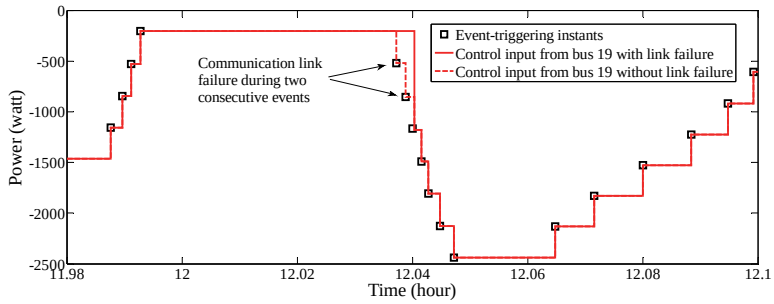

(a)

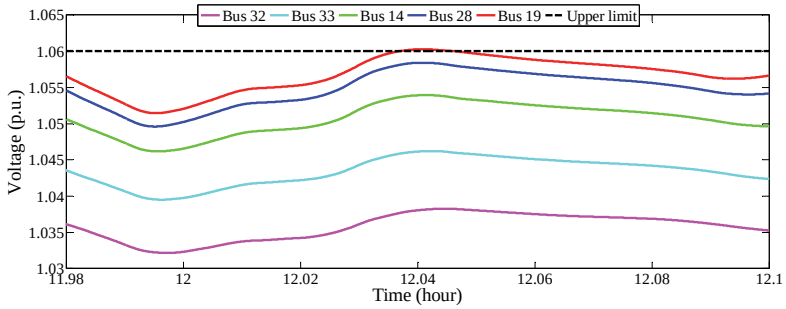

(b)

Figure 5.19. (a) Control input from bus 19 to bus 28 with communication link failure for two consecutive communication instants (b) V19 exceeds the allowable limit.

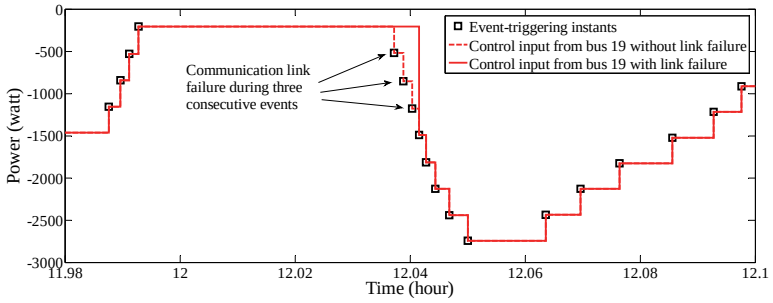

(a)

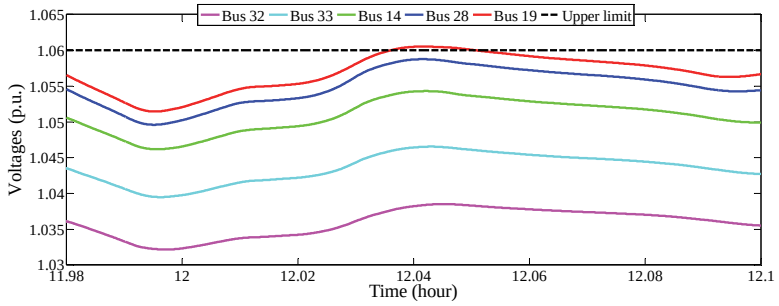

(b)

Figure 5.20. (a) Control input from bus 19 to bus 28 with communication link failure for three consecutive communication instants (b) V19 exceeds the allowable limit.

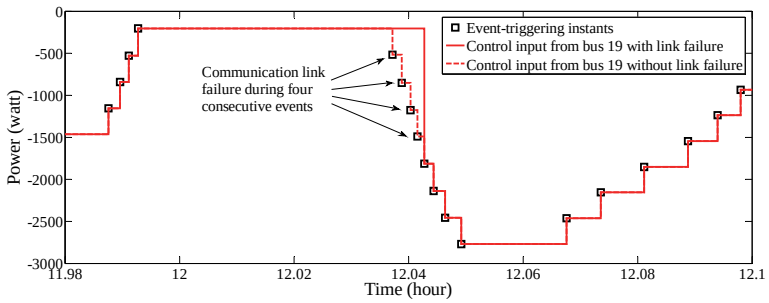

(a)

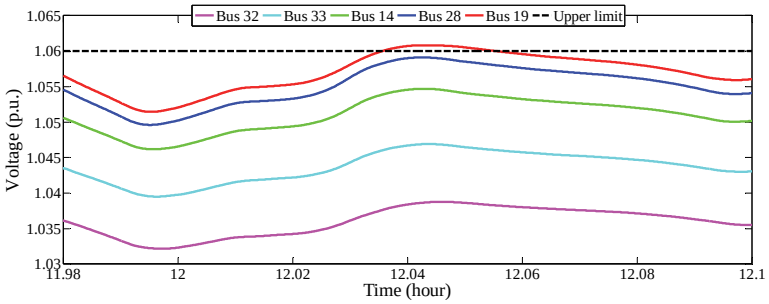

(b)

Figure 5.21. (a) Control input from bus 19 to bus 28 with communication link failure for four consecutive communication instants (b) V19 exceeds the allowable limit.

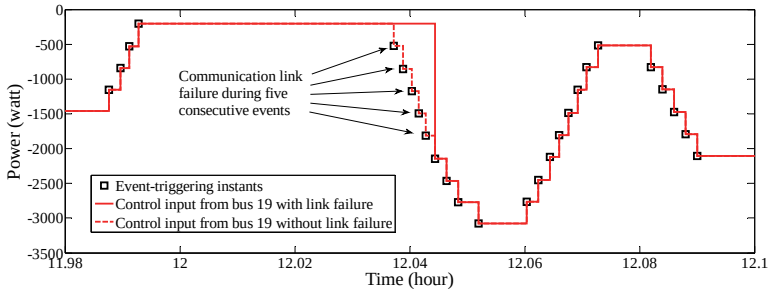

(a)

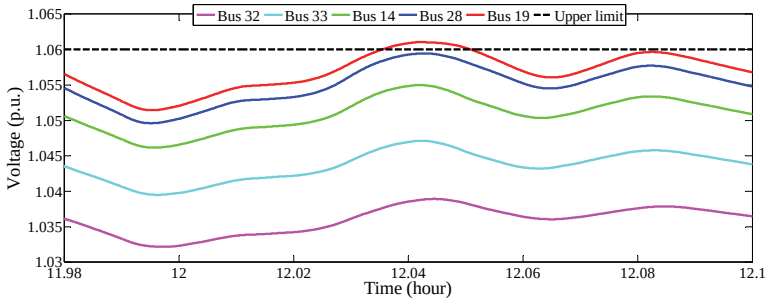

(b)

Figure 5.22. (a) Control input from bus 19 to bus 28 with communication link failure for five consecutive communication instants (b) V19 exceeds the allowable limit.

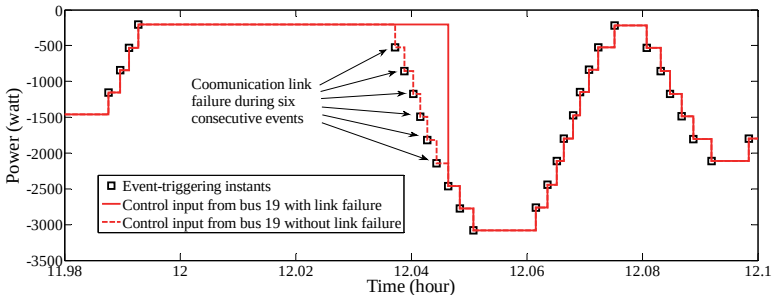

(a)

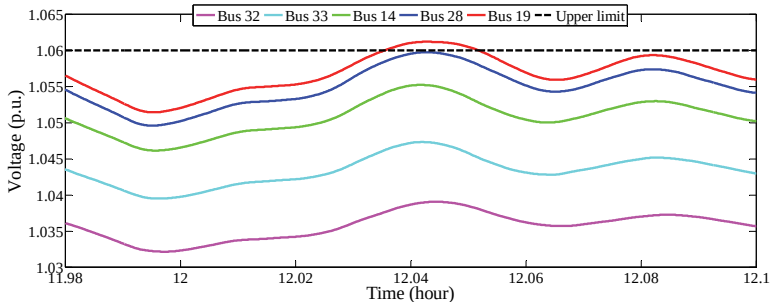

(b)

Figure 5.23. (a) Control input from bus 19 to bus 28 with communication link failure for six consecutive communication instants (b) V19 exceeds the allowable limit.

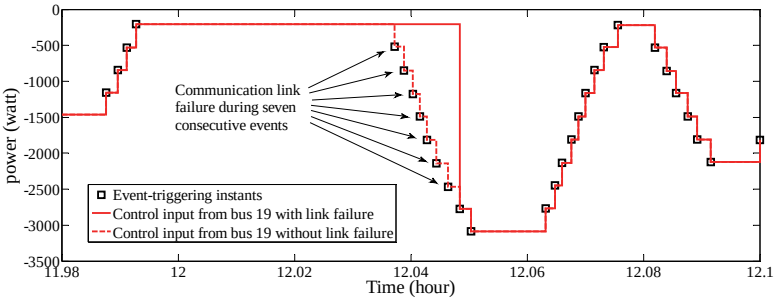

(a)

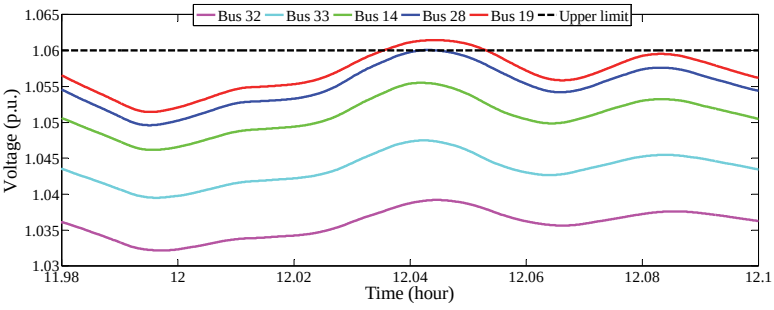

(b)

Figure 5.24. (a) Control input from bus 19 to bus 28 with communication link failure for seven consecutive communication instants (b) V19 and V28 exceed the allowable limit.

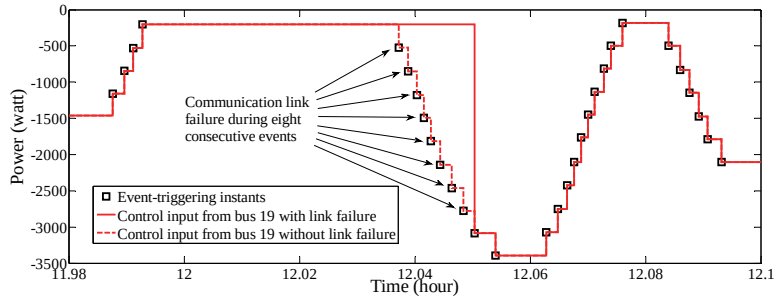

(a)

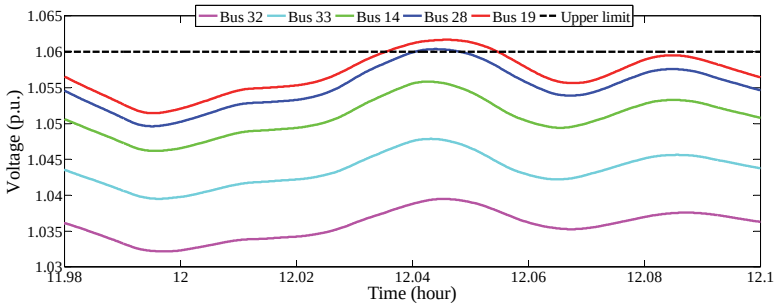

(b)

Figure 5.25. (a) Control input from bus 19 to bus 28 with communication link failure for eight consecutive communication instants (b) V19 and V28 exceed the allowable limit.

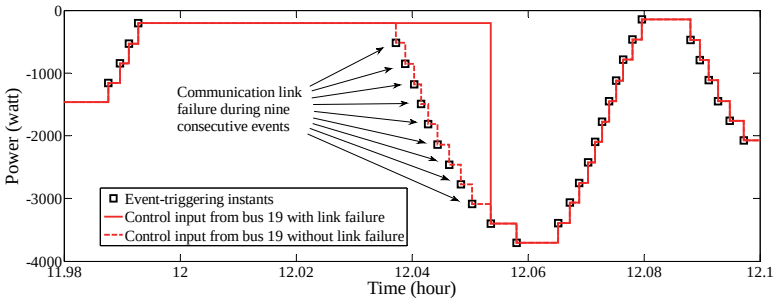

(a)

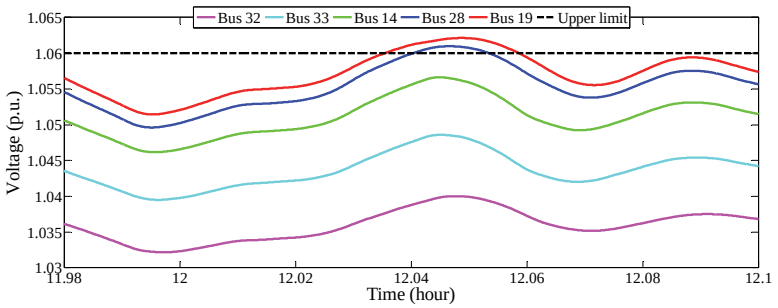

(b)

Figure 5.26. (a) Control input from bus 19 to bus 28 with communication link failure for nine consecutive communication instants (b) V19 and V28 exceed the allowable limit.

Figure 5.17 illustrates a part of the partly cloudy day (11.98-12.1 hours) with no communication link failure between neighbour buses. It shows that, when there is no disruption in the communication between neighbour agents, the discrete event-triggered communication-based distributed voltage controller perfectly regulates the critical bus voltages within allowable limit. Figure 5.18-figure 5.26 illustrate the impact of communication link failure between bus 19 and bus 28 for a series of communication instants on the performance of the distributed voltage controller. In figure 5.18-figure 5.26 and figure 5.27 one can see that, the more is the failed consecutive communication instants, the more is the voltage deviation exceeding the allowable zone.

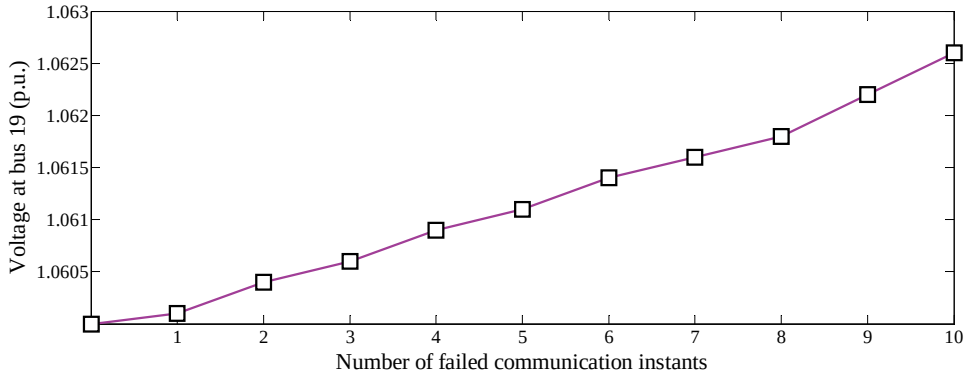

Figure 5.27. Relation between number of failed consecutive communication instants and voltage rise during day time on a partly cloudy day.

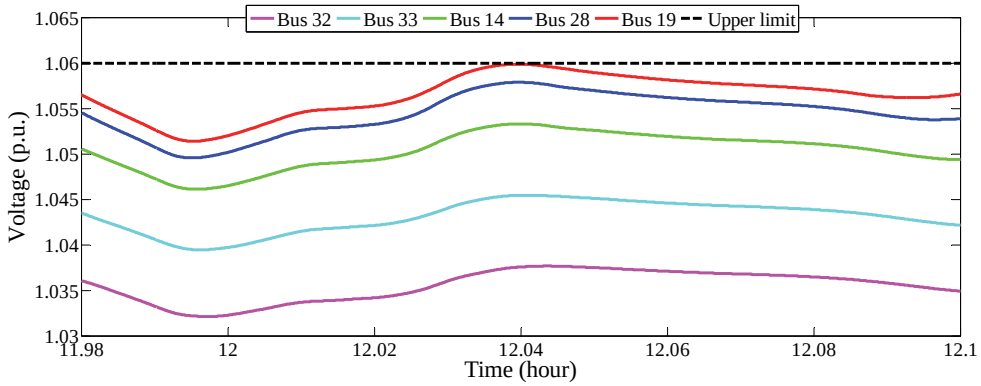

Figure 5.28. Voltage profile of the critical buses when alternate path routing algorithm is implemented in the event of communication link failure for four consecutive communication instants between bus 19 and bus 28.

Figure 5.28 illustrates the voltage profile of critical buses when the proposed alternate path routing algorithm is implemented in the event of communication link failure for four consecutive communication instants between bus 19 and bus 28. In this figure, one can see that the voltage profile of the critical buses is almost similar to the voltage profile when no communication link failure occurs. A time delay of 35 ms has been considered for the data transmission through alternate path considering that the usual communication delay for wireless-based network is 20 ms [41].

Figure 5.29 illustrates the voltage profile of the critical buses during the occurrences of communication link failure between bus 19 and bus 28 for four consecutive communication instants (12.037 hour- 12.043 hour) and communication link failure between bus 28 and bus 14 for three consecutive communication instants (11.498 hour- 11.504 hour) and five consecutive communication instants (12.314 hour- 12.332 hour). It shows that these communication link failure events affect the performability of the discrete event-triggered communication-based distributed voltage controller and V_{19} exceeds the allowable voltage limit.

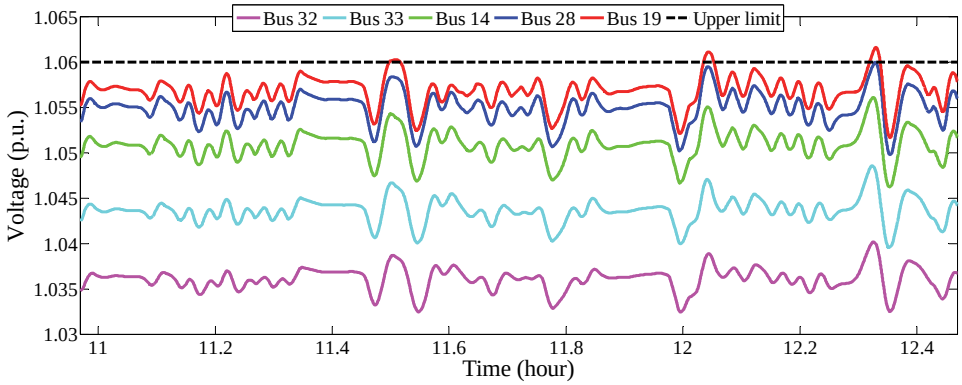

Figure 5.29. Voltage profile of the critical buses when communication link failures occur between different adjacent critical buses.

Figure 5.30 illustrates the voltage profile of critical buses when the proposed alternate path routing algorithm is implemented in the occurrences of communication link failures illustrated in figure 5.29. It shows that the voltage rise at bus 19 is totally mitigated and the robust performance of the proposed voltage controller is restored. Time delay for data transmission through alternate path has been considered as 35 ms.

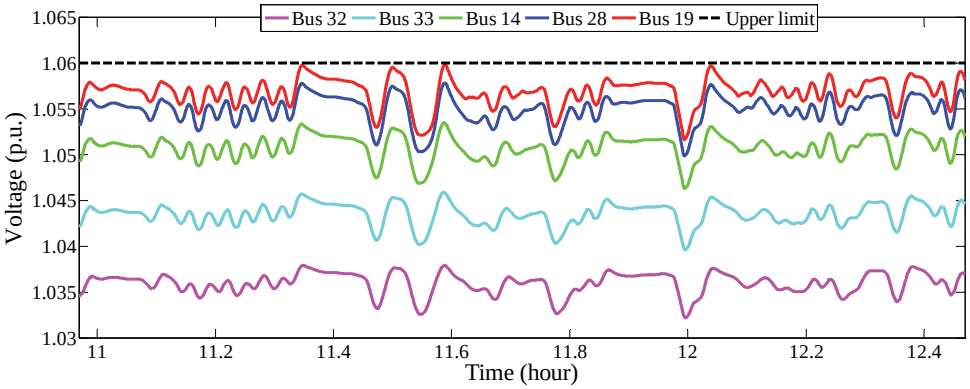

Figure 5.30. Voltage profile of the critical buses when alternate path routing algorithm is implemented in the event of communication link failures between multiple adjacent buses on a partly cloudy day.

In this section, one can see that the proposed alternate path routing algorithm can provide robustness to discrete event-triggered communication-based distributed voltage controller against random communication failures.

5.6 Conclusion

In this paper, the performance of an event-triggered communication-based distributed cooperative voltage control strategy implemented on adjacent BESSs and PV inverters has been evaluated to control the feeder voltage of grid-tied PV system on a partly cloudy day. Case studies have been performed to evaluate the performance of each separated control layer on a partly cloudy day. Case studies have shown that the communication instants between neighbour agents are more frequent and significantly larger in number on a partly cloudy day comparing to a clear sunny day. The significance of a reliable communication network to ensure the desirable performance of proposed discrete event-triggered communication-based distributed voltage controller has been illustrated by analysing the impacts of random communication link failures. Case study showed that the disruption of data transmission between neighbour agents during communication instants affects the controller performability and bus voltages exceed the allowable limit. The performance of the proposed alternate path routing algorithm has been evaluated where it has been showed that this algorithm provides robustness to the voltage controller against random communication link failures. The simulation test results were obtained from a realistic low-voltage distribution network model interconnected with large-scale PVs and actual network data, load profile data, solar irradiance

and ambient temperature data have been used to evaluate the performance of proposed control strategy in realistic environment.

References

[1] International Energy Agency, “Technology roadmap: Solar photovoltaic energy,” Sep. 2014. [Online]. Available: https://www.iea.org/publications/freepublications/publication/TechnologyRoadmapSolarPhotovoltaicEnergy_2014edition.pdf

[2] Mahmud, N., & Zahedi, A. (2016). Review of control strategies for voltage regulation of the smart distribution network with high penetration of renewable distributed generation. *Renewable and Sustainable Energy Reviews*, *64*, 582-595.

[3] Masters, C. L. (2002). Voltage rise: the big issue when connecting embedded generation to long 11 kV overhead lines. *Power engineering journal*, *16*(1), 5-12.

[4] Ranamuka, D., Agalgaonkar, A. P., & Muttaqi, K. M. (2014). Online voltage control in distribution systems with multiple voltage regulating devices. *IEEE Transactions on Sustainable Energy*, *5*(2), 617-628.

[5] Todorovski, M. (2014). Transformer voltage regulation—Compact expression dependent on tap position and primary/secondary voltage. *IEEE Transactions on Power Delivery*, *29*(3), 1516-1517.

[6] Rahman, M. S., Hossain, M. J., & Lu, J. (2016). Coordinated control of three-phase AC and DC type EV–ESSs for efficient hybrid microgrid operations. *Energy Conversion and Management*, *122*, 488-503.

[7] Ghosh, S., Rahman, S., & Pipattanasomporn, M. (2017). Distribution voltage regulation through active power curtailment with PV inverters and solar generation forecasts. *IEEE Transactions on Sustainable Energy*, *8*(1), 13-22.

[8] Li, P., Ji, H., Wang, C., Zhao, J., Song, G., Ding, F., & Wu, J. (2017). A Coordinated Control Method of Voltage and Reactive Power for Active Distribution Networks Based on Soft Open Point. *IEEE Transactions on Sustainable Energy*.

[9] Jayasekara, N., Masoum, M. A., & Wolfs, P. J. (2016). Optimal operation of distributed energy storage systems to improve distribution network load and generation hosting capability. *IEEE Transactions on Sustainable Energy*, *7*(1), 250-261.

[10] Wang, Lei, et al. "Coordination of Multiple Energy Storage Units in a Low-Voltage Distribution Network." *IEEE Transactions on Smart Grid* 6.6 (2015): 2906-2918.

[11] Mahmud, N., Zahedi, A., & Mahmud, A. (2017). A cooperative operation of novel PV inverter control scheme and storage energy management system based on ANFIS for voltage regulation of grid-tied PV system. *IEEE Transactions on Industrial Informatics*.

[12] Xin, H., Zhang, M., Seuss, J., Wang, Z., & Gan, D. (2013). A real-time power allocation algorithm and its communication optimization for geographically dispersed energy storage systems. *IEEE Transactions on Power Systems*, *28*(4), 4732-4741.

[13] Xu, Y., Zhang, W., Hug, G., Kar, S., & Li, Z. (2015). Cooperative control of distributed energy storage systems in a microgrid. *IEEE Transactions on smart grid*, *6*(1), 238-248.

[14] Oliveira, T. R., Silva, W. W. A. G., & Donoso-Garcia, P. F. (2016). Distributed secondary level control for energy storage management in dc microgrids. *IEEE Transactions on Smart Grid*.

[15] Morstyn, T., Hredzak, B., & Agelidis, V. G. (2015). Distributed cooperative control of microgrid storage. *IEEE transactions on power systems*, *30*(5), 2780-2789.

[16] Morstyn, T., Hredzak, B., & Agelidis, V. G. (2016). Cooperative multi-agent control of heterogeneous storage devices distributed in a DC microgrid. *IEEE Transactions on Power Systems*, *31*(4), 2974-2986.

[17] Schiffer, J., Seel, T., Raisch, J., & Sezi, T. (2016). Voltage stability and reactive power sharing in inverter-based microgrids with consensus-based distributed voltage control. *IEEE Transactions on Control Systems Technology*, *24*(1), 96-109.

[18] Lai, J., Zhou, H., Lu, X., Yu, X., & Hu, W. (2016). Droop-based distributed cooperative control for microgrids with time-varying delays. *IEEE Transactions on Smart Grid*, *7*(4), 1775-1789.

[19] Wang, Y., Tan, K. T., Peng, X. Y., & So, P. L. (2016). Coordinated control of distributed energy-storage systems for voltage regulation in distribution networks. *IEEE Transactions on Power Delivery*, *31*(3), 1132-1141.

[20] Yang, Q., Barria, J. A., & Green, T. C. (2011). Communication infrastructures for distributed control of power distribution networks. *IEEE Transactions on Industrial Informatics*, *7*(2), 316-327.

[21] Yang, Q., Barria, J. A., & Green, T. C. (2011). Communication infrastructures for distributed control of power distribution networks. *IEEE Transactions on Industrial Informatics*, *7*(2), 316-327.

[22] Li, C., Yu, X., Yu, W., Huang, T., & Liu, Z. W. (2016). Distributed event-triggered scheme for economic dispatch in smart grids. *IEEE Transactions on Industrial Informatics*, *12*(5), 1775-1785.

[23] Zhang, X. M., Han, Q. L., & Zhang, B. L. (2017). An overview and deep investigation on sampled-data-based event-triggered control and filtering for networked systems. *IEEE Transactions on Industrial Informatics*, *13*(1), 4-16.

[24] Henriksson, E., Quevedo, D. E., Peters, E. G., Sandberg, H., & Johansson, K. H. (2015). Multiple-loop self-triggered model predictive control for network scheduling and control. *IEEE Transactions on Control Systems Technology*, *23*(6), 2167-2181.

[25] Pezeshki, H., Wolfs, P. J., & Ledwich, G. (2014). Impact of high PV penetration on distribution transformer insulation life. *IEEE Transactions on Power Delivery*, *29*(3), 1212-1220.

[26] Trindade, F. C., Ferreira, T. S., Lopes, M. G., & Freitas, W. (2017). Mitigation of Fast Voltage Variations During Cloud Transients in Distribution Systems With PV Solar Farms. *IEEE Transactions on Power Delivery*, *32*(2), 921-932.

[27] Çetinkaya, E. K., Broyles, D., Dandekar, A., Srinivasan, S., & Sterbenz, J. P. (2013). Modelling communication network challenges for future internet resilience, survivability, and disruption tolerance: A simulation-based approach. *Telecommunication Systems*, 1-16.

[28] Hasan, M. Z., Al-Rizzo, H., & Al-Turjman, F. (2017). A Survey on Multipath Routing Protocols for QoS Assurances in Real-Time Wireless Multimedia Sensor Networks. *IEEE Communications Surveys & Tutorials*.

[29] Jones, N. M., Paschos, G. S., Shrader, B., & Modiano, E. (2017). An overlay architecture for throughput optimal multipath routing. *IEEE/ACM Transactions on Networking*.

[30] Hasan, M. Z., Al-Turjman, F., & Al-Rizzo, H. (2017). Optimized multi-constrained quality-of-service multipath routing approach for multimedia sensor networks. *IEEE Sensors Journal*, *17*(7), 2298-2309.

[31] Gupta, M., & Kumar, N. (2013). Node-disjoint on-demand multipath routing with route utilization in ad-hoc networks. *International Journal of Computer Applications*, *70*(9).

[32] Pu, J., Manning, E., & Shoja, G. C. (2001). Routing reliability analysis of partially disjoint paths. In *Communications, Computers and signal Processing, 2001. PACRIM. 2001 IEEE Pacific Rim Conference on* (Vol. 1, pp. 79-82). IEEE.

[33] Jayashree, A., Biradar, G. S., & Mytri, V. D. (2012). Review of Multipath Routing Protocols in Wireless Multimedia Sensor Network–A Survey. *International Journal of Scientific & Engineering Research*, *3*(7), 1-9.

[34] Somaa, F., Korbi, I. S. E., & Saidane, L. A. (2017). Proactive vs. reactive multipath routing for mobility enabled RPL. *International Journal of Space-Based and Situated Computing*, *7*(2), 94-107.

[35] Anita, R. (2017). Joint cost and secured node disjoint energy efficient multipath routing in mobile ad hoc network. *Wireless Networks*, *23*(7), 2307-2316.

[36] Das, I., Lobiyal, D. K., & Katti, C. P. (2016). An Analysis of Link Disjoint and Node Disjoint Multipath Routing for Mobile Ad Hoc Network. *International Journal of Computer Network and Information Security*, *8*(3), 52.

[37] Al-Ariki, H. D. E., & Swamy, M. S. (2017). A survey and analysis of multipath routing protocols in wireless multimedia sensor networks. *Wireless Networks*, *23*(6), 1823-1835.

[38] Wu, G., Lin, C., Xia, F., Yao, L., Zhang, H., & Liu, B. (2010). Dynamical jumping real-time fault-tolerant routing protocol for wireless sensor networks. *Sensors*, *10*(3), 2416-2437.

[39] Yang, Y., Zhong, C., Sun, Y., & Yang, J. (2010). Network coding based reliable disjoint and braided multipath routing for sensor networks. *Journal of Network and Computer Applications*, *33*(4), 422-432.

[40] Trindade, F. C., Ferreira, T. S., Lopes, M. G., & Freitas, W. (2017). Mitigation of Fast Voltage Variations During Cloud Transients in Distribution Systems With PV Solar Farms. *IEEE Transactions on Power Delivery*, *32*(2), 921-932.

[41] Refaat, T. K., Daoud, R. M., Amer, H. H., & Makled, E. A. (2010, June). Wifi implementation of wireless networked control systems. In *Networked Sensing Systems (INSS), 2010 Seventh International Conference on* (pp. 145-148). IEEE.

Chapter 6

CONCLUSION AND FUTURE WORKS

Voltage regulation challenge along the distribution feeder has attracted the attention of industries and researchers and this challenge will be more crucial in near future due to increased integration of renewable DGs in the low/ medium voltage distribution network. Renewable DGs are generally small-scale electric power generators those generate electricity from renewable sources such as solar, wind, tide etc. Among various sorts of renewable DGs, solar PVs are most popular for grid interconnected operation. Increased interconnection of solar PVs with low-voltage distribution network arises several challenges among which voltage regulation challenge is the most significant. In this thesis, the voltage regulation challenge in low-voltage power distribution network when increased amount of solar PVs are penetrated has been addressed and intelligent mitigation strategies have been designed and their performances have been evaluated in realistic test environment. As traditional control devices like OLTCs, SVRs or SCs are not efficient enough to regulate the voltage when large amount of intermittent solar PVs are interconnected, development of advanced control strategies is the fundamental key for unlimited solar PV penetration without putting significant adverse impact on distribution network operation and stability.

6.1 Impact analysis and qualitative comparison

The impact of interconnecting renewable DGs with traditional low-voltage distribution system has been mathematically analysed in *chapter 2*. Qualitative analysis has been performed for different existing voltage control approaches and recent developments in control structures like centralized control structure, decentralized control structure and distributed control structure have been summarized.

6.2 Design and implementation of two-stage cooperative voltage control at PCC and performance evaluation

Voltage regulation challenge mainly arises because of the reverse power flow to grid during high solar irradiation period. A two-stage cooperative operation of ANFISPID-based PV inverter control scheme and ANFIS-based supervisory EMS has been implemented in *chapter 3* in real time to regulate the PCC voltage of low-voltage distribution network interconnected with large-scale solar PVs. Traditionally, the utility operators need to manually adjust the conventional PID control parameters at a regular practice by a trial-and-error method which is expensive, time-consuming and tedious. The adjusted PID parameters can go obsolete in a short time due to rapidly changing system dynamics which will make the utility operators run the trial-and-error process again. Moreover, when large-scale of intermittent solar PVs are interconnected with low-voltage distribution system, an increased amount of nonlinearities are introduced in the system dynamics. Conventional PID-based control scheme may fail to provide appropriate response in this scenario due to their linear nature that can cause oscillation and system instability. However, when ANFISPID is applied, the expensive manual trial-and-error tuning is not required anymore. To train ANFIS, a number of simulations in different operating conditions are necessary and this is a one-time process and far lesser time-consuming and tedious comparing to manual trial-and-error tuning at a regular practice. Once ANFIS is trained, it provides 'plug-and-play' feature to auto-tune appropriate PID parameters in accordance with system operating conditions in real time. Moreover, ANFISPID-based control scheme provides robust response to system dynamic changes & noises and damps oscillation. Case studies performed in *chapter 3* showed that oscillatory responses provided by the conventional PID can cause the PCC voltage to exceed allowable limit which will arise several critical power system contingencies which are expensive to recover. On the other hand, ANFISPID-based control scheme provides robust responses and damps oscillations even in worst case scenarios and regulates PCC/ feeder voltage within permissible ranges. Besides, ANFIS is easier to implement, faster, stronger in generalization skills and more accurate. The ANFIS controller implemented in this thesis (for ANFISPID) has only two inputs and one output which makes the algorithm very simple, easy and inexpensive to implement. Case studies performed in *chapter 3* also showed that the ANFIS-based supervisory EMS cooperates with ANFISPID-based PV inverter control scheme by reducing PCC voltage deviation thus reducing necessary reactive power injection/ absorption by the inverter for voltage regulation. This reduces line losses through the system and overall expenses. Besides, simulation studies

showed that ANFIS-based supervisory EMS ensures longer BESS life span and better BESS efficiency which increases economic feasibility.

6.3 Design and implementation of discrete event-triggered distributed cooperative voltage control for radial distribution feeder with multiple buses and performance evaluation

For implementing distributed cooperative voltage control along the feeder, a reliable communication network with appropriate bandwidth between neighbour agents is necessary. However, the bandwidth for the communication network of low-voltage distribution grid is very limited. Therefore, in the case of large-scale penetration of solar PVs, the tremendous data exchange while implementing distributed cooperative voltage control along the feeder will rapidly make the network exhausted and communication bottleneck will occur. This bottleneck will put adverse impact on the voltage control performance. Therefore, a strategy is required to reduce the occupancy of communication network bandwidth while preserving the desirable distributed cooperative voltage control performance. In *chapter 4* of this thesis, a novel discrete event-triggered communication-based distributed cooperative voltage control strategy implemented on adjacent BESSs and PV inverters has been designed, implemented and its performance has been evaluated. The designed distributed cooperative voltage control scheme efficiently utilizes the storage capacity of neighbour BESSs and reactive power capacity of PV inverters and it has been separated into two different control layers that reduces necessary communication between neighbour agents. Then, discrete event-triggered communication scheme has been implemented in each control layer that dramatically reduces data transmission between agents and significantly releases communication bandwidth. Three case studies have shown the significance of each control layer for feeder voltage regulation throughout the day. They have shown that the cooperation among neighbour BESSs and PV inverters reduces the BESS sizing requirement and reactive power injection/ absorption requirement at each bus, which eventually reduces capital costs and power losses through the system. Case studies have also proved that separating the distributed cooperative control into different layers and implementing discrete event-triggered communication scheme between agents decrease communication instants in remarkable extent. This significantly reduces the occupancy of limited communication bandwidth and prevents communication bottleneck.

6.4 Performance evaluation of designed discrete event-triggered distributed cooperative control in the occurrences of random communication link failures and design and implementation of alternate path routing algorithm to provide robustness and performance evaluation

The threshold for computed errors has been defined in this thesis in such a way that the communication instants between agents are reduced as much as possible without affecting the performance of the distributed controller. Therefore, if there is a failure of data transmission during an event-triggered communication instant between agents, it can significantly affect the performance of the distributed controller. Besides, on a partly cloudy day, fast variation of solar irradiation associated with cloud transients causes rapid voltage variations through the distribution feeder with highly penetrated PVs. This phenomenon will trigger very frequent and increased number of communication instants which requires highly reliable and resilient communication network for stable distributed voltage control operation. However, communication networks can be subjected to numbers of disturbances and challenges in normal operation due to attacks, large-scale disasters, mobility and characteristics of wireless communication channels. Attacks against the communication network is very frequent and it is practically impossible to achieve fully resilient network because of cost constraints and design flaws. Therefore, it is necessary to evaluate the dependability and performability of the discrete event-triggered communication-based distributed cooperative voltage control strategy when subjected to communication disruptions such as, communication link failures. In *chapter 5*, the performance of an event-triggered communication-based distributed cooperative voltage control strategy implemented on adjacent BESSs and PV inverters has been evaluated to control the feeder voltage of grid-tied PV system on a partly cloudy day. Case studies have been performed to evaluate the performance of each separated control layer on a partly cloudy day and they have shown that the communication instants between neighbour agents are more frequent and significantly larger in number on a partly cloudy day comparing to a clear sunny day. The significance of a reliable communication network to ensure the desirable voltage control performance has been illustrated by analysing the impacts of random communication link failures. Case study showed that the disruption of data transmission between neighbour agents during communication instants affects the controller performability and bus voltages exceed the allowable limit. To provide robustness against these random communication link failures, an alternate path routing algorithm has been proposed. In this algorithm, each node on

the radial communication network selects their back up node so that if there is a communication link failure from the node upstream, an alternate path can be constructed without that node. The performance of the proposed alternate path routing algorithm has been evaluated where it has been shown that this algorithm provides robustness to the voltage controller against random communication link failures.

The simulation results in this thesis were obtained from a realistic model replicating an actual low-voltage distribution network integrated with large-scale of solar PVs. Actual customer load profile data, actual solar irradiance and ambient temperature data had been used to evaluate the performance of the developed voltage control strategies in real scenarios.

6.5 Recommendations for future works

- As a continuation to this work, in the future, variable threshold can be considered in real time for computed errors which will allow more reduction of communication instants all though the day.
- The impact of solar PV penetration can be evaluated for different R/X values and a cooperative strategy utilizing BESS, PV inverter and OLTC can be implemented for distribution feeders with very high R/X values.
- A detailed trade-off analysis can be performed between the maintenance overhead of alternate path and the financial benefit of constructing alternate path in the occurrences of random communication link failures. Maintenance overhead is the measure of the energy required to maintain these alternate paths using periodic keep-alives.
- ANFIS-based supervisory energy management system can be modified and implemented for distributed coordinated voltage control through the feeder with multiple buses.
- A new reactive power control method that is based on sensitivity analysis can be introduced. A location-dependent power factor set value can be assigned to each inverter, and the grid voltage support can be achieved with less total reactive power consumption. In order to prevent unnecessary reactive power absorption from the grid during admissible voltage range or to increase reactive power contribution from the inverters that are closest to the transformer during grid overvoltage condition, this method can combine into two droop functions that can be inherited from the standard cos φ (P) and Q (U) strategies.
- An effective sizing strategy for distributed BESS can be developed in the distribution networks under high PV penetration level. The size of the distributed BESS can be optimized and the cost-benefit analysis can be derived. The cost-benefit analysis can

consider factors of BESS influence on the work stress of voltage regulation devices, load shifting and peaking power generation, as well as individual BESS cost with its lifetime estimation. Based on the cost-benefit analysis, the cost-benefit size can be determined for the distributed BESS.

- A central voltage-control strategy can be developed for smart LV distribution networks, by using a novel optimal power flow (OPF) methodology in combination with the information collected from smart meters for the power flow calculation. This strategy can simultaneously mitigate the PV reactive power fluctuations, as well as minimize the voltage rise and power losses. The results can be very promising, as voltage control can be achieved fast and accurately, the reactive power can be smoothed in reference to the typical optimization techniques and the local control strategies can be validated with a real-time simulator.
- Through a parametric study, various inverter settings can be considered and compared for a real medium voltage network with a high PV penetration level and for which a demonstration can be planned. The purpose of this work can be to investigate the suitability of such control concepts to compensate the voltage rise caused by the PV power feed-in and to provide some guidance on the adjustment of the settings of such control mechanisms. For the assessment of the performance of the control concept with different settings, extensive load flow simulations can be performed for a voltage-dependent reactive power control (Q(V) characteristics) on the basis of 15-minute profiles. As a result, voltage time-series over a period of 1 year can be obtained for each case and analysed. Apart from the voltage profiles, other features such as network losses and reactive energy import can be quantified because they are also of noticeable importance for network operators.
- The Solar PV inverter operation in mitigating the voltage quality issues in various scenarios through RSCAD real-time simulations can be investigated.
- Field measurement data monitoring at the distribution transformer levels can be analysed for better management of the LV network and for maximizing PV penetration. Further research can be performed to understand and mitigate the harmonic resonance issues accompanied with PV systems penetration.
- In future, Energy storage systems will play a vital role in the LV networks. The collective impact of PV and energy storage technology need to be studied. Also, the proposals like community energy storage and distributed energy storage systems installation in the network could be interesting.